ANALYSIS OF ERBB RECEPTORS:

REGULATION OF ERBB-1 KINASE ACTIVATION AND

LOCALIZATION OF ERBB-4 TO MEMBRANE MICRODOMAINS

By

Kristina Wyatt Thiel

Dissertation

Submitted to the Faculty of the

Graduate School of Vanderbilt University

in partial fulfillment of the requirements

for the degree of

DOCTOR OF PHILOSOPHY

in

Biochemistry

December, 2007

Nashville, Tennessee

Approved:

Professor Graham F. Carpenter

Professor Bruce D. Carter

Professor Robert J. Coffey, Jr.

Professor Anne K. Kenworthy

Professor Charles R. Sanders

OVERVIEW

      Two distinct and exclusive projects are combined for this doctoral dissertation, and are separated into two parts. Part I describes the localization of ErbB-4 to membrane microdomains, and Part II reports the importance of the intracellular juxtamembrane region for ErbB-1 kinase activation. Each part contains separate chapters for the introduction, methods and results, conclusions, and references.

ACKNOWLEDGEMENTS

TABLE OF CONTENTS

Part I: ErbB-4 Localization to Membrane Microdomains

Chapter

LIST OF TABLES

LIST OF FIGURES

Part I

Part II

Part I

ErbB-4 Localization to Membrane Microdomains

CHAPTER I

INTRODUCTION

ErbB-4 is the fourth member of the ErbB family of receptor tyrosine kinases. Full-length ErbB-4 behaves as a typical receptor tyrosine kinase in terms of ligand binding, dimerization (both homo- and heterodimerization with other ErbB family members) and tyrosine phosphorylation. In contrast to ErbB-1 and ErbB-2, however, less is understood about the role of ErbB-4 in homeostasis and disease given that it is rarely expressed in immortalized cell lines. Furthermore, its proteolytically-generated intracellular domain fragment has functions distinct from that of the intact receptor. This chapter focuses on the characteristics that distinguish ErbB-4 from the other ErbB receptors.

ErbB-4

Ligand-Dependent Activation and Signaling Pathways

ErbB-4 was originally identified as the receptor for heregulin in 1993 by Plowman, *et al.,* and placed in the ErbB family of receptor tyrosine kinases based on a high degree homology with the other previously identified members, ErbB-1, -2, and -3 [1, 2]. It is now known that ErbB-4 is the receptor for multiple ligands, including the heregulins 1-4 (also neuregulins) [1, 3-5], betacellulin [6], epiregulin [7], and heparin-binding epidermal growth factor (HB-EGF) [8]. The crystal

structure of the ErbB-4 ectodomain, solved by Leahy and colleagues, revealed significant structural similarities in the ligand-unbound state of the ectodomains of ErbB-1, ErbB-3, and ErbB-4 [9], but to date there is no published structure of a ligand-bound ErbB-4 ectodomain. This similarity in ectodomain structure explains why some ErbB-4 ligands also bind to ErbB-1 and/or ErbB-3.

In accord with canonical receptor tyrosine kinase signaling, ligand binding to the ectodomain of ErbB-4 results in tyrosine autophosphorylation [1] as well as tyrosine phosphorylation of downstream substrates such as phospholipase C-γ1 [10], Shc [11, 12] and phosphatidylinositol 3-kinase (PI3K) [12], which are also phosphorylated by other ErbB receptors [13]. Quite interestingly, alternative splicing of the ErbB-4 cytoplasmic domain results in two populations of receptors: a 16-residue insert that contains a PI3K binding site, CYT-1, and another that lacks this insert, CYT-2 (Figure I-1). No differences in ligand-stimulated proliferation were observed in cell lines expressing either the CYT-1 or CYT-2 isoform [14]. However, this same group reported a difference in survival, depending on the isoform expressed, and expression of the CYT-1 isoform, but not the CYT-2 isoform, was found to protect cells from apoptosis [14]. Since PI3K phosphorylation of Akt regulates survival, this result is not surprising. Both isoforms are found in normal breast tissue and in some breast cancer cell lines, such as T47D [15].

Intrinsically coupled to receptor activation is a mechanism for receptor inactivation, and this often includes a negative feedback loop initiated by ligand binding. For ErbB-1, the receptor is rapidly internalized following ligand addition

3
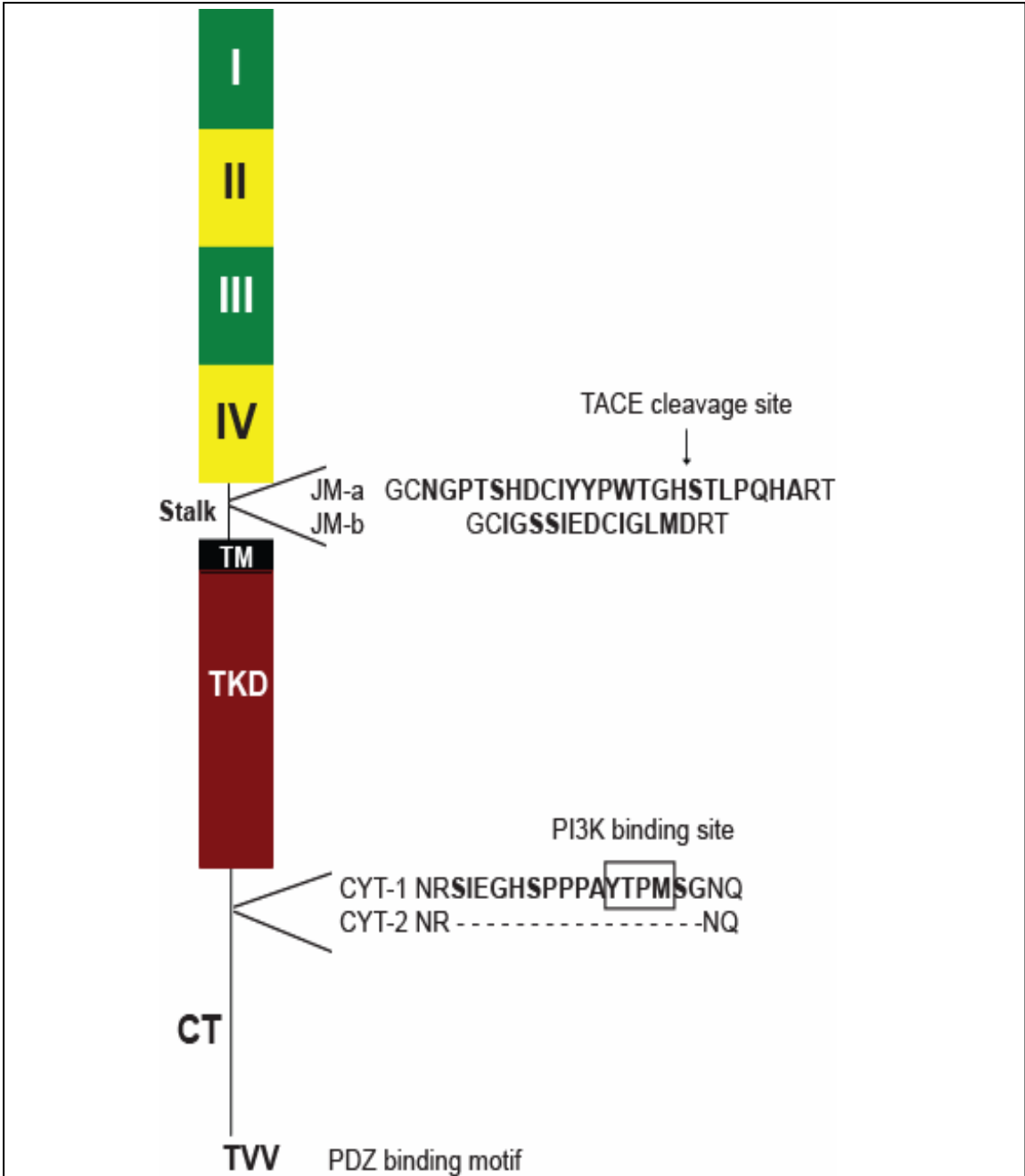
Figure I-1: Schematic of ErbB-4. Domains I-IV represent the ectodomain, with domains I and III (green) being the regions of ligand binding and domains II and IV (yellow) being the cysteine-rich regions involved in ectodomain dimerization. The stalk region connects the ectodomain to the transmembrane and is one site of alternative splicing as well as the location of TACE cleavage (JM-a isoform only). A second site of alternative splicing is in the carboxyterminal (CT) domain. At the extreme CT is a PDZ binding motif. TM (black): transmembrane domain; TKD (red): tyrosine kinase domain. JM-a and JM-b and CYT-1 and CYT-2 splice isoforms are described in the text.

and degraded in response to ubiquitination by the E3 ligase Cbl [16]. However, Cbl does not regulate ErbB-4 stability [17].

ErbB-4 has been reported to be ubiquitinated in a non-Cbl manner, and this event is linked with decreases in its expression. For example, overexpression of LRIG1 results in an increase in heregulin-dependent ubiquitination of ErbB-4 as well as a decrease in overall ErbB-4 levels [18]. Overexpression of the E3 ligases Nrdp1 [19] and Aip4/Itch [20] also cause a decrease in ErbB-4 in a ligand-independent manner, and Aip4/Itch was shown to promote ErbB-4 ubiquitination [20]. In comparison to ErbB-1, ErbB-4 displays impaired internalization following heregulin addition [21]. However, the unanswered critical question is how ligand addition mechanistically promotes ErbB-4 ubiquitination, and why ErbB-4 internalization occurs at a slower pace than ErbB-1, i.e., why is it advantageous to retain a cell-surface activated ErbB-4.

Proteolytic Processing by TACE and γ-Secretase

An unexpected finding occurred in experiments geared towards understanding the slow internalization of ErbB-4. Treatment with the phorbol ester, 12-tetradecanolyphorbol-13-acetate (TPA), an activator of protein kinase C (PKC), results in phosphorylation-dependent inactivation of ErbB-1 kinase activity [22]. However, in the case of ErbB-4, TPA promoted proteolysis of ErbB-4 in a PKC-dependent manner [10]. Two fragments were initially identified: a 120-kDa fragment arising from the ectodomain that is shed into the media, and an 80-kDa membrane-tethered intracellular domain fragment, termed m80 (Figure I-2) [10].

No physiological function has been assigned to the shed ectodomain fragment.

Ectodomain proteolysis is also ligand-mediated, as treatment with heregulin promotes generation of the membrane-tethered fragment [23]. The membrane tethered fragment is tyrosine phosphorylated and interacts with Shc, PLC-γ1, and ErbB-2 [10, 24]. The membrane-tethered m80 fragment is also ubiquitinated [25], hinting that proteolysis may be a mechanism for receptor

Figure I-2: Proteolytic processing of ErbB-4 by TACE and γ-secretase to yield the soluble E4ICD fragment.
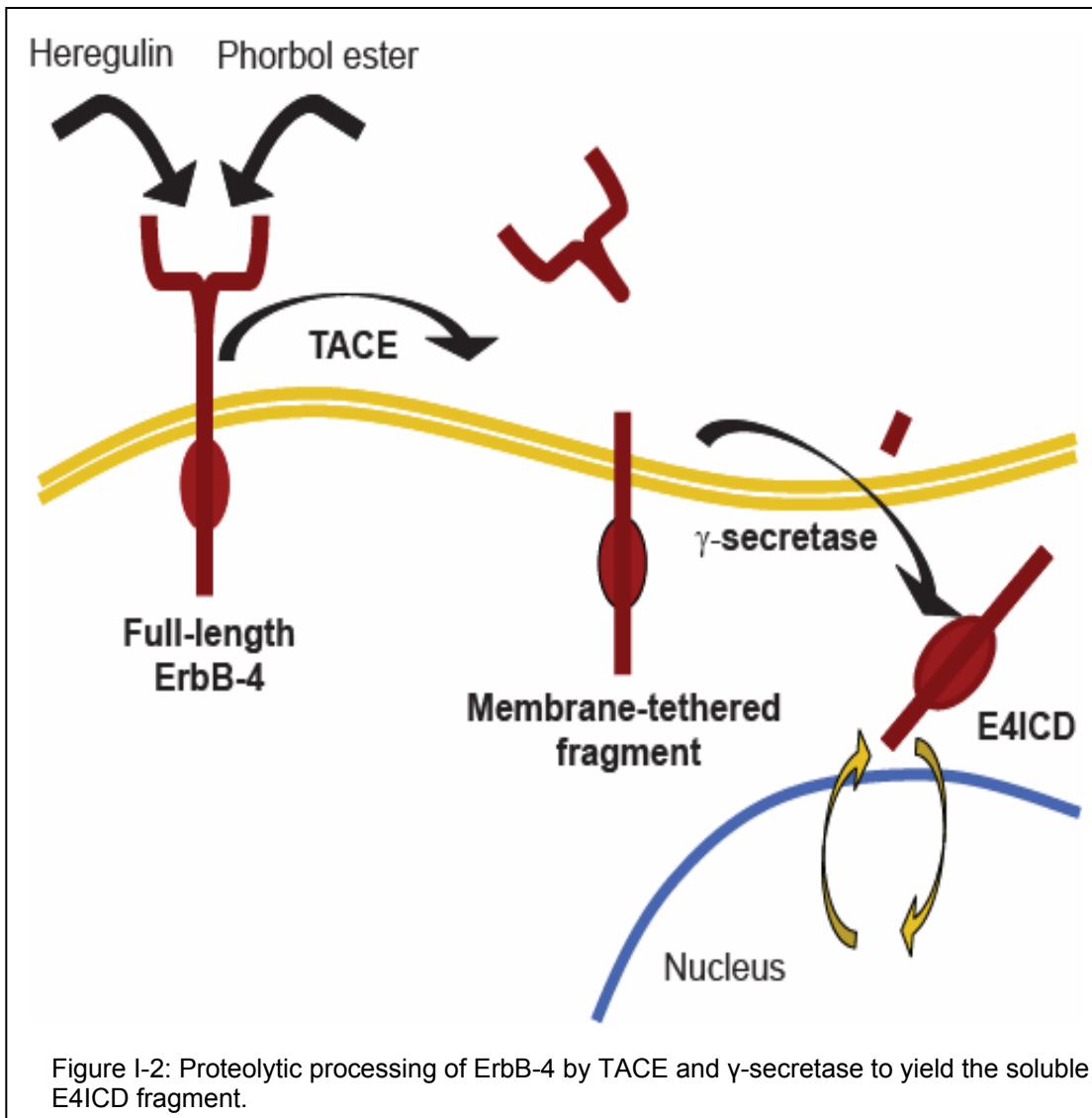
inactivation. The N-terminal cleavage site is located in the stalk region that connects the ectodomain to the transmembrane domain (Figure I-1) [24]. Early studies found that the ectodomain cleavage event is sensitive to metalloprotease inhibitors [25], and thereafter tumor necrosis factor-α converting enzyme (TACE) was identified as the sheddase that generates the membrane-tethered fragment [26]. TACE is a member of the ADAM (a disintegrin and metalloprotease) family of matrix metalloproteases and also cleaves a growing list of proteins, including the ErbB ligands [27], Notch [28] and CD44 [29]. While other members of the ADAM family, such as ADAM9, display sheddase activity towards other substrates, such as CD44 [29], no other members of the ADAM family have been shown to cleave ErbB-4 and ErbB-4 cleavage does not occur in TACE-null fibroblasts [26]. Interestingly, alternative splicing within the stalk region generates a metalloprotease cleavage-resistant isoform, termed JM-b, that has a shorter stalk region than the cleavable JM-a isoform [30]. No substrate-specific recognition sequence has been identified for TACE. Instead, the length of the stalk region may determine a protein's potential as a TACE substrate [31]. Of all the ErbB receptors, the stalk region of the JM-a ErbB-4 isoform is the longest, and TACE has not been shown to cleave any other ErbB receptors; however, the ectodomain of ErbB-2 is shed by a metalloprotease activity [32] or generated by alternate translation initiation [33].

Subsequent data defined a novel role for the m80 cleavage product distinct from that of the full-length receptor. Following TACE cleavage of the ectodomain, transmembrane cleavage of the m80 fragment generates a soluble

intracellular domain (ICD) fragment, termed s80 or ErbB-4ICD [34, 35]. Intramembrane proteolysis of ErbB-4 only occurs subsequent to ectodomain cleavage. The enzyme responsible for intramembrane cleavage is the aspartyl protease complex γ-secretase, which also cleaves two well-known and important plasma membrane proteins: amyloid precursor protein (APP) and Notch [36, 37]. Cleavage of APP by ectodomain sheddases and γ-secretase generates the Aβ fragment found in Alzheimer's disease [36]. The function of the Notch ICD is well-characterized as a transcriptional co-activator with important roles in development [38]. The γ-secretase complex is minimally composed of presenilin-1 or -2, nicastrin, Aph-1, and Pen-2 [39-41]. Presenilin-1 or -2 constitutes the catalytic enzyme portion of the complex [42], and nicastrin recognizes substrates by their lack of an ectodomain [43]. In addition to this function, nicastrin is involved in assembly and cell surface expression of the γ-secretase complex, as are Aph-1 and Pen-2 [44].

One lingering question is how this protease complex manages to cleave transmembrane proteins in the hydrophobic environment of the plasma membrane, because proteases generally require water for cleavage. While a structure of the intact γ-secretase complex has not been solved, the structure of another transmembrane protease rhomboid has been solved by several groups (reviewed in ref. [45]), and lends great insight into how these transmembrane proteases function. Two transmembrane domains act as a lateral gate to allow the substrate to enter the catalytic core of the protease, where hydrolysis of water can catalyze proteolysis. While rhomboid is a serine protease, the idea of

a gating mechanism for substrate access may be applicable to the γ-secretase complex as well.

A PDZ binding motif at the extreme carboxyterminal region of ErbB-4 (Figure I-1) is also required for intramembrane proteolysis by serving to recruit the presenilin-1 subunit of the γ-secretase complex [46]. Mutation of the PDZ motif on ErbB-4 prevents generation of the soluble ICD fragment from the membrane-tethered fragment [46].

The parameters that must be fulfilled for ErbB-4 proteolysis by TACE and γ-secretase are still under investigation. One study found that m80 interacts with ErbB-2 but not full-length ErbB-4 [24], suggesting that an ErbB-4:ErbB-2 dimer may be the substrate for ErbB-4 regulated proteolysis. In addition to ligand binding, tyrosine kinase activity is required for proteolysis, as pretreatment with a tyrosine kinase inhibitor prevents cleavage of ErbB-4 [24]. The tyrosine phosphatase inhibitor, pervanadate, also promotes cleavage of ErbB-4, although pervanadate- and heregulin-stimulated cleavage are PKC-independent [23, 47]. These two pieces of data indicate that kinase activity and/or tyrosine phosphorylation are required for ErbB-4 cleavage, but not understood is how ligand binding triggers ectodomain proteolysis of ErbB-4 in parallel with canonical receptor signaling. Specifically, if tyrosine phosphorylation occurs within five minutes of ligand addition [2], but cleavage occurs optimally at 30-60 minutes [23], what additional steps are required to active cleavage of ErbB-4? Two possibilities are re-localization of the protein or activation of downstream signaling pathways because the time course of cleavage is not likely to be

sufficient for regulation at the transcriptional level. Also, cycloheximide treatment did not prevent ectodomain [10] or transmembrane proteolysis of ErbB-4 (Ni and Carpenter, unpublished data).

Role of ErbB-4 Cleavage in Development and Disease

Generation of a soluble protein from a membraneous precursor increases the number of potential kinase substrates, since the ICD has been detected in the cytosol, nucleus, and mitochondria [34, 48]. Because γ-secretase-mediated ErbB-4 cleavage induces cell death of T47D breast cancer cells [34], many of the ICD-interacting proteins identified to date have some role in cell death, although a few studies have successfully linked E4ICD-associated target proteins to cell death. For example, E4ICD interacts with and tyrosine phosphorylates the E3 ligase Mdm2 [49]. This E4ICD:Mdm2 interaction results in the ubiquitination of Mdm2, which translates to an increase in expression of the pro-apototic protein p53 [49].

A second interacting partner is the Yes-associated protein (YAP), a transcriptional co-activator that interacts with nuclear E4ICD via a WW domain [50, 51]. Overexpression of WWOX, another WW-domain-containing protein with cytosolic localization, results in a loss of the E4ICD:YAP interaction and retention of E4ICD in the cytosol [52]. However, the precise transcriptional target of the E4ICD:YAP complex was not identified, nor was it determined whether E4ICD phosphorylates YAP or WWOX.

10

One link between E4ICD and cell death in mammary tissue has come from studies by Jones and colleagues. Surprisingly, this group found that E4ICD contains a BH3 domain that induces E4ICD localization to the mitochondria in breast cancer cells [48]. E4ICD expression was correlated with an increase in cytochrome C release from the mitochondria, a hallmark of cell death. Furthermore, E4ICD-dependent apoptosis was inhibited by overexpression of the anti-apoptotic protein Bcl-2, similar to other BH3-containing proteins BAX and BAK [48]. While it was initially believed that ErbB-4-mediated cell death required nuclear localization and transcriptional activation of pro-apoptotic genes (or suppression of anti-apoptotic genes), mitochondrial localization represents an alternate mechanism by which ErbB-4 proteolysis promotes cell death.

Consistent with the fact that ErbB receptors promote mitogenic signaling, heregulin treatment results in increased DNA synthesis compared to NIH 3T3 cells without ErbB-4 [21]. Also, HB-EGF promotes chemotaxis in NIH 3T3 cells stably expressing only ErbB-4 [8]. However, treatment with an ErbB-4 ligand also promotes differentiation of MDA-MD-453 breast cancer cells that express both ErbB-2 and ErbB-4 [2]. Loss of mammary gland differentiation and lactation are two phenotypes of an ErbB-4 conditional knockout animal [53], confirming the role of ErbB-4 in differentiation previously observed with a breast cancer cell line [1, 2]. Experimental data suggest a link between ErbB-4 cleavage and mammary gland differentiation. Linggi, *et al*, detected an interaction between E4ICD and Eto2, a transcriptional corepressor of genes that regulate differentiation. Expression of the E4ICD inhibits Eto2 transcriptional repression [54]. E4ICD also

serves as a chaperone to shuttle the transcriptional activator STAT5A into the nucleus, whereupon STAT5A activates transcription of β-casein, a gene involved in lactation [55, 56].

The ErbB-4 knockout mouse is embryonic lethal at E10.5 due to defects in the development of the heart and brain [57]. Not coincidentally, the knockout animals both for TACE [58] and heregulin [59] also exhibit defects in heart development. The fact that this phenotype is shared with ErbB-4 -/- mice may be due to ineffective TACE processing of the ligand rather than the receptor because, in the adult heart, only the non-cleavable (JM-b) isoform of ErbB-4 is expressed [30]. As described above, a conditional knockout mouse in which ErbB-4 is re-expressed in the heart displayed loss of mammary gland differentiation and lactation [53], and the role of E4ICD as a nuclear chaperone for STAT5A [55] may explain the importance of ErbB-4 proteolysis in the mammary gland development.

It was first thought that proteolytic liberation of the E4ICD was a means to promote cell death in breast cancer cells [34], such that the intact ErbB-4 signaled for cell growth while the cleavage fragment signaled for cell death. However, the story is undoubtedly more complicated and the true function of ErbB-4 and its cleavage fragment in normal and pathologic mammary tissues remains an unanswered question. Precise function seems to be defined by isoform, cell type, and subcellular localization. Nuclear ErbB-4 has been detected in medulloblastoma [60] and breast cancer [61], but these studies did not differentiate between the full-length receptor and the cleavage product.

A recent study demonstrated that E4ICD is a negative regulator of astrocyte differentiation [62] and this is the only study to date proving that ErbB-4 cleavage is biologically important. This role for E4ICD is mediated via interaction with the transcriptional co-repressor complex of TAB2 and NCoR. Inhibition of ErbB-4 intramembrane cleavage or expression of the non-cleavable JM-b isoform prevents nuclear localization of TAB2, a step that is required for ErbB-4-mediated co-repression activity, i.e., inhibits transcription of genes that promote differentiation of a precursor to an astrocyte [62]. This group went on to show that the cleavable JM-a isoform but not the non-cleavable JM-b isoform inhibits astrogenesis, thus defining a role for ErbB-4 in development [62]. This study defined a role for E4ICD in cell fate determination of neuronal precursors and implicated ErbB-4 proteolysis in potential brain pathologies, such as Alzheimer's disease [62].

Membrane Microdomains

Current Theories

For many years, the fluid-mosaic model , in which proteins diffuse freely in the plane of the phospholipid membrane, was the accepted model for plasma membrane organization [63]. When the distribution of cholesterol in the membrane was considered, the idea of liquid-ordered and liquid-disordered phases emerged [64]. In 1997, Simons and Ikonen coined the term "lipid rafts" to describe cholesterol and sphingolipid-enriched regions of the plasma membrane

that serve to concentrate signaling molecules [65]. Given the surface area of the plasma membrane, it stands to reason that some mechanism must be in place to increase the chance interactions between proteins to efficiently propagate a signal transduction cascade. The most significant roadblock for the lipid raft model has been an inability to directly visualize these structures in living cells.

In addition to the difficulty in imaging lipid rafts, there is also debate as to the size of lipid rafts, as well as whether lipid rafts are pre-formed structures that proteins migrate into or whether raft components cluster around pre-formed protein complexes. Also poorly understood is what signals/sequences/domains exist on proteins to target them to lipid rafts. Thus far, no raft-localization domain has been identified. Post-translational modifications, such as palmitoylation, may promote localization to lipid rafts, but not all raft-localized proteins are palmitoylated or modified otherwise (reviewed in ref. [66]).

Caveolae are a type of lipid-enriched membrane microdomain that were first identified over 50 years ago due to the presence of invaginations in the plasma membrane, or "little caves," detectable by electron microscopy. This property makes caveolae distinct from lipid rafts and thus not subject to as much controversy.

Techniques for Detection

No one technique is accepted for biochemical isolation of lipid rafts from cells. One common way to extract raft-associated proteins relies on the relative insolubility of rafts in detergents, such as Triton X-100 and Brij 98 at 4°C, a technique pioneered by Deborah Brown (Figure I-3, reviewed in ref. [67]).

14

However, some proteins, such as ErbB-1, can be extracted from a lipid-raft fraction to a non-raft fraction by Triton X-100 [68]. Thus the detergent-insoluble fraction does not completely represent the lipid raft proteins found in a living cell. Also, there is an issue of whether detergents induce the formation of rafts.

A second method developed by Smart and Anderson is a detergent-free method that takes into account the relative buoyant density of cholesterol-enriched regions of the plasma membrane [69]. By this technique, the raft-associated proteins "float" to the low-density region of a continuous OptiPrep density gradient and the non-raft associated proteins remain in the lower higher-density region of the gradient (Figure I-4). While this technique yields a relatively pure raft fraction, it also requires a large amount of starting material.

Several live-cell imaging techniques are also designed to assess raft properties, as well as protein localization to lipid rafts. One method to investigate lateral mobility of known raft-associated proteins is fluorescent recovery after photobleaching (FRAP), which can lend insight into the raft composition of cells by measuring the velocity of fluorescence recovery into the bleached region [70]. Methods to assess raft localization of proteins in living cells include Förster resonance energy transfer (FRET) [71] or co-patching [72] with known raft-associated proteins, such as GPI-anchored proteins. As an alternative system to imaging rafts in intact cells, unilamellar vesicles that include physiological concentrations of cholesterol and sphingolipids are also employed [73].

Concomitant with defining the parameters that constitute protein localization to a lipid raft are methods to disrupt lipid rafts in order to compare

protein localization in both experimental conditions. The typical method for raft perturbation is to deplete cholesterol from the membranes of cells with methyl-β-cyclodextrin. However, cholesterol depletion has also been shown have effects aside from lipid raft disruption [74]. Comparing protein localization to a lipid raft before and after cyclodextrin treatment is not ideal, but cholesterol depletion is the most widely used method for raft perturbation.

ErbB Family Localization to Membrane Microdomains

All ErbB family members have been detected in some type of cholesterol-enriched membrane microdomain. Anderson and colleagues, using a detergent-free technique, were the first to reported that ErbB-1 localizes to caveolae, and EGF treatment promotes movement out of caveolar membranes [69, 75]. This finding seems counterintuitive because most proteins are thought to move into lipid rafts as a means to concentrate signaling molecules and thereby facilitate activation of signal transduction cascades. It is possible that ligand-dependent ErbB-1 translocation out of rafts may represent a mechanism to prevent sustained activation of downstream pathways.

One study reported that raft-localized ErbB-1 is tyrosine phosphorylated [76], whereas another study concluded that ErbB-1 localization to lipid rafts prevents EGF binding [77], suggesting ligand-independent activation of raft-associated ErbB-1. Furthermore, cholesterol depletion promotes ligand-independent tyrosine phosphorylation of ErbB-1, as well as activation of the Ras/MAPK pathway [78, 79]. ErbB-1 interacts with the raft-associated proteins

caveolin-1 [80] and phospholipid scramblase 1 [81], but direct phosphorylation of these proteins by ErbB-1 has not been reported. The second cysteine-rich region of ErbB-1 is required for localization to caveolae [82], and this region is conserved in ErbB-4.   In summary, many studies detect ErbB-1 in a membrane microdomain, but the data are conflicting in terms of how this localization regulates ligand binding, activation, and downregulation.

Even less is known about ErbB-2 and ErbB-3 localization to membrane microdomains.   ErbB-2 has been detected in membrane microdomains of fibroblasts and two breast cancer cell lines by a variety of methodologies [75, 83, 84]. Most of the studies detected tyrosine phosphorylation of raft-localized ErbB-2, but do not connect localization to function at the post-receptor level (i.e., activation of downstream substrates). In one of the above studies, ErbB-2 and ErbB-3 were found to colocalize with the raft marker GM1 [83], but there are no other reports of ErbB-3 localization in or translocation in/out of membrane microdomains or the effect of ligand addition on this localization.

Only five reports of ErbB-4 localization to lipid rafts can be found in the literature.   The first study of heregulin-dependent trafficking of ErbB-4 into detergent-insoluble fraction was conducted in T47D breast cancer cells that lack caveolae and showed that ErbB-4 translocates to the Triton X-100-insoluble fraction within 10 min. of ligand addition [23]. A subsequent study showed that this translocation is also dependent on kinase activity, because pre-treatment with an ErbB tyrosine kinase inhibitor prevented heregulin-dependent ErbB-4 translocation [24]. A second group showed ligand-mediated ErbB-4 movement

17

into a detergent-resistant fraction of cortical neurons with the same time course, and cholesterol depletion prevented ErbB-4 translocation [85]. In contrast, ErbB-4 appears to be constitutively localized to lipid rafts in cardiomyocytes, and heregulin treatment actually promotes translocation out of the lipid raft [86]. A study of ErbB-4 localization to lipid rafts is presented in the following chapter and compares heregulin-dependent ErbB-4 translocation to detergent-insoluble fractions and lipid rafts by three different methodologies [87]. Thus, the role of ErbB-4 raft localization in function seems to differ by cell type, and the use of different methodologies makes comparison between studies difficult.

Regulation of RIP by Membrane Microdomains

While little information currently exists evaluating ErbB-4 translocation into or out of lipid rafts and whether this influences its proteolytic regulation, the importance of raft localization in APP processing has been investigated by several groups. A study by Ehehalt, *et al*., determined that depletion of cholesterol shifted APP processing from β-secretase-mediated cleavage in lipid rafts to α-secretase-mediated cleavage outside lipid rafts [88]. In the context of Alzheimer's disease, β-secretase cleavage followed by γ-secretase cleavage produces the Aβ peptide found in senile plaques [89]. These data suggest that lipid rafts on normal cells serve to segregate proteases from their substrates, and diseases, such as Alzheimer's, may be associated with the mislocalization of substrates into lipid rafts. Cleavage of prion protein has also been reported to occur in lipid rafts, as disruption of rafts abrogrates its cleavage [90].

In addition to determining localization of substrates to lipid rafts, a great deal of work has analyzed the localization of proteolytic enzymes to lipid rafts. For example, β-secretase localizes to lipid rafts that do not contain caveolin [91], and the activity of this protease is influenced by the type of lipids in its local environment, with cholesterol and glycosphingolipids serving to increase activity [92]. Only a portion of total β-secretase is raft-associated [92, 93], and addition of a GPI-anchor to force localization of β-secretase to lipid rafts results in significantly increased cleavage of APP [93]. Components of the γ-secretase complex (presenilin-1, nicastrin, APH-1, and PEN-2 have also been found in lipid raft fractions from neurons [94], indicating that total APP cleavage, and cleavage of other γ-secretase substrates occurs in lipid rafts.

CHAPTER II

ERBB-4 AND TNF-α CONVERTING ENZYME
LOCALIZATION TO MEMBRANE MICRODOMAINS

Based on data that ErbB-4 translocates to the detergent-insoluble fraction in a heregulin-dependent manner [23], and the literature documenting localization of proteolytic machinery to lipid rafts for cleavage of APP [89], I hypothesized that ErbB-4 movement into lipid rafts is required for its proteolytic processing. However, reports from other groups indicated that ErbB-1 localization is highly influenced by detergents such as Triton X-100 [68], so the experimental approaches for this project were Triton X-100 insolubility, Brij 98 insolubility, and a detergent-free methodology. This study employs two cell lines, T47D breast cancer cells, which express endogenous ErbB-4, and COS-7 cells stably expressing two isoforms of ErbB-4, JM-a (cleavable) CYT-2 or JM-b (non-cleavable) CYT-2.

Methods

Cell Culture and Transfection

T47D and COS-7 cells were maintained in Dulbecco's Modified Eagle's Medium (DMEM) supplemented with 10% fetal bovine serum (FBS) at 37°C with 5% CO_2. For generation of JM-a CYT-2 and JM-b CYT-2 ErbB-4 stable cell

lines, COS-7 cells were transfected with 2 µg DNA using Lipofectamine 2000 (Invitrogen) per manufacturer's instructions. Next, cells were selected with 500 µg/ml G418 for 10 days, and then maintained in 200 µg/ml G418. Wild-type and S674A ErbB-4 (JM-a CYT-2) stable cell lines were similarly generated.

Separation of Detergent-Soluble and –Insoluble Fractions

For all treatments, cells were starved overnight in serum-free DMEM before treatment. Cells were fractionated as previously described (Figure I-3) [23]. In brief, cells were lysed with cold TGH (1% Triton X-100, 10% glycerol, 50 mM Hepes, pH 7.2, 100 mM NaCl, 10 mM 1,10-phenanthroline, 5 mM NaF, 1

Figure I-3: Separation of detergent-soluble and -insoluble fractions using Triton X-100 or Brij 98.
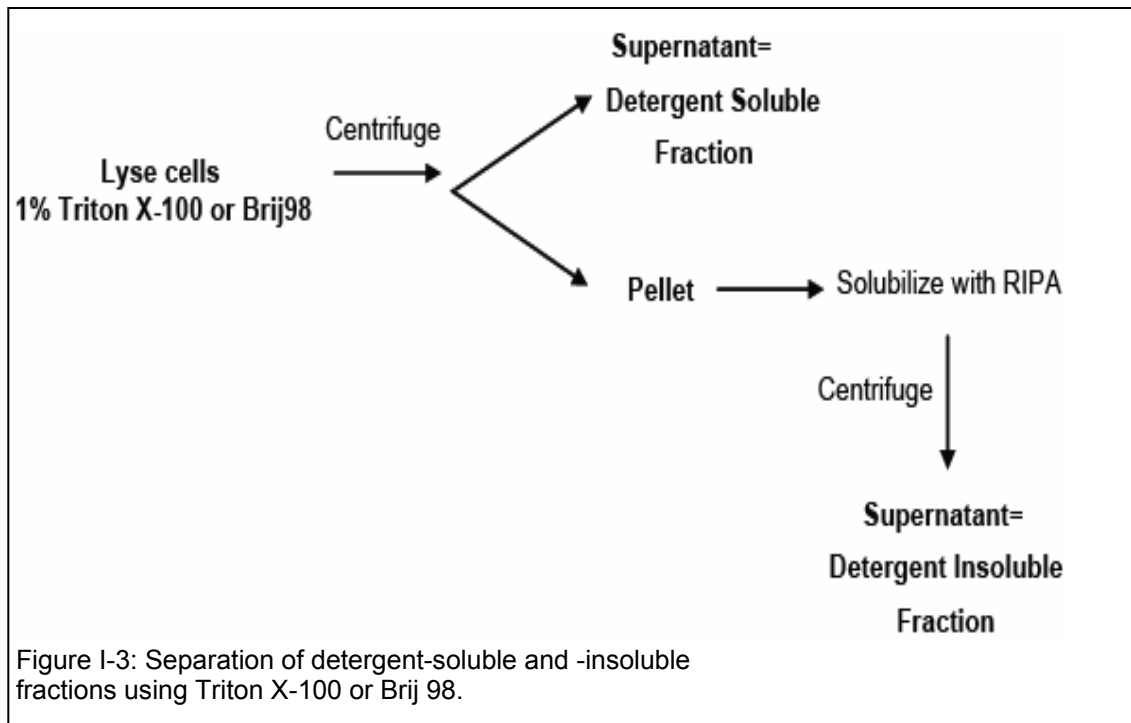
mM Na$_3$VO$_4$, and Roche Complete-Mini protease inhibitor cocktail tablet) or BGH (TGH substituted with 1% Brij 98 in place of Triton). Lysates were centrifuged at 14, 000 x g for 10 min. at 4°C, and the resulting supernatant is the detergent-soluble fraction. The pellet was next washed with TGH and solubilized with RIPA buffer (1% deoxycholate, 1% Triton X-100, 0.1% SDS, 150 mM NaCl, 1 mM EDTA, 50 mM Tris-HCl, pH 7.4, and protease inhibitors). The resulting supernatant is the detergent-insoluble fraction. Equal volumes of each lysate were either subjected to SDS-PAGE followed by immunoblotting with TACE (epitope: 802-823, Calbiochem) or flotillin-1 (BD Transduction Laboratories) antibodies, or immunoprecipitated with ErbB-4 (C-18, Santa Cruz Biotechnology) and immunoblotted with ErbB-4 prepared as described elsewhere [21].

Detergent-Free Lipid Raft Isolation

Lipid rafts were isolated from five 150 mm dishes of confluent cells per treatment according to the method of Smart, *et al.* [69]. This technique, diagrammed in Figure I-4, involves separation of the plasma membrane fraction on a 30% Percoll gradient and flotation of the plasma membrane fraction on two density gradients: a continuous 20-10% OptiPrep gradient followed by a discontinuous 25%-15%-5% OptiPrep gradient. Lipid rafts are contained at the 5%-15% OptiPrep interface of the discontinuous gradient, in fraction 1. Equal volumes of each lipid raft fraction were subjected to immunoblot analysis with ErbB-4, TACE, or flotillin-1 antibodies.

Figure I-4: Detergent-free lipid raft isolation, based on the technique developed by Smart, *et al.* PM: plasma membrane
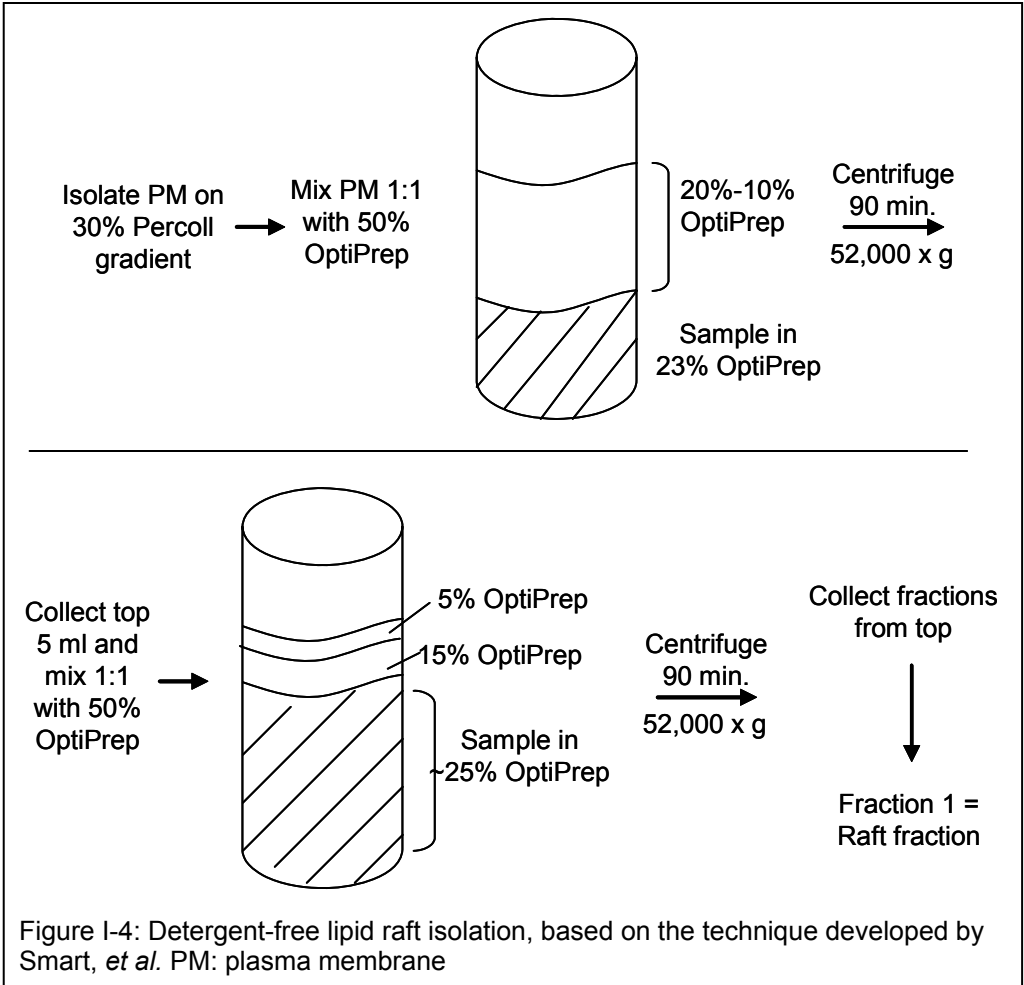
Results

Heregulin-Induced ErbB-4 Translocation to a Triton X-100-Insoluble Fraction

As previously reported [23], treatment of T47D cells with heregulin, but not the PKC activator TPA, promoted ErbB-4 translocation to a Triton-insoluble fraction (Figure I-5A). To test the generality of this finding, two ErbB-4 isoforms, JM-a CYT-2 or JM-b CYT-2, were stably expressed in COS-7 cells. These isoforms were included because the JM-b species is reported to be resistant to ectodomain cleavage due to sequence changes around the cleavage site [30]. As shown in Figure I-5B, heregulin treatment did not promote translocation to the Triton-insoluble fraction for either isoform compared to that obtained with T47D cells. Thus, these data demonstrate that the ErbB-4 translocation to a Triton-insoluble fraction is not a general phenomenon or that stable expression of ErbB-4 leads to a result that is not generalizable. While the composition of the Triton-insoluble fraction is not known in detail, a lipid raft marker, flotillin-1, is present in this fraction in both cell types. The mature form of TACE was detected in the Triton-insoluble fraction as a 100-kDa band in T47D cells (Figure I-5A), but not in the Triton-insoluble fractions derived from COS-7 cells (Figure I-5B). This difference reflects endogenous proteins, not transfected proteins. The enzyme furin processes immature 120-kDa TACE in the Golgi apparatus to a 100-kDa activated form [95].

Figure I-5: Heregulin-induced ErbB-4 translocation to a Triton X-100-insoluble fraction. T47D **(Panel A)** or COS-7 **(Panel B)** cells stably expressing JM-a or JM-b ErbB-4 were starved overnight, then treated with heregulin (20 ng/ml) or the phorbol ester TPA (100 ng/ml) for 15 min. Cells were separated into Triton X-100-soluble and –insoluble fractions as described in the Methods section. Equal volumes of soluble and insoluble fractions were either precipitated with anti-ErbB-4 (upper panels) or directly subjected to SDS-PAGE and blotted with antibodies directed against ErbB-4, TACE or flotillin-1. ErbB-4 bands in the Triton-insoluble fraction were subjected to densitometric analysis, normalized for flotillin-1 levels, and quantitated relative to untreated samples. Asterisks indicate immature (upper arrow, 120 kDa) and mature (lower arrow, 100 kDa) forms of TACE (center panels).

Effect of Cholesterol Depletion on ErbB-4 Localization

Since membrane microdomains are by definition enriched with cholesterol, one frequently used method to disrupt these microdomains is treatment with methyl-β-cyclodextrin (MβCD), which depletes cholesterol from membranes [96]. T47D cells treated with MβCD displayed a loss of basal ErbB-4 in the Triton-insoluble fraction (Figure I-6), but not when treated with α-cyclodextrin, which does not deplete cholesterol. Interestingly, MβCD pretreatment did not significantly affect heregulin-stimulated ErbB-4 translocation to this fraction

Figure I-6: Cholesterol depletion does not inhibit heregulin-dependent translocation of ErbB-4 to a Triton-insoluble fraction. T47D cells were pretreated treated with either methyl-β-cyclodextrin (MβCD, 5 mM) or α-cyclodextrin (α-CD, 5 mM) for 30 min. followed by heregulin (20 ng/ml) for an additional 15 min. and separated into Triton X-100-soluble and insoluble fractions. The Triton-insoluble fractions were precipitated with anti-ErbB-4 and blotted for ErbB-4 (upper panel). Lysates were blotted for flotillin-1 expression (lower panel).

(Figure I-6). Therefore, ErbB-4 migration to the Triton-insoluble fraction of T47D cells does not represent association with a cholesterol-dependent microdomain.

Constitutive ErbB-4 and TACE Localization to a Brij 98-Insoluble Fraction

A recent report compared ErbB-1 localization to lipid rafts using an array of detergents, including Triton X-100 and two detergent-free methods [68]. The data show that, in the absence of ligand stimulation, ErbB-1 segregates to a lipid raft fraction as determined by detergent-free methods or the use of Brij 98, but remains in a non-raft fraction when Triton X-100 is included. Hence, the experiments in Figure I-5 were repeated with Brij 98. Brij 98 and Triton X-100 are both non-ionic detergents. When either T47D (Figure I-7A) or COS-7 cells expressing JM-a or JM-b ErbB-4 (Figure I-7B) were separated into Brij 98-soluble and -insoluble fractions, the resulting analysis revealed that, in both the absence or presence of heregulin stimulation, ErbB-4 was primarily associated with the Brij 98-insoluble fraction. Only a small proportion of total receptor localized to the Brij-98 soluble fraction. This is in marked contrast to the results obtained with

Figure I-7: Constitutive ErbB-4 and TACE localization to a Brij 98-insoluble fraction. T47D **(Panel A)** or COS-7 **(Panel B)** cells stably expressing JM-a or JM-b ErbB-4 were treated and lysed as described in Figure I-5 with the following modification: 1% Brij 98 was used instead of 1% Triton X-100. Equal volumes of lysates were either immunoprecipitated with ErbB-4 (Panel A, top) or directly subjected to SDS-PAGE and blotted with anti-ErbB-4, anti-TACE or anti-flotillin-1 as in Figure I-5. Asterisks denote the mature (100 kDa) and immature (120 kDa) forms of TACE (center panels).

Triton X-100. Flotillin-1 was enriched in the Brij 98-insoluble fractions of T47D and COS-7 cells and equivalent amounts of mature TACE were found in the Brij 98-soluble and Brij 98–insoluble fractions of both cell types (Figure I-7).

Distribution of ErbB-4 Isoforms in Lipid Rafts Using a Detergent-Free Technique

Data from Figures I-5A and I-7A indicate that TACE localizes to both Triton- and Brij 98-insoluble fractions of T47D cells. In these same cells, however, ErbB-4 localization to membrane microdomains is highly dependent on the detergent used for solubilization. To rule out detergent-dependent effects, a detergent-free methodology developed by Smart, *et al.* [69] was employed. Consistent with the Brij 98 data, ErbB-4 was present in equal amounts in the raft fraction of control and heregulin-treated T47D cells (Figure I-8A). The mature

form of TACE was constitutively present in this fraction (Figure I-8A), also in agreement with the data in Figures I-5A and I-7A.
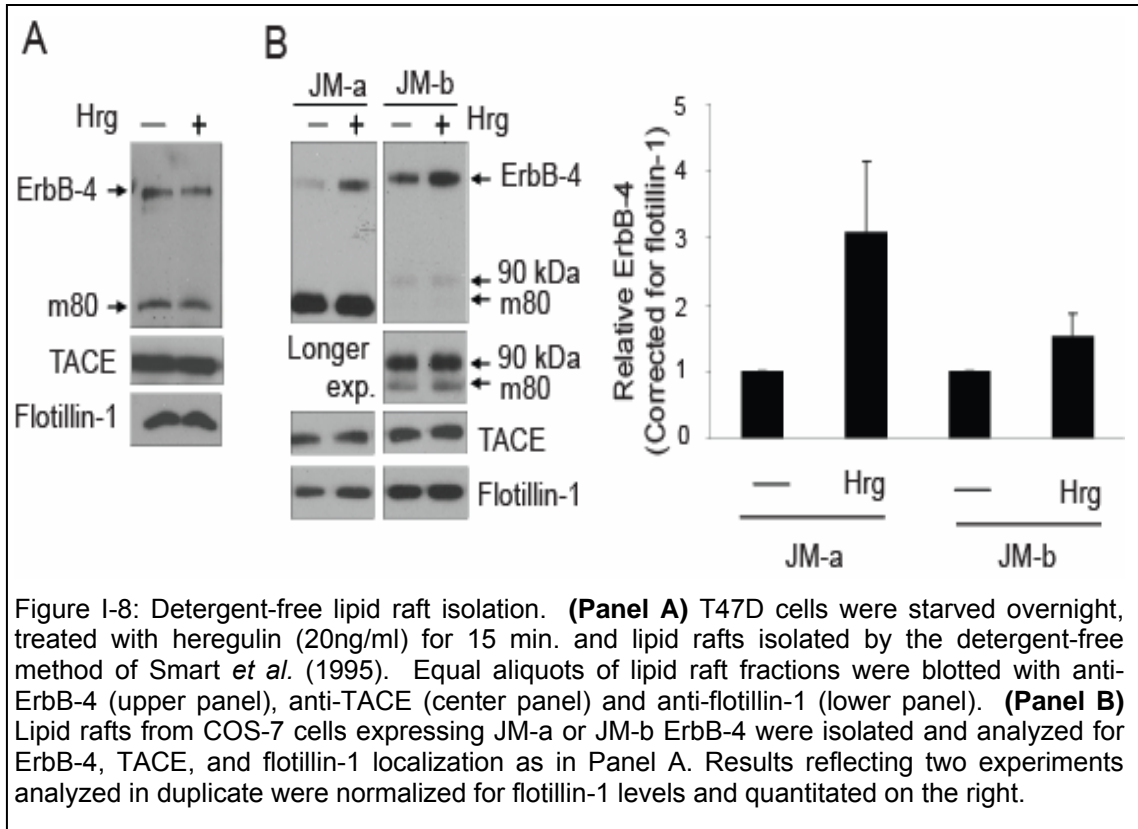
Figure I-8: Detergent-free lipid raft isolation. **(Panel A)** T47D cells were starved overnight, treated with heregulin (20ng/ml) for 15 min. and lipid rafts isolated by the detergent-free method of Smart *et al.* (1995). Equal aliquots of lipid raft fractions were blotted with anti-ErbB-4 (upper panel), anti-TACE (center panel) and anti-flotillin-1 (lower panel). **(Panel B)** Lipid rafts from COS-7 cells expressing JM-a or JM-b ErbB-4 were isolated and analyzed for ErbB-4, TACE, and flotillin-1 localization as in Panel A. Results reflecting two experiments analyzed in duplicate were normalized for flotillin-1 levels and quantitated on the right.

Detergent-free lipid rafts were also isolated from COS-7 cells containing JM-a or JM-b ErbB-4 isoforms. The JM-a isoform migrated into the raft fraction after heregulin treatment (Figure I-8B). In contrast, the JM-b isoform was constitutively present in the raft fraction and only slightly increased following heregulin addition (Figure I-8B). Also detected were the m80 fragment in the JM-a ErbB-4 raft fractions (in both T47D and COS7 cells) and 80- and 90-kDa fragments in JM-b ErbB-4 raft fractions (Figure I-8B, right panel). The m80 fragment represents the TACE cleavage product that is a substrate for γ-

secretase-mediated intramembrane proteolysis [10, 34]. The m80 fragment was not detected in the Triton-insoluble fraction derived from T47D cells [23]. The identity of the 90-kDa fragment is not known, but others have detected a similar fragment recognized by an ErbB-4 extreme carboxyterminal antibody [97]. Mature TACE was also present constitutively in the raft fraction of all cells analyzed (Figure I-8).

The intracellular juxtamembrane region of ErbB-1 contains a well-documented PKC phosphorylation site [22], and a bioinformatic screen indicated that ErbB-4 likely contains a PKC phosphorylation site (Ser 679) in this region [98]. Mutations of this putative PKC phosphorylation site did not prevent TPA or heregulin-stimulated cleavage (data not shown), but this does not rule out other regulatory PKC phosphorylation sites. Based on data that PKC phosphorylation of hematopoietic protein tyrosine phosphatase promotes localization to lipid rafts [99], the localization of wild-type and Ser679A ErbB-4 to lipid rafts was also compared. However, both isoforms were constitutively localized to lipid rafts in the absence of heregulin addition (Figure I-9), and the effect of heregulin stimulation on localization was not tested.
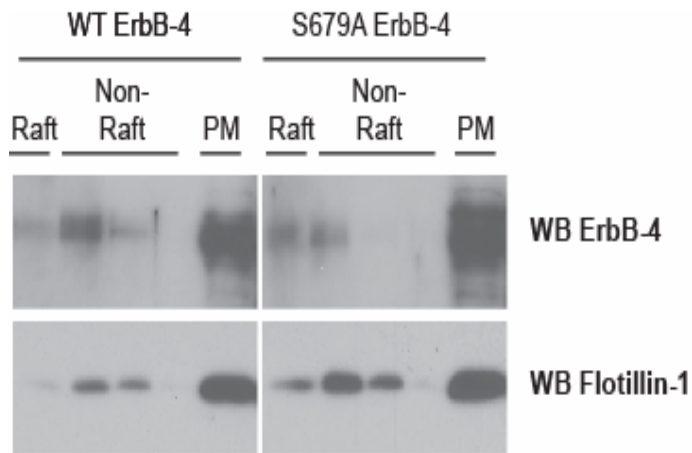
Figure I-9: Comparison of wild-type and S679A ErbB-4 localization in the lipid raft fraction. Cells stably expressing either wild-type or S679A ErbB-4 (JM-a CYT-2) were subjected to detergent-free lipid raft isolation as in Figure I-8. Raft (fraction 1), non-raft (fractions 2-4), and plasma membrane (PM) fractions were immunoblotted with either ErbB-4 (top panel) or flotillin-1 (bottom panel).

CHAPTER III

CONCLUSIONS

Using three separate techniques, membrane microdomains were isolated from T47D cells that express endogenous ErbB-4 and COS-7 cells that stably express two ErbB-4 isoforms, JM-a CYT-2 and JM-b CYT-2. T47D cells were chosen because a previous report demonstrated heregulin-stimulated cleavage and translocation of ErbB-4 to a Triton X-100-insoluble fraction in these cells [23]. The ErbB-4 JM isoforms were also use for analysis in order to assess the role of ErbB-4 membrane microdomain localization in cleavage as the JM-b isoform is thought to be resistant to TACE cleavage [30]. For consistency, CYT-2 isoforms were used in conjunction with both JM isoforms. Heregulin promoted movement of endogenous ErbB-4 to a Triton-insoluble fraction in T47D cells, but not ErbB-4 expressed exogenously in COS-7 cells. Depletion of cholesterol from T47D cells did not significantly affect heregulin-induced ErbB-4 translocation to the Triton-insoluble fraction, indicating that ErbB-4 movement into the Triton-insoluble fraction is not cholesterol dependent. Rather, this may reflect translocation induced by protein:protein interactions instead of protein:lipid interactions within a lipid raft [100]. ErbB-4 was present at high levels in the Brij 98-insoluble fractions of all cells tested regardless of heregulin treatment (Figure I-7). The effect of cholesterol depletion on protein association with the Brij 98-insoluble fraction was not assessed.

The data in Figure I-8 suggest that the cleavable and non-cleavable isoforms differentially associate with membrane microdomains. Strikingly, only the JM-a isoform of ErbB-4 expressed in COS-7 cells displayed marked heregulin-stimulated translocation to lipid rafts isolated by a detergent-free method. No significant difference was detected in heregulin-stimulated JM-b ErbB-4 migration into or out of membrane microdomains in COS-7 cells expressing this isoform. Furthermore, no differences were detected in association of these isoforms with the detergent-insoluble fractions (Figure I-5 and I-7). Because T47D cells express both the JM-a and JM-b isoforms (K. Elenius, University of Turku, personal communication), a valuable experiment would be to selectively knockdown the JM-b isoform and compare ErbB-4 localization in that experimental scenario. No group has co-expressed ErbB-4 isoforms in an ErbB-4-free background, so this experiment would determine whether one JM isoform influences the localization of another. Alternately, both isoforms could be exogenously expressed in COS-7 or another recipient cell line.

An interesting finding of Figure I-8 is that an 80-kDa cleavage product was detected at high levels in the lipid raft fraction derived from T47D cells and COS-7 cells expressing JM-a ErbB-4. This fragment likely represents the membrane-anchored m80 fragment, but could also be the soluble s80 (E4ICD) fragment associating with the membrane. Was this fragment produced in the lipid raft, or did it migrate into the lipid raft post-cleavage? A study by Vetrivel, *et al.*, concluded that the membrane-anchored C-terminal fragment of APP migrates into detergent-insoluble membranes, where it is cleaved by the γ-secretase

complex [101]. It is possible that a similar phenomenon occurs for transmembrane proteolysis of ErbB-4, and the time course in this study did not allow for appreciable γ-secretase cleavage.

Also detected in the detergent-free lipid raft fraction of COS-7 cells expressing JM-b CYT-2 were 80-kDa and 90-kDa species that did not increase with heregulin treatment (Figure I-8). Metalloprotease inhibitors were maintained throughout all steps of isolation, so it is unlikely that these cleavage fragments are an artifact generated post-lysis by TACE. Of course, this does not rule out cleavage by other proteases. Määttä, *et al.*, also detected a 90-kDa band in MCF-7 cells transfected with JM-b CYT-2 ErbB-4 and theorized that represents an N-terminal truncation fragment [97], but this fragment has not been characterized.

ErbB-4 expression and heregulin treatment did not alter TACE localization to membrane microdomains of either cell line. Importantly, the mature form of TACE was the predominant form in all detergent-insoluble or lipid-enriched microdomains tested. This finding suggests the potential for TACE activity in a membrane microdomain. While several pieces of data point to the importance of lipid rafts for γ-secretase cleavage of substrates [89], this is the first report to localize the mature form of TACE, an α-secretase, to a membrane microdomain.

I first proposed studying the role of ErbB-4 membrane microdomain localization as a potential regulatory step in ectodomain and transmembrane domain cleavage of the receptor. While these data confirm that ErbB-4 is localized to a membrane microdomain, they provide no direct evidence that

ErbB-4 translocation to the Triton-insoluble fraction regulates cleavage. It seems likely that the data obtained using the detergent-free methodology in Figure I-8 is the most accurate indicator of ErbB-4 localization in the intact membrane because detergent insolubility may not necessarily translate to raft association in a living cell. ErbB-4 localization to membrane microdomains is highly influenced by cell type as evidenced by the difference observed between T47D and COS7 cells plus previously reported data in neurons [85] and cardiomyocytes [86]. Regulatory factors that influence membrane localization, such as phospholipid scramblase-1 for ErbB-1 [81], may be differentially expressed in each of these tissues, which would account for the discrepancies in ErbB-4 translocation amongst studies. Alternatively, the techniques used to detect ErbB-4 translocation in these cell types may not be comparable. No group has incorporated fluorescent-based approaches to assess heregulin-dependent ErbB-4 localization to membrane microdomains.

Comparison of breast (T47D, SkBr3) and ovarian (OVCAR3, OVCAR429) cancer cell lines that express ErbB-4 revealed that only a subset undergo heregulin-induced cleavage, while all display tyrosine phosphorylation in response to heregulin binding [23]. All of these cell lines displayed TPA-induced cleavage, so the JM-a form is present [23]. I theorized that ErbB-4 localization to rafts may be different in cell lines that cleave ErbB-4 in response to heregulin and those that do not. However, I did not detect heregulin-stimulated translocation of ErbB-4 into or out of lipid rafts derived from T47D, SkBr3, OVCAR3, and OVCAR429 cells using the detergent-free methodology (data not shown).

The CYT-2 isoform was chosen as the cytoplasmic isoform for all raft-localization experiments. Both the JM-a CYT-1 and JM-a CYT-2 isoforms are similarly cleaved in response to TPA [97], but heregulin-stimulated cleavage has not been investigated. Elenius and colleagues recently reported that the CYT-2 isoform localizes to the nucleus better than the CYT-1 isoform [102]. It may have been valuable to compare localization of both CYT isoforms, not just the CYT-2 lacking the PI3K binding site. It is possible that signal transduction pathways initiated by PI3K binding to the CYT-1 isoform play a role in membrane microdomain localization. It should be noted that T47D cells, which undergo heregulin-stimulated translocation to the Triton X-100-insoluble fraction [23], contain both CYT isoforms (K. Elenius, personal communication). Because an antibody to distinguish the different isoforms is not available, the relative expression on the cell surface of each isoform cannot be estimated. The JM-a CYT-2 isoform did migrate into the detergent-free lipid raft in response to heregulin (Figure I-8B). If each isoform is expressed equally in T47D cells, then perhaps migration of one particular isoform into the raft fraction is not detectable in the context of this experimental approach.

Many of the same questions that were originally proposed at the beginning of this study remain. One of those questions is where in the cell cleavage of ErbB-4 occurs. While the shed ErbB-4 ectodomain has been detected in the media of cells [10], inhibition of heregulin-stimulated endocytosis prevents ligand-dependent generation of the 80-kDa intracellular cleavage product [23]. Therefore, it remains to be determined if ErbB-4 is cleaved while residing on the

cell surface or in an internalized vesicle with subsequent exocytosis of the 120-kDa ectodomain fragment. There is a precedent in the literature for cleavage of APP [103] and the neurotrophin receptor p75 [104] in a vesicle, and inhibition of internalization prevents Notch ectodomain cleavage [105]. Cleavage of APP and p75 has been shown to be regulated by localization to a lipid raft/detergent-insoluble fraction [88, 106]. There are no reports of localization of these receptors to lipid rafts in an internalized compartment, but components of the γ-secretase complex have been found to reside in rafts derived from endosomes [94]. Because the detergent-free method separates the plasma membrane fraction from other intracellular membranes, it is possible that heregulin-activated ErbB-4 localizes to a raft in an internalized compartment, where it is cleaved by TACE and γ-secretase.

While TPA is routinely used to induce cleavage of many substrates, including ErbB-4, it is not known how this occurs mechanistically. Inhibition of PKC combined with TPA treatment protects ErbB-4 from TPA-induced cleavage [10]. Therefore, the mechanism of TPA action is thought to be through activation of PKC, but a link between PKC activation and ErbB-4 cleavage has not been reported. Although heregulin-stimulated cleavage requires kinase activation, TPA stimulated cleavage does not [24]. ErbB-4 interacts with PLC-γ-1 [10], which, through generation of the second messenger diacylglycerol, serves to activate PKC. TPA treatment may circumvent this normal ligand-mediated and kinase-dependent process. The potency of TPA as a PKC agonist may explain,

in part, the increased proportion of ErbB-4 receptors cleaved by TPA treatment compared to heregulin treatment [23].

Alternatively, PKC may phosphorylate the sheddase or an adaptor protein that links ErbB-4 to its sheddase. ERK-mediated phosphorylation of TACE at Thr 735 is required for cell surface expression [107]. Seemingly contradictory, however, is the finding that deletion of the entire intracellular domain of TACE does not prevent proteolysis of TNF-α induced by TPA [108]. If phosphorylation is required for trafficking of TACE to the cell surface, then how is a mutant that lacks an intracellular domain able to be signaled to cleave its cell-surface substrate? In addition to promoting shedding of many TACE substrates, treatment with TPA also induces internalization and downregulation of TACE [109].

The story of ErbB-4 proteolysis is far from complete. Most of the focus in the field has been targets of the ICD fragment, both in the cytosol and the nucleus, that regulate cell growth and differentiation. The finding that ErbB-4 cleavage regulates neuronal cell fate determination [62] has finally assigned to ErbB-4 cleavage a biological relevance. As future studies reveal new functions of ErbB-4 proteolysis in development and disease, it will be especially important to understand the precise mechanisms that initiate the rate-limiting steps of ErbB-4 cleavage. Manipulating these steps may eventually provide a novel therapeutic approach for ErbB-4-associated diseases.

REFERENCES

1.   Plowman, G.D., J.M. Green, J.M. Culouscou, G.W. Carlton, V.M. Rothwell, and S. Buckley. (1993). Heregulin induces tyrosine phosphorylation of HER4/p180erbB4. *Nature* **366**: 473-5.

2.   Plowman, G.D., J.M. Culouscou, G.S. Whitney, J.M. Green, G.W. Carlton, L. Foy, et al. (1993). Ligand-specific activation of HER4/p180erbB4, a fourth member of the epidermal growth factor receptor family. *Proc Natl Acad Sci U S A* **90**: 1746-50.

3.   Chang, H., D.J. Riese, 2nd, W. Gilbert, D.F. Stern, and U.J. McMahan. (1997). Ligands for ErbB-family receptors encoded by a neuregulin-like gene. *Nature* **387**: 509-12.

4.   Hobbs, S.S., E.M. Cameron, R.P. Hammer, A.T. Le, R.M. Gallo, E.N. Blommel, et al. (2004). Five carboxyl-terminal residues of neuregulin2 are critical for stimulation of signaling by the ErbB4 receptor tyrosine kinase. *Oncogene* **23**: 883-93.

5.   Hobbs, S.S., S.L. Coffing, A.T. Le, E.M. Cameron, E.E. Williams, M. Andrew, et al. (2002). Neuregulin isoforms exhibit distinct patterns of ErbB family receptor activation. *Oncogene* **21**: 8442-52.

6.   Riese, D.J., 2nd, Y. Bermingham, T.M. van Raaij, S. Buckley, G.D. Plowman, and D.F. Stern. (1996). Betacellulin activates the epidermal growth factor receptor and erbB-4, and induces cellular response patterns distinct from those stimulated by epidermal growth factor or neuregulin-beta. *Oncogene* **12**: 345-53.

7.   Komurasaki, T., H. Toyoda, D. Uchida, and S. Morimoto. (1997). Epiregulin binds to epidermal growth factor receptor and ErbB-4 and induces tyrosine phosphorylation of epidermal growth factor receptor, ErbB-2, ErbB-3 and ErbB-4. *Oncogene* **15**: 2841-8.

8.   Elenius, K., S. Paul, G. Allison, J. Sun, and M. Klagsbrun. (1997). Activation of HER4 by heparin-binding EGF-like growth factor stimulates chemotaxis but not proliferation. *Embo J* **16**: 1268-78.

9.   Bouyain, S., P.A. Longo, S. Li, K.M. Ferguson, and D.J. Leahy. (2005). The extracellular region of ErbB4 adopts a tethered conformation in the absence of ligand. *Proc Natl Acad Sci U S A* **102**: 15024-15029.

10.   Vecchi, M., J. Baulida, and G. Carpenter. (1996). Selective cleavage of the heregulin receptor ErbB-4 by protein kinase C activation. *J Biol Chem* **271**: 18989-95.

11.   Fiddes, R.J., P.W. Janes, G.M. Sanderson, S.P. Sivertsen, R.L. Sutherland, and R.J. Daly. (1995). Heregulin (HRG)-induced mitogenic signaling and cytotoxic activity of a HRG/PE40 ligand toxin in human breast cancer cells. *Cell Growth Differ* **6**: 1567-77.

12.   Cohen, B.D., J.M. Green, L. Foy, and H.P. Fell. (1996). HER4-mediated biological and biochemical properties in NIH 3T3 cells. Evidence for HER1-HER4 heterodimers. *J Biol Chem* **271**: 4813-8.

13.   Yarden, Y. and M.X. Sliwkowski. (2001). Untangling the ErbB signalling network. *Nat Rev Mol Cell Biol* **2**: 127-37.

14.   Kainulainen, V., M. Sundvall, J.A. Maatta, E. Santiestevan, M. Klagsbrun, and K. Elenius. (2000). A natural ErbB4 isoform that does not activate phosphoinositide 3-kinase mediates proliferation but not survival or chemotaxis. *J Biol Chem* **275**: 8641-9.

15.   Sawyer, C., I. Hiles, M. Page, M. Crompton, and C. Dean. (1998). Two erbB-4 transcripts are expressed in normal breast and in most breast cancers. *Oncogene* **17**: 919-24.

16.   Levkowitz, G., H. Waterman, E. Zamir, Z. Kam, S. Oved, W.Y. Langdon, et al. (1998). c-Cbl/Sli-1 regulates endocytic sorting and ubiquitination of the epidermal growth factor receptor. *Genes Dev.* **12**: 3663-3674.

17.   Levkowitz, G., L.N. Klapper, E. Tzahar, A. Freywald, M. Sela, and Y. Yarden. (1996). Coupling of the c-Cbl protooncogene product to ErbB-1/EGF-receptor but not to other ErbB proteins. *Oncogene* **12**: 1117-25.

18.   Laederich, M.B., M. Funes-Duran, L. Yen, E. Ingalla, X. Wu, K.L. Carraway, 3rd, et al. (2004). The leucine-rich repeat protein LRIG1 is a

negative regulator of ErbB family receptor tyrosine kinases. *J Biol Chem* **279**: 47050-6.

19.   Diamonti, A.J., P.M. Guy, C. Ivanof, K. Wong, C. Sweeney, and K.L. Carraway, 3rd. (2002). An RBCC protein implicated in maintenance of steady-state neuregulin receptor levels. *Proc Natl Acad Sci U S A* **99**: 2866-71.

20.   Omerovic, J., L. Santangelo, E.M.-R. Puggioni, J. Marrocco, C. Dall'Armi, C. Palumbo, et al. (2007). The E3 ligase Aip4/Itch ubiquitinates and targets ErbB-4 for degradation. *FASEB J.* Epub April 26, 2007.

21.   Baulida, J., M.H. Kraus, M. Alimandi, P.P. Di Fiore, and G. Carpenter. (1996). All ErbB receptors other than the epidermal growth factor receptor are endocytosis impaired. *J Biol Chem* **271**: 5251-7.

22.   Hunter, T., N. Ling, and J.A. Cooper. (1984). Protein kinase C phosphorylation of the EGF receptor at a threonine residue close to the cytoplasmic face of the plasma membrane. *Nature* **311**: 480.

23.   Zhou, W. and G. Carpenter. (2000). Heregulin-dependent trafficking and cleavage of ErbB-4. *J Biol Chem* **275**: 34737-43.

24.   Cheng, Q.C., O. Tikhomirov, W. Zhou, and G. Carpenter. (2003). Ectodomain cleavage of ErbB-4: characterization of the cleavage site and m80 fragment. *J Biol Chem* **278**: 38421-7.

25.   Vecchi, M. and G. Carpenter. (1997). Constitutive proteolysis of the ErbB-4 receptor tyrosine kinase by a unique, sequential mechanism. *J Cell Biol* **139**: 995-1003.

26.   Rio, C., J.D. Buxbaum, J.J. Peschon, and G. Corfas. (2000). Tumor necrosis factor-alpha-converting enzyme is required for cleavage of erbB4/HER4. *J Biol Chem* **275**: 10379-87.

27.   Sunnarborg, S.W., C.L. Hinkle, M. Stevenson, W.E. Russell, C.S. Raska, J.J. Peschon, et al. (2002). Tumor Necrosis Factor-alpha Converting Enzyme (TACE) Regulates Epidermal Growth Factor Receptor Ligand Availability. *J. Biol. Chem.* **277**: 12838-12845.

28.   Brou, C., F. Logeat, N. Gupta, C. Bessia, O. LeBail, J.R. Doedens, et al. (2000). A novel proteolytic cleavage involved in Notch signaling: the role of the disintegrin-metalloprotease TACE. *Mol Cell* **5**: 207-16.

29.   Nagano, O., D. Murakami, D. Hartmann, B. de Strooper, P. Saftig, T. Iwatsubo, et al. (2004). Cell-matrix interaction via CD44 is independently regulated by different metalloproteinases activated in response to extracellular Ca2+ influx and PKC activation. *J. Cell Biol.* **165**: 893-902.

30.   Elenius, K., G. Corfas, S. Paul, C.J. Choi, C. Rio, G.D. Plowman, et al. (1997). A novel juxtamembrane domain isoform of HER4/ErbB4. Isoform-specific tissue distribution and differential processing in response to phorbol ester. *J Biol Chem* **272**: 26761-8.

31.   Hinkle, C.L., S.W. Sunnarborg, D. Loiselle, C.E. Parker, M. Stevenson, W.E. Russell, et al. (2004). Selective Roles for Tumor Necrosis Factor {alpha}-converting Enzyme/ADAM17 in the Shedding of the Epidermal Growth Factor Receptor Ligand Family: THE JUXTAMEMBRANE STALK DETERMINES CLEAVAGE EFFICIENCY. *J. Biol. Chem.* **279**: 24179-24188.

32.   Christianson, T.A., J.K. Doherty, Y.J. Lin, E.E. Ramsey, R. Holmes, E.J. Keenan, et al. (1998). NH2-terminally truncated HER-2/neu protein: relationship with shedding of the extracellular domain and with prognostic factors in breast cancer. *Cancer Res* **58**: 5123-9.

33.   Anido, J., M. Scaltriti, J.J. Bech Serra, B.S. Josefat, F.R. Todo, J. Baselga, et al. (2006). Biosynthesis of tumorigenic HER2 C-terminal fragments by alternative initiation of translation. *Embo J* **25**: 3234-44.

34.   Ni, C.Y., M.P. Murphy, T.E. Golde, and G. Carpenter. (2001). gamma - Secretase cleavage and nuclear localization of ErbB-4 receptor tyrosine kinase. *Science* **294**: 2179-81.

35.   Lee, H.J., K.M. Jung, Y.Z. Huang, L.B. Bennett, J.S. Lee, L. Mei, et al. (2002). Presenilin-dependent gamma-secretase-like intramembrane cleavage of ErbB4. *J Biol Chem* **277**: 6318-23.

36.   Rochette, M.J. and M.P. Murphy. (2002). Gamma-secretase: substrates and inhibitors. *Mol Neurobiol* **26**: 81-95.

37. De Strooper, B., W. Annaert, P. Cupers, P. Saftig, K. Craessaerts, J.S. Mumm, et al. (1999). A presenilin-1-dependent [gamma]-secretase-like protease mediates release of Notch intracellular domain. *Nature* **398**: 518.

38. Shih, I.-M. and T.-L. Wang. (2007). Notch Signaling, {gamma}-Secretase Inhibitors, and Cancer Therapy. *Cancer Res* **67**: 1879-1882.

39. Takasugi, N., T. Tomita, I. Hayashi, M. Tsuruoka, M. Niimura, Y. Takahashi, et al. (2003). The role of presenilin cofactors in the [gamma]-secretase complex. *Nature* **422**: 438.

40. Kimberly, W.T., M.J. LaVoie, B.L. Ostaszewski, W. Ye, M.S. Wolfe, and D.J. Selkoe. (2003). {gamma}-Secretase is a membrane protein complex comprised of presenilin, nicastrin, aph-1, and pen-2. *Proc Natl Acad Sci U S A* **100**: 6382-6387.

41. Edbauer, D., E. Winkler, J.T. Regula, B. Pesold, H. Steiner, and C. Haass. (2003). Reconstitution of [gamma]-secretase activity. *Nat Cell Biol* **5**: 486.

42. Wolfe, M.S., W. Xia, B.L. Ostaszewski, T.S. Diehl, W.T. Kimberly, and D.J. Selkoe. (1999). Two transmembrane aspartates in presenilin-1 required for presenilin endoproteolysis and [gamma]-secretase activity. *Nature* **398**: 513.

43. Shah, S., S.F. Lee, K. Tabuchi, Y.H. Hao, C. Yu, Q. LaPlant, et al. (2005). Nicastrin functions as a gamma-secretase-substrate receptor. *Cell* **122**: 435-47.

44. Wolfe, M.S. (2006). The Gamma-Secretase Complex: Membrane-Embedded Proteolytic Ensemble. *Biochemistry* **45**: 7931-7939.

45. Lieberman, R.L. and M.S. Wolfe. (2007). From rhomboid function to structure and back again. *Proc Natl Acad Sci U S A* **104**: 8199-8200.

46. Ni, C.Y., H. Yuan, and G. Carpenter. (2003). Role of the ErbB-4 carboxyl terminus in gamma-secretase cleavage. *J Biol Chem* **278**: 4561-5.

47. Vecchi, M., L.A. Rudolph-Owen, C.L. Brown, P.J. Dempsey, and G. Carpenter. (1998). Tyrosine phosphorylation and proteolysis.

Pervanadate-induced, metalloprotease-dependent cleavage of the ErbB-4 receptor and amphiregulin. *J Biol Chem* **273**: 20589-95.

48.   Naresh, A., W. Long, G.A. Vidal, W.C. Wimley, L. Marrero, C.I. Sartor, et al. (2006). The ERBB4/HER4 intracellular domain 4ICD is a BH3-only protein promoting apoptosis of breast cancer cells. *Cancer Res* **66**: 6412-20.

49.   Arasada, R.R. and G. Carpenter. (2005). Secretase-dependent tyrosine phosphorylation of Mdm2 by the ErbB-4 intracellular domain fragment. *J Biol Chem* **280**: 30783-7.

50.   Komuro, A., M. Nagai, N.E. Navin, and M. Sudol. (2003). WW domain-containing protein YAP associates with ErbB-4 and acts as a co-transcriptional activator for the carboxyl-terminal fragment of ErbB-4 that translocates to the nucleus. *J Biol Chem* **278**: 33334-41.

51.   Omerovic, J., E.M. Puggioni, S. Napoletano, V. Visco, R. Fraioli, L. Frati, et al. (2004). Ligand-regulated association of ErbB-4 to the transcriptional co-activator YAP65 controls transcription at the nuclear level. *Exp Cell Res* **294**: 469-79.

52.   Aqeilan, R.I., V. Donati, A. Palamarchuk, F. Trapasso, M. Kaou, Y. Pekarsky, et al. (2005). WW domain-containing proteins, WWOX and YAP, compete for interaction with ErbB-4 and modulate its transcriptional function. *Cancer Res* **65**: 6764-72.

53.   Long, W., K.U. Wagner, K.C. Lloyd, N. Binart, J.M. Shillingford, L. Hennighausen, et al. (2003). Impaired differentiation and lactational failure of Erbb4-deficient mammary glands identify ERBB4 as an obligate mediator of STAT5. *Development* **130**: 5257-68.

54.   Linggi, B. and G. Carpenter. (2006). ERBB-4 s80 intracellular domain abrogates ETO2-dependent transcriptional repression. *J Biol Chem*.

55.   Williams, C.C., J.G. Allison, G.A. Vidal, M.E. Burow, B.S. Beckman, L. Marrero, et al. (2004). The ERBB4/HER4 receptor tyrosine kinase regulates gene expression by functioning as a STAT5A nuclear chaperone. *J Cell Biol* **167**: 469-78.

56.   Clark, D.E., C.C. Williams, T.T. Duplessis, K.L. Moring, A.R. Notwick, W. Long, et al. (2005). ERBB4/HER4 potentiates STAT5A transcriptional activity by regulating novel STAT5A serine phosphorylation events. *J Biol Chem* **280**: 24175-80.

57.   Gassmann, M., F. Casagranda, D. Orioli, H. Simon, C. Lai, R. Klein, et al. (1995). Aberrant neural and cardiac development in mice lacking the ErbB4 neuregulin receptor. *Nature* **378**: 390-4.

58.   Shi, W., H. Chen, J. Sun, S. Buckley, J. Zhao, K.D. Anderson, et al. (2003). TACE is required for fetal murine cardiac development and modeling. *Dev Biol* **261**: 371-80.

59.   Meyer, D. and C. Birchmeier. (1995). Multiple essential functions of neuregulin in development. *Nature* **378**: 386-90.

60.   Gilbertson, R.J., R.H. Perry, P.J. Kelly, A.D. Pearson, and J. Lunec. (1997). Prognostic significance of HER2 and HER4 coexpression in childhood medulloblastoma. *Cancer Res* **57**: 3272-80.

61.   Kew, T.Y., J.A. Bell, S.E. Pinder, H. Denley, R. Srinivasan, W.J. Gullick, et al. (2000). c-erbB-4 protein expression in human breast cancer. *Br J Cancer* **82**: 1163-70.

62.   Sardi, S.P., J. Murtie, S. Koirala, B.A. Patten, and G. Corfas. (2006). Presenilin-Dependent ErbB4 Nuclear Signaling Regulates the Timing of Astrogenesis in the Developing Brain. *Cell* **127**: 185.

63.   Singer, S.J. and G.L. Nicolson. (1972). The fluid mosaic model of the structure of cell membranes. *Science* **175**: 720-31.

64.   Ipsen, J.H., G. Karlstrom, O.G. Mouritsen, H. Wennerstrom, and M.J. Zuckermann. (1987). Phase equilibria in the phosphatidylcholine-cholesterol system. *Biochim Biophys Acta* **905**: 162-72.

65.   Simons, K. and E. Ikonen. (1997). Functional rafts in cell membranes. *Nature* **387**: 569.

66. Resh, M.D. (2006). Palmitoylation of Ligands, Receptors, and Intracellular Signaling Molecules. *Sci. STKE* **2006**: re14-.

67. Brown, D.A. (2006). Lipid Rafts, Detergent-Resistant Membranes, and Raft Targeting Signals. *Physiology* **21**: 430-439.

68. Pike, L.J., X. Han, and R.W. Gross. (2005). Epidermal growth factor receptors are localized to lipid rafts that contain a balance of inner and outer leaflet lipids: a shotgun lipidomics study. *J Biol Chem* **280**: 26796-804.

69. Smart, E.J., Y.S. Ying, C. Mineo, and R.G. Anderson. (1995). A detergent-free method for purifying caveolae membrane from tissue culture cells. *Proc Natl Acad Sci U S A* **92**: 10104-8.

70. Kenworthy, A.K., B.J. Nichols, C.L. Remmert, G.M. Hendrix, M. Kumar, J. Zimmerberg, et al. (2004). Dynamics of putative raft-associated proteins at the cell surface. *J. Cell Biol.* **165**: 735-746.

71. Varma, R. and S. Mayor. (1998). GPI-anchored proteins are organized in submicron domains at the cell surface. *Nature* **394**: 798.

72. Friedrichson, T. and T.V. Kurzchalia. (1998). Microdomains of GPI-anchored proteins in living cells revealed by crosslinking. *Nature* **394**: 802.

73. Kahya, N. (2006). Targeting membrane proteins to liquid-ordered phases: molecular self-organization explored by fluorescence correlation spectroscopy. *Chem Phys Lipids* **141**: 158-68.

74. London, E. (2005). How principles of domain formation in model membranes may explain ambiguities concerning lipid raft formation in cells. *Biochimica et Biophysica Acta (BBA) - Molecular Cell Research* **1746**: 203.

75. Mineo, C., G.N. Gill, and R.G.W. Anderson. (1999). Regulated Migration of Epidermal Growth Factor Receptor from Caveolae. *J. Biol. Chem.* **274**: 30636-30643.

76.   Adachi, S., T. Nagao, H.I. Ingolfsson, F.R. Maxfield, O.S. Andersen, L. Kopelovich, et al. (2007). The Inhibitory Effect of (-)-Epigallocatechin Gallate on Activation of the Epidermal Growth Factor Receptor Is Associated with Altered Lipid Order in HT29 Colon Cancer Cells. *Cancer Res* **67**: 6493-6501.

77.   Roepstorff, K., P. Thomsen, K. Sandvig, and B. van Deurs. (2002). Sequestration of Epidermal Growth Factor Receptors in Non-caveolar Lipid Rafts Inhibits Ligand Binding. *J. Biol. Chem.* **277**: 18954-18960.

78.   Pike, L.J. and L. Casey. (2002). Cholesterol levels modulate EGF receptor-mediated signaling by altering receptor function and trafficking. *Biochemistry* **41**: 10315-22.

79.   Chen, X. and M.D. Resh. (2002). Cholesterol Depletion from the Plasma Membrane Triggers Ligand-independent Activation of the Epidermal Growth Factor Receptor. *J. Biol. Chem.* **277**: 49631-49637.

80.   Abulrob, A., S. Giuseppin, M.F. Andrade, A. McDermid, M. Moreno, and D. Stanimirovic. (2004). Interactions of EGFR and caveolin-1 in human glioblastoma cells: evidence that tyrosine phosphorylation regulates EGFR association with caveolae. *Oncogene* **23**: 6967-79.

81.   Sun, J., M. Nanjundan, L.J. Pike, T. Wiedmer, and P.J. Sims. (2002). Plasma Membrane Phospholipid Scramblase 1 Is Enriched in Lipid Rafts and Interacts with the Epidermal Growth Factor Receptor. *Biochemistry* **41**: 6338-6345.

82.   Yamabhai, M. and R.G.W. Anderson. (2002). Second Cysteine-rich Region of Epidermal Growth Factor Receptor Contains Targeting Information for Caveolae/Rafts. *J. Biol. Chem.* **277**: 24843-24846.

83.   Nagy, P., G. Vereb, Z. Sebestyen, G. Horvath, S.J. Lockett, S. Damjanovich, et al. (2002). Lipid rafts and the local density of ErbB proteins influence the biological role of homo- and heteroassociations of ErbB2. *J Cell Sci* **115**: 4251-4262.

84.   Zhou, W. and G. Carpenter. (2001). Heregulin-dependent translocation and hyperphosphorylation of ErbB-2. *Oncogene* **20**: 3918-20.

85. Ma, L., Y.Z. Huang, G.M. Pitcher, J.G. Valtschanoff, Y.H. Ma, L.Y. Feng, et al. (2003). Ligand-dependent recruitment of the ErbB4 signaling complex into neuronal lipid rafts. *J Neurosci* **23**: 3164-75.

86. Zhao, Y.Y., O. Feron, C. Dessy, X. Han, M.A. Marchionni, and R.A. Kelly. (1999). Neuregulin signaling in the heart. Dynamic targeting of erbB4 to caveolar microdomains in cardiac myocytes. *Circ Res* **84**: 1380-7.

87. Thiel, K.W. and G. Carpenter. (2006). ErbB-4 and TNF-[alpha] converting enzyme localization to membrane microdomains. *Biochemical and Biophysical Research Communications* **350**: 629.

88. Ehehalt, R., P. Keller, C. Haass, C. Thiele, and K. Simons. (2003). Amyloidogenic processing of the Alzheimer {beta}-amyloid precursor protein depends on lipid rafts. *J. Cell Biol.* **160**: 113-123.

89. Hooper, N.M. (2005). Roles of proteolysis and lipid rafts in the processing of the amyloid precursor protein and prion protein. *Biochem Soc Trans* **33**: 335-8.

90. Taraboulos, A., M. Scott, A. Semenov, D. Avrahami, L. Laszlo, S.B. Prusiner, et al. (1995). Cholesterol depletion and modification of COOH-terminal targeting sequence of the prion protein inhibit formation of the scrapie isoform. *J. Cell Biol.* **129**: 121-132.

91. Riddell, D.R., G. Christie, I. Hussain, and C. Dingwall. (2001). Compartmentalization of beta-secretase (Asp2) into low-buoyant density, noncaveolar lipid rafts. *Curr Biol* **11**: 1288-93.

92. Kalvodova, L., N. Kahya, P. Schwille, R. Ehehalt, P. Verkade, D. Drechsel, et al. (2005). Lipids as Modulators of Proteolytic Activity of BACE: INVOLVEMENT OF CHOLESTEROL, GLYCOSPHINGOLIPIDS, AND ANIONIC PHOSPHOLIPIDS IN VITRO. *J. Biol. Chem.* **280**: 36815-36823.

93. Cordy, J.M., I. Hussain, C. Dingwall, N.M. Hooper, and A.J. Turner. (2003). Exclusively targeting {beta}-secretase to lipid rafts by GPI-anchor addition up-regulates {beta}-site processing of the amyloid precursor protein. *Proceedings of the National Academy of Sciences* **100**: 11735-11740.

94.   Vetrivel, K.S., H. Cheng, W. Lin, T. Sakurai, T. Li, N. Nukina, et al. (2004). Association of {gamma}-Secretase with Lipid Rafts in Post-Golgi and Endosome Membranes. *J. Biol. Chem.* **279**: 44945-44954.

95.   Schlondorff, J., J.D. Becherer, and C.P. Blobel. (2000). Intracellular maturation and localization of the tumour necrosis factor alpha convertase (TACE). *Biochem J* **347 Pt 1**: 131-8.

96.   Smart, E.J., R.G.W. Anderson, and K.S.a.L.P. Chandan, *Alterations in membrane cholesterol that affect structure and function of caveolae*, in *Methods in Enzymology*. 2002, Academic Press. p. 131.

97.   Maatta, J.A., M. Sundvall, T.T. Junttila, L. Peri, V.J.O. Laine, J. Isola, et al. (2006). Proteolytic Cleavage and Phosphorylation of a Tumor-associated ErbB4 Isoform Promote Ligand-independent Survival and Cancer Cell Growth. *Mol. Biol. Cell* **17**: 67-79.

98.   Fujii, K., G. Zhu, Y. Liu, J. Hallam, L. Chen, J. Herrero, et al. (2004). Kinase peptide specificity: Improved determination and relevance to protein phosphorylation. *Proc Natl Acad Sci U S A* **101**: 13744-13749.

99.   Nika, K., C. Charvet, S. Williams, L. Tautz, S. Bruckner, S. Rahmouni, et al. (2006). Lipid Raft Targeting of Hematopoietic Protein Tyrosine Phosphatase by Protein Kinase C {theta}-Mediated Phosphorylation. *Mol. Cell. Biol.* **26**: 1806-1816.

100.   Douglass, A.D. and R.D. Vale. (2005). Single-molecule microscopy reveals plasma membrane microdomains created by protein-protein networks that exclude or trap signaling molecules in T cells. *Cell* **121**: 937-50.

101.   Vetrivel, K.S., H. Cheng, S.-H. Kim, Y. Chen, N.Y. Barnes, A.T. Parent, et al. (2005). Spatial Segregation of {gamma}-Secretase and Substrates in Distinct Membrane Domains. *J. Biol. Chem.* **280**: 25892-25900.

102.   Sundvall, M., L. Peri, J.A. Maatta, D. Tvorogov, I. Paatero, M. Savisalo, et al. (2007). Differential nuclear localization and kinase activity of alternative ErbB4 intracellular domains. *Oncogene*.

103. Rajendran, L., M. Honsho, T.R. Zahn, P. Keller, K.D. Geiger, P. Verkade, et al. (2006). Alzheimer's disease beta-amyloid peptides are released in association with exosomes. *Proc Natl Acad Sci U S A* **103**: 11172-11177.

104. Urra, S., C.A. Escudero, P. Ramos, F. Lisbona, E. Allende, P. Covarrubias, et al. (2007). TrkA Receptor Activation by Nerve Growth Factor Induces Shedding of the p75 Neurotrophin Receptor Followed by Endosomal {gamma}-Secretase-mediated Release of the p75 Intracellular Domain. *J. Biol. Chem.* **282**: 7606-7615.

105. Gupta-Rossi, N., E. Six, O. LeBail, F. Logeat, P. Chastagner, A. Olry, et al. (2004). Monoubiquitination and endocytosis direct {gamma}-secretase cleavage of activated Notch receptor. *J. Cell Biol.* **166**: 73-83.

106. Gil, C., R. Cubi, and J. Aguilera. (2007). Shedding of the p75NTR neurotrophin receptor is modulated by lipid rafts. *FEBS Letters* **581**: 1851.

107. Soond, S.M., B. Everson, D.W.H. Riches, and G. Murphy. (2005). ERK-mediated phosphorylation of Thr735 in TNF{alpha}-converting enzyme and its potential role in TACE protein trafficking. *J Cell Sci* **118**: 2371-2380.

108. Reddy, P., J.L. Slack, R. Davis, D.P. Cerretti, C.J. Kozlosky, R.A. Blanton, et al. (2000). Functional Analysis of the Domain Structure of Tumor Necrosis Factor-alpha Converting Enzyme. *J. Biol. Chem.* **275**: 14608-14614.

109. Doedens, J.R. and R.A. Black. (2000). Stimulation-induced Down-regulation of Tumor Necrosis Factor-alpha Converting Enzyme. *J. Biol. Chem.* **275**: 14598-14607.

Part II

Regulation of ErbB-1 Kinase Activation

CHAPTER I

INTRODUCTION

Epidermal growth factor (EGF) receptor, or ErbB-1, is the prototypical member of the ErbB family of type I receptor tyrosine kinases (RTK). ErbB-1 (170 kDa) is comprised of an ectodomain (100 kDa), a single transmembrane domain, and a 60 kDa intracellular domain (see Figure II-1). The ectodomain can be divided into four structural subdomains: two subdomains, I and III, involved in ligand binding and two cysteine-rich subdomains, II and IV [2]. An α-helical transmembrane domain connects the ectodomain to the intracellular domain (ICD). Within the ICD are a juxtamembrane (JM) region, the tyrosine kinase domain (TKD), and a carboxyterminal (CT) region [2].

Figure II-1: Schematic of ErbB-1 domains. Green: ligand-binding regions; yellow: cysteine-rich regions; TM: transmembrane domain; JM: juxtamembrane region; TKD, tyrosine kinase domain; CT: carboxyterminal region.
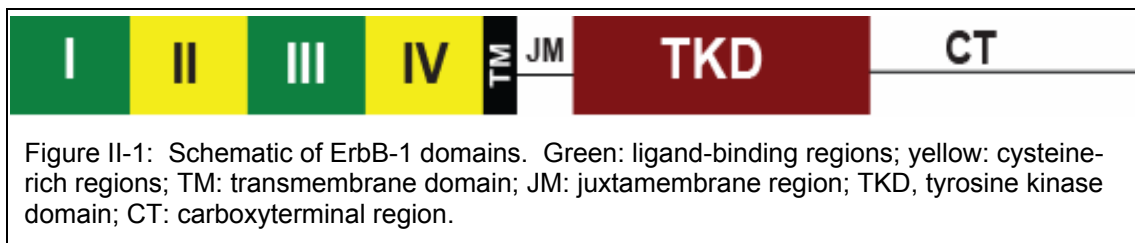
The importance of each of these regions of ErbB-1 in dimerization and kinase activation are discussed in detail in this chapter. Since ErbB-2, -3, and -4 are similarly organized, the lessons learned from ErbB-1 may be applicable in part (ErbB-2, -3) or in full (ErbB-4).

Ligand-Dependent ErbB-1 Activation and Signaling Pathways

Transmembrane proteins receive signals to alter cellular processes from the extracellular environment and transmit those signals across the plasma membrane to effect changes inside the cell. For ErbB-1, EGF-like ligands specifically associate with the receptor and a series of receptor conformational changes ensue in response to ligand binding, culminating in activation of mitogenic signaling pathways. ErbB-1 serves as a receptor for several related growth factors, including EGF, transforming growth factor-α, betacellulin, amphiregulin, epiregulin, epigen, and heparin-binding EGF [1]. Ligand binding to regions I and III in the ectodomain induces a conformational change to convert the ErbB-1 ectodomain from a tethered, inactive conformation to an extended, active conformation, as determined by high-resolution crystal structures [5, 6].

This and further conformational changes result in intracellular tyrosine kinase activity and spawn a cascade of activated downstream signaling molecules. Proteins containing a src homology-2 (SH2) or protein tyrosine binding (PTB) domain are recruited to sites of autophosphorylation in the ErbB-1 carboxyterminal region and many are then phosphorylated by the ErbB-1 TKD [2]. This constitutes a receptor-proximal activation step. For example, ErbB-1 tyrosine phosphorylation of phospholipase C-γ1 (PLC-γ1) promotes results in PLC-γ1 hydrolysis of phosphatidyl-inositol-4,5-bisphosphate (PIP_2) to form the two second messengers inositol 1,4,5-trisphosphate (IP_3) and diacylglycerol (DAG) which, respectively, promote release of calcium from the endoplasmic reticulum and activation of protein kinase C (PKC) [7, 8]. Receptor

phosphorylation also serves to recruit adaptor proteins to the cytosolic face of the plasma membrane. For example, Grb2 also binds to ErbB-1 but is not phosphorylated [9], acting as an adaptor protein to facilitate ErbB-1 activation of Ras [10].

Separate from a cell-surface signaling molecule, full-length ErbB-1 also translocates to the nucleus where it is required for activating transcription of several genes, including cyclin D1 and c-myb [11]. The mechanism of ErbB-1 nuclear localization involves retrograde translocation from the endoplasmic reticulum (ER) by interaction with the translocon Sec61 [12]. Normally, this translocon functions as a pore to integrate newly synthesized transmembrane proteins into the ER membrane, but Sec61 can also remove misfolded proteins from their membrane environment through a retrotranslocation process termed ER-associated degradation, or ERAD [13]. Certain toxins, such as cholera toxin, exploit the ERAD pathway to gain access to the cytosol and nucleus [14], and a recent report suggests that the ER may also serve as a intermediate localization for cell-surface transmembrane proteins to reach the nucleus in a non-membraneous state [12]. Knockdown of Sec61β by siRNA prevents both nuclear localization of ErbB-1 and EGF-induced cyclin D1 expression, revealing that the mechanism of ErbB-1-dependent cyclin D1 transcription relies on retrograde transport to the ER [12].

Since ErbB-1 activates an array of signaling pathways that result in cell growth and proliferation, controls exist to prevent sustained activation of the receptor. The short-term mechanism for ErbB-1 inactivation is

dephosphorylation by protein tyrosine phosphatases ([15] and references therein). The long-term mechanism for ErbB-1 inactivation is downregulation via clathrin-mediated endocytosis and lysosomal degradation [16-18]. Ligand binding promotes rapid internalization of ErbB-1, but not other ErbB receptors [19], and three fates exist for the internalized receptor: 1) recycling to the cell surface, 2) lysosomal degradation, and 3) transport to the nucleus. Internalization, however, does not necessarily translate to inactivation because signaling still occurs from endocytic vesicles [20, 21], and ErbB-1 activates transcription in the nucleus [12].

Activation of ErbB-1 in Tumorigenesis

Proteins involved in cell survival and proliferation are frequently overexpressed or mutated in malignant tissues. ErbB-1 was first termed an oncogene in 1984 when Downward *et al.* identified similarities between the intracellular domain sequences of ErbB-1 and the avian erythroblastosis virus [22]. Overexpression of ErbB-1 is well-documented in a variety of tumor types, including non-small cell lung cancer (NSCLC) [23], head and neck squamous cell carcinoma (HNSCC) [24], colorectal cancer [25], pancreatic cancer [26], renal cell carcinoma [27], ovarian cancer [28], and esophageal cancer [29].

In addition to overexpression, mutant forms of ErbB-1 have also been detected in glioblastoma multiforme, the most common mutation being a splice variant, ErbB-1vIII, that results in deletion of exon 3 [30]. Deletion of this region creates a constitutively active receptor, thus circumventing the need for ligand-

dependent activation [30]. More recently, mutations within the tyrosine kinase domain (exons 18-21) of ErbB-1 were identified in lung cancer patients that render the receptor partially constitutively active and more sensitive to some small-molecule tyrosine kinase inhibitors (TKIs) [31-33]. The two most common mutations are Δ746-750 in exon 19 and L858R in exon 21 [23]. These and other TKD mutations in ErbB-1 have been detected primarily in Asian women non-smokers with bronchiolar adenocarcinoma [23], while ErbB-1vIII has also been detected in squamous cell lung carcinoma in addition to glioblastoma [34]. Three mouse models have been developed that inducibly express mutant forms of ErbB-1 targeted to lung type II pneumocytes: L858R mutation, exon 19 deletion [35] and ErbB-1vIII [34]. The TKD mutant animals develop tumors after prolonged mutant ErbB-1 expression and these tumors are sensitive to ErbB-1 TKIs [35]. Animals expressing ErbB-1vIII develop NSCLC, but these tumors are only sensitive to the irreversible TKI HKI-272 [34].

As can be imagined, inhibition of ErbB-1 represents a desirable avenue for treatment of cancer. Currently, two modes of ErbB-1 inhibition are under investigation: TKIs and monoclonal antibodies. The TKIs gefitinib (Iressa) and erlotinib (Tarceva) bind to the ATP binding site of ErbB-1. Crystal structures of erlotinib [4] and gefitinib [36] bound to the tyrosine kinase domain of ErbB-1 revealed that these 4-anilinoquinazolines bind to the open conformation of ErbB-1 TKD, i.e., when the activation loop is exposed. Lapatinib is a ErbB TKI that targets both ErbB-1 and ErbB-2 and, in contrast to erlotinib and gefitinib, binds to the closed conformation of the TKD when the activation loop is buried within the

ATP binding pocket [37]. The irreversible inhibitors EKB-569, HKI-357, and HKI-272 act as Michael acceptors to form a covalent bond with a cysteine residue in the ErbB-1 binding pocket [23].

The monoclonal antibodies cetuximab (C-225, Erbitux) and panitumumab (ABX-EGF) target the extracellular region of ErbB-1 to block ligand binding and induce receptor internalization without activating the receptor [23]. The TKIs gefitinib and erlotinib are more effective clinically in lung cancer patients expressing ErbB-1 TKD mutations [38], whereas the monoclonal antibodies display better effectiveness in colorectal cancer [39, 40].

The ligands of ErbB-1, and not the receptor *per se*, may also be inappropriately in disease, which leads to sustained activation of the receptor [24]. Hence, assessment of ErbB-1 expression alone may not be an adequate prognostic marker for an increase in ErbB-1 activity in malignant carcinoma. Aside from classical activation by ligand binding, transactivation of ErbB-1 occurs through a variety of heterologous receptors or stimuli, such as G-protein coupled receptors, and these pathways could also contribute to disease [1].

Dimerization of ErbB-1

Joseph Schlessinger first proposed that dimerization of ErbB receptors is a critical step in activation of the receptors [41]. Based on high-resolution crystal structures, it is now known that regions within the ectodomain [5, 42-44] and tyrosine kinase domains [3] dimerize subsequent to ligand binding. Dimerization motifs are also found in the transmembrane domains of the ErbB receptors [45];

however, the extent to which these mediate or are required for ligand-dependent receptor activation is not clear.

Ectodomain

In the absence of ligand, a critical dimerization arm present in ErbB-1 [5, 6], ErbB-3 [42], and ErbB-4 [44] is in a tethered conformation that is maintained by contacts between subdomains II and IV (Figure II-2). The additional of ligand

Figure II-2: Conformational changes in the ectodomain associated with ligand binding. In the absence of ligand, ErbB-1, -3, and -4 are in a tethered state. Ligand binding to subdomains I and III induces a conformation change to an extended state. Exposure of the dimerization arm in subdomain II facilitates ectodomain dimerization (right). Adapted from Linggi and Carpenter [1].
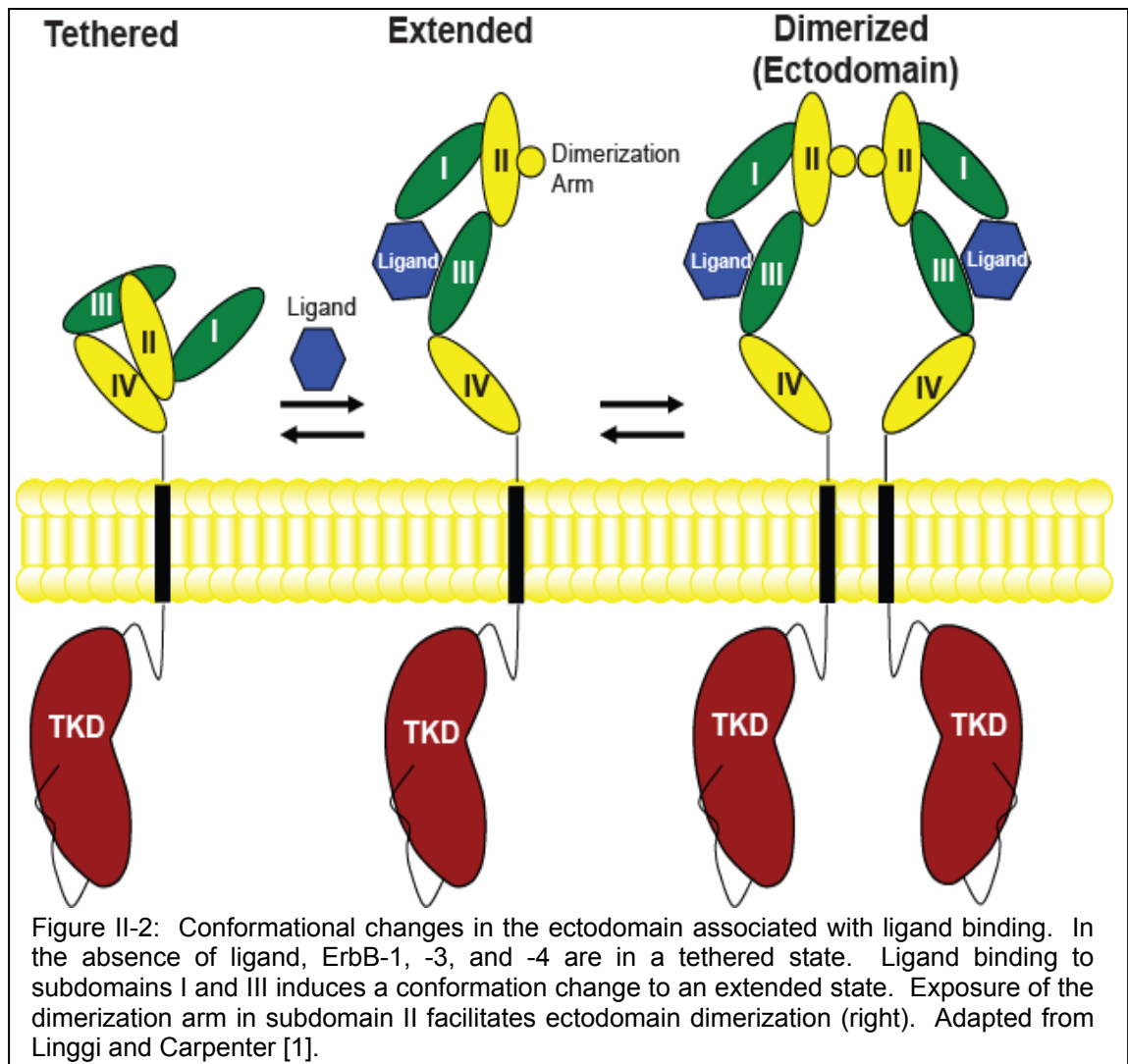
(i.e., EGF, TGF-α) to ErbB-1 induces a conformational change that results in exposure of the dimerization arm, located in the first cysteine-rich region (subdomain II), and promotes a back-to-back mode of extracellular dimerization [5, 6]. Although mutagenesis of the dimerization arm prevents EGF-induced receptor activation and mitogenesis [46, 47], exposure of the dimerization , while a necessary first step, is probably not sufficient for activation. For example, deletion of the region just below the dimerization arm also inhibits ErbB-1 activity, indicating a role for those sequences in activation of the receptor [47]. This mode of ectodomain dimerization is well-accepted in the field, and no structural alternatives have been presented in the literature.

Biochemical experiments and crystal structures of the ErbB-1 ectodomain bound to ligand revealed that the stoichiometry of ligand:receptor is 1:1 [5, 6, 48], and that the ligand does not directly participate in dimerization (ligand-mediated dimerization). The ligand simply induces the conformational changes necessary to facilitate receptor-mediated dimerization [5, 6]. In contrast to ErbB-1, -3, and -4, ErbB-2 is found in an extended, pseudo-ligand-bound conformation in the absence of ligand [49]. ErbB-2 is an orphan receptor as no ligand binding step is required to induce the conformational change that exposes the dimerization arm, as is the case for the other ErbBs. In fact, the constitutively extended conformation with the exposed dimerization arm allows ErbB-2 to rapidly dimerize with ligand-activated ErbB-1, ErbB-3, and ErbB-4. The conformation of the ErbB-2 ectodomain may explain why overexpression of this protein is often oncogenic.

Interestingly, biochemical experiments revealed that ErbB-1 vIII mutant receptor does not homodimerize [50]. Therefore, other regions of the receptor must contribute to activation since deletion of exon 3, a region that participates in ligand binding, is capable of ligand-independent activation.

Transmembrane Domain

Originally identified in the TM domain of glycoporin A, the GXXXG and GXXXG-like motifs are associated with interactions between TM domains [51]. All ErbB receptors (except ErbB-3) contain N- and C-terminal GXXXG-like dimerization motifs in their TM domains (see Figure II-3) [45]. Mutations of these

```
ErbB-1    SIATGMVGALLLLLVVALGIGLFM
ErbB-2    LTSIVSAVVGILLVVVLGVVFGILI
ErbB-3    LTMALTVIAGLVVIFMMLGGTFLYW
ErbB-4    LIAAGVIGGLFILVIVGLTFAVYV
```
Figure II-3: Alignment of the ErbB transmembrane domains. Yellow boxes denote GXXXG-like motifs classically associated with transmembrane domain dimerization. ErbB-2 V664 is underlined.
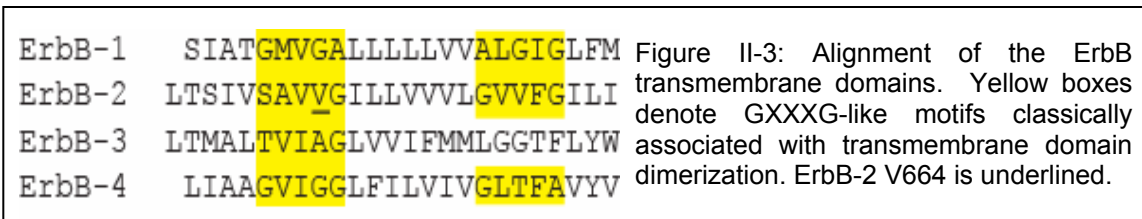
putative dimerization motifs led to a theory of TM domain dimerization in which the C-terminal GXXXG-like motif in ErbB-1 mediates homodimerization [45], whereas the N-terminal GXXXG-like motif is involved in heterodimerization with other ErbB TM domains, such as ErbB-2 [52].   Mutation of Val664 to Glu in the TM domain of ErbB-2 results in constitutive activation of the receptor [53] by promoting dimerization [54], though not necessarily TM domain dimerization [45]. A similar mutation (I658E) in the TM of ErbB-4 also results in a constitutively

active receptor, although this group did not compare dimerization of wild-type and I658E ErbB-4 [55].

Tyrosine Kinase Domain

The tyrosine kinase domain of ErbB receptors is divided into two lobes, termed the N-lobe and the C-lobe, with a short connector between the two [56]. This bi-lobed architecture is found in all protein kinases, although some receptors contain a larger linker between the N- and C-lobes [56]. In the absence of ligand or another activating element, kinases are in an inactive conformation, with the active site in the N-lobe occluded by the activation loop (A-loop) in the C-lobe [56]. Conformational changes that occur in response to ligand binding facilitate kinase activation, and most receptor tyrosine kinases require phosphorylation of a residue within the A-loop of the TKD for full catalytic activation [56]. For example, autophosphorylation of Tyr1163 within the A-loop of the insulin receptor induces a conformational change in the A-loop that exposes the ATP binding site, leading to subsequent catalytic activity [57, 58]. The ErbB family, however, is an exception to this general mechanism. While there is a tyrosine residue (Tyr845) within the A-loop of ErbB-1 that is phosphorylated, this site is phosphorylated by Src [59, 60]. This site is not known to be an autophosphorylation site. However, in one study mutation of Tyr845 to phenylalanine reduced EGF-induced DNA synthesis [59], while a second report found this same mutation does not inhibit EGF-dependent ERK activation [61]. This seeming contradiction has not been resolved.

It is widely accepted in the field that, in addition to ectodomain dimerization, intracellular domain dimerization is also required for ErbB-1 tyrosine kinase activation. Until recently, it was assumed, based on a crystal structure of the ErbB-1 TKD, that ErbB-1 intracellular dimerization occurs in a symmetrical fashion [4]. However, mutation of residues at the symmetrical interface failed to

Figure II-4: Asymmetrical dimerization of ErbB-1 TKD. The N-lobe of an acceptor monomer interacts with the C-lobe of a donor monomer. This allosteric interaction results in activation of the acceptor monomer.
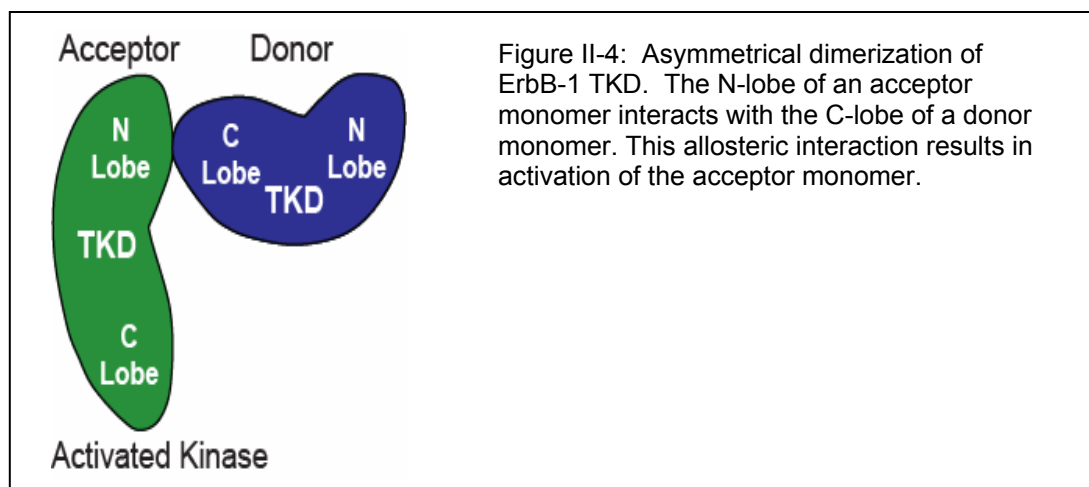
inhibit tyrosine kinase activity of full-length ErbB-1 [3]. A recent publication by Zhang, *et al.,* instead describes an allosteric mechanism for intracellular kinase activation via asymmetrical dimerization of TKD monomers (Figure II-4) [3].

Crystallographical studies combined with cell biological verification by Kuriyan and colleagues elegantly revealed that ligand binding promotes interaction of the N-lobe of an acceptor monomer with the C-lobe of a donor monomer, resulting in activation of the acceptor monomer (Figure II-4) [3]. This mode of interaction is similar to that of the cyclin-CDK complex, in which the donor is the cyclin-like monomer, and the acceptor is the CDK-like monomer [62].

Importantly, single point mutations at key residues in the dimer interface abolish EGF-induced tyrosine phosphorylation of full-length ErbB-1 expressed in cells [3]. Dimer interface residues in the N-lobe of the acceptor monomer are Pro675, Iso682, and Lys736, while contact residues in the C-lobe of the donor monomer are Iso917, Met921, Val924, and Met928 [3]. Mutation of any single N-lobe or C-lobe contact residue theoretically forces that monomer to be a donor or acceptor, respectively.

Intracellular Juxtamembrane Region of ErbB-1

Extending from the last residue of the transmembrane domain is the 37-residue juxtamembrane region (Figure II-1), which is highly conserved amongst ErbB family members (Figure II-5).

Structural Features of the Juxtamembrane Region

Attempts to determine a structure for the JM region of ErbB-1 using NMR and circular dichroism have been limited to peptides comprising the JM region [63, 64] or the N-terminal portion of the JM region with a transmembrane domain linker [65]. Using a peptide of R645-G697, which includes 15 residues of the

```
ErbB-1 RRR--HIVRKRTLRRLLQERELVEPLTPSGEAPNQALLRI
ErbB-2 KRRQQKIR-KYTMRRLLQETELVEPLTPSGAMPNQAQMRI
ErbB-3 WRGRR-IQNKRAMRRYLERGESIEPLDPS-EKANKVLARI
ErbB-4 RRK--SIKKKRALRRFL-ETELVEPLTPSGTAPNQAQLRI
```

Figure II-5: Alignment of ErbB JM regions. Yellow: conserved in all 4 proteins; grey: conserved in 3.
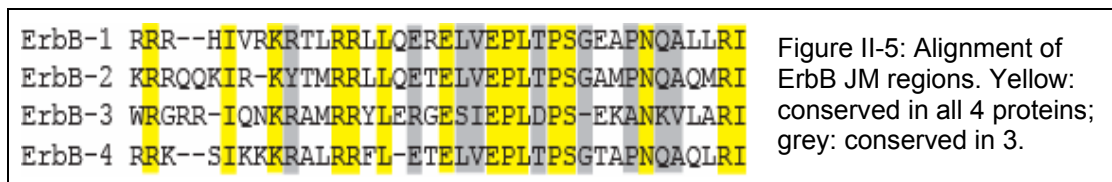
TKD, one group concluded, based on NMR data, that the JM region is relatively unordered in solution and forms three amphipathic helices connected by two unstructured regions in detergent micelles [63]. To date, no structure of the JM region together with the TKD or the complete ICD has been published, so the fold of the JM region may be different in the context of the full receptor than that observed using the TM and portions of the JM region.

Contained within the JM region of ErbB-1 are lysosomal [66] and basolateral sorting signals [67], a tripartite nuclear localization sequence [11, 68], as well as one PKC [69, 70] and two mitogen-activated protein kinase (MAPK) [71, 72] phosphorylation sites. Calmodulin [73] and the α-subunit of G_s proteins [74] are also reported bind to the JM region of ErbB-1 *in vivo* and *in vitro*. In detergent micelles, the dominant basolateral sorting signal is located in an unordered loop, the PKC phosphorylation site and calmodulin binding region are found in the first amphipathic helix, and the lysosomal sorting signal is located in the second helix [64]. PKC and calmodulin may compete for binding to the same site, as calmodulin binding does not occur when the JM region is phosphorylated by PKC, and PKC phosphorylation of the JM cannot be detected in the presence of bound calmodulin in *in vitro* studies [73]. Hence, a great deal of sequence information that potentially regulates functions, including receptor localization, inactivation, and degradation, is localized within the small region of the receptor. Furthermore, the significant degree of homology with other ErbB receptors suggests that these sorting signals and binding sites in the ErbB-1 JM region are also contained within ErbB-2, -3, and -4.

PKC Phosphorylation of Thr654

PKC phosphorylation of ErbB-1 was first reported in 1984 when it was determined that treatment with the phorbol ester TPA prevents EGF-induced tyrosine phosphorylation of the receptor [75] and promotes threonine phosphorylation of ErbB-1 [76]. Soon afterwards, two separate reports identified Thr654 within the juxtamembrane region as the major site of PKC phosphorylation [69, 70]. Subsequent studies sought to understand how PKC phosphorylation mediates receptor inactivation. Several groups compared EGF binding to ErbB-1 before and after treatment with TPA; however, the results are conflicting and vary depending on the technique used. For example, Rosner and colleagues found that phorbol ester treatment did not affect ^{125}I-EGF binding using A431 cells [75], whereas Parker and colleagues observed a 3-fold decrease in EGF affinity for ErbB-1 purified from A431 cells and phosphorylated *in vitro* by PKC [77]. Davis also detected a decrease in EGF binding to both wild-type ErbB-1 and T654A ErbB-1 expressed in CHO cells after pretreatment with TPA [78]. A phosphomimetic mutant, T654E, displayed no difference in EGF binding, tyrosine phosphorylation, or DNA synthesis as compared to the wild-type receptor in the absence of TPA [79].

Interestingly, platelet-derived growth factor (PDGF), the ligand for the PDGF receptor, also promotes ErbB-1 Thr654 phosphorylation, presumably through PDGF activation of PKC [80]. Importantly, EGF [81, 82] and TGF-α [83] also provoke Thr654 phosphorylation, indicating that a negative feedback loop exists involving ErbB-1 activation of PLC-γ1, which then hydrolyzes PIP$_2$ to

generate the second messengers IP_3 and DAG. The latter activates PKC resulting in phosphorylation of ErbB-1 on Thr654 and other sites.

PKC phosphorylation of Thr654 has also been linked to receptor endocytosis. Early studies showed that phorbol ester treatment (in the absence of ligand) induces internalization of wild-type ErbB-1 [84, 85], yet others observed that phosphorylation at Thr654 (i.e., pretreatment with phorbol ester) inhibits ligand-mediated receptor internalization [86]. A PKC-phosphorylated receptor is subjected to recycling following endocytosis but a non-phosphorylated receptor (T654A) is degraded [87]. Collectively, these data indicate that Thr654 phosphorylation by PKC inhibits EGF-stimulated degradation of the receptor. However, the mechanism is still unclear, such as how a PKC-phosphorylated receptor is distinguished from a non-phosphorylated receptor.

The JM region of the ErbB receptors is unique compared to other tyrosine kinase receptors in that it contains a large stretch of basic residues immediately following the transmembrane domain. One hypothesis is that these residues mediate an electrostatic interaction with negatively-charged phospholipids in the lipid bilayer, and this interaction promotes an inactive conformation of the TKD [88]. Calmodulin binding to a peptide representing this region in ErbB-1 (residues 645-660) inhibits the electrostatic interaction of the peptide with phospholipids to potentially allow activation of intracellular kinase activity [65, 88]. Relevant to PKC phosphorylation of Thr654 within this region, calmodulin does not bind a Thr654-phosphorylated ErbB-1 JM peptide [88], but this data has not been replicated in an intact cell.

A conserved PKC phosphorylation site that results in receptor downregulation has also been identified at Thr686 in the JM region of ErbB-2 [89, 90], but this site has not been studied as extensively as Thr654 in ErbB-1. Based on the consensus site for PKC phosphorylation, ErbB-4 contains a putative PKC phosphorylation site at Ser679 [91], five residues after the transmembrane domain; the positioning of this site is not conserved with ErbB-1 and ErbB-2 (see Figure II-5) and has not been directly validated in the literature. PKC phosphorylation sites have also been identified in the juxtamembrane regions of the RTKs c-met [92, 93] and the insulin receptor [94] and result in a decrease in receptor tyrosine kinase activity when phosphorylated.

Carboxyterminal Region of ErbB-1

The carboxyterminal region of all ErbB receptors is the exclusive site for tyrosine autophosphorylation. The first sites to be identified in Erb-1 were tyrosines 1068, 1148, and 1173 [95], and later autophosphorylation was detected on tyrosine residues 992, 1045, and 1086 [96-98]. Subsequent studies of catalytically-inactive receptors (K721 mutation) co-expressed with carboxy-truncated receptors revealed that autophosphorylation occurs in *trans* [99, 100]. Quite interestingly, mutation of any one tyrosine to phenylalanine does not inhibit activation of downstream signaling molecules and induction of mitogenesis [101, 102]. This is in direct contrast to the PDGF receptor in which, for example, PLC-γ1 exclusively binds to tyrosine 1021 and Grb2 to tyrosine 716 of the PDGF-β receptor [103]. Hence mutation of any one of these residues in PDGF receptor

selectively turns off one signaling pathway while maintaining others, whereas the signaling properties of the same proteins are not affected by mutation of a single tyrosine residue in ErbB-1.

Aside from providing a docking site for SH2 or PTB-containing proteins, the carboxyterminal region of ErbB-1 may also play a role in receptor autoinhibition and internalization. For example, deletion of the carboxyterminal region beginning at residues 1052, 1022, 991, and 973, but not 944, results in increased activation of target proteins [96], and a receptor truncated at residue 973 displays higher activity towards ErbB-2 than the intact ErbB-1 [104]. The mechanism of autoinhibition has not been elucidated. One theory is that the carboxyterminal region interacts with the ATP binding site [105]. By assessing FRET activity between a fluoresecent-tagged ATP analog and a C-terminal fluorophore on ErbB-1 ICD, Koland and colleagues demonstrated that tyrosine phosphorylation of the carboxyterminal residues of ErbB-1 abolishes the interaction between the extreme C-terminus and ATP observed with the inactive ICD [105]. An alternative theory is that a patch of acidic residues in the carboxyterminal region (residues 979-991) interacts with the basic residues in the juxtamembrane region (residues 645-660) to lock the TKD in an inactive conformation [106]. However, no structural information is available that validates or disproves either of these theories, as the TKD crystal structures reported to date omit the carboxyterminal region as well as the JM region.

Collectively, the last 5 years have yielded an immense amount of information about the conformational changes that occur in response to ligand

binding to create an active kinase. Future studies will determine how these distinct regions interact with each other to both activate and inactivate the receptor, and also define the role of the transmembrane domain. The data in the following chapter describe a role for the juxtamembrane region of ErbB-1 in allosteric tyrosine kinase activation. Initially, I hypothesized that the juxtamembrane region negatively regulated tyrosine kinase activity upon PKC phosphorylation, but subsequent experiments led me to change the hypothesis. The current theory is that the juxtamembrane region is required for kinase activation.

CHAPTER II

EPIDERMAL GROWTH FACTOR RECEPTOR JUXTAMEMBRANE REGION
REGULATES ALLOSTERIC TYROSINE KINASE ACTIVATION

Experimental Approach

The goal of this project is to identify the role of the ErbB-1 intracellular juxtamembrane region in kinase activation. In the literature, several approaches have been adopted to define the importance of this region of ErbB-1 relative to kinase function. Early studies incorporated juxtamembrane insertions [107] or deletions [108-110] in the full-length receptor to assess the effects of these modifications on kinase activity or binding to interacting proteins. The advantage to this strategy is the ability to determine ligand-dependent effects. Deletion of residues 645-660 (polybasic region) [108] or residues 670-674 [109] in the full-length receptor resulted in loss of tyrosine phosphorylation, but no mechanistic information was determined. Complicating the interpretation of experiments with the intact receptor is the fact that mutations with the juxtamembrane region result in a decreased population of cell-surface receptors [111].

A minimalist approach for the study of tyrosine kinase activation adopted by Kuriyan and others is to use the isolated tyrosine kinase domain [3, 4]. The limitation to this experimental strategy is that the contribution of other regions to

kinase activation cannot be determined, in addition to precluding study of ligand-mediated activation.

I chose to study the role of the juxtamembrane region in tyrosine kinase activation using a fragment comprised of the entire intracellular domain in cells. This experimental approach is intermediary between use of the intact receptor in cells and the isolated TKD *in vitro*. Other groups have used purified ICD fragments for *in vitro* studies [112-114], including creating point mutations in the ICD to assess the effect on activity [115, 116]. The drawbacks to this approach include the following: the transmembrane domain may be necessary to properly orient intracellular domains; ligand-dependent activation cannot be assessed; and the soluble ICD interacts with proteins that the intact receptor does not normally contact, which may contribute artifactually to kinase activation.

Methods

Construction of ErbB-1 ICD and Mutants

Wild-type and ΔJM mutant ICDs were completely sequenced to ensure no secondary mutations occurred during PCR amplification. Point mutants arising from wild-type or ΔJM ICD templates (T654A, T654D, I682Q, or V924R) were sequenced at the region of mutation.

All primer sequences for ICD mutants are located in Table II-1. PCR was used to amplify the entire intracellular domain of ErbB-1 (residues 645-1186) from ErbB-1-EGFP (gift of Dr. Alexander Sorkin, University of Colorado Health

Sciences). The forward primer included a HindIII restriction site, Kozak sequence and start codon; the reverse primer retained the stop codon immediately followed by an XbaI site. The ErbB-1 ICD PCR product was cloned into a pFlag CMV 5.1+ vector (Sigma). Site-directed mutagenesis (Quik-Change, Stratagene) was utilized to remove the stop codon and allow coding of the Flag epitope at the C-terminus, and the entire cDNA of ErbB-1 ICD-Flag was subjected to sequencing. The Flag epitope did not influence ErbB-1 ICD expression or tyrosine phosphorylation (data not shown), and all experiments herein utilize the ErbB-1 ICD-Flag construct unless otherwise noted. All point mutations (T654A, T654D, K721R, L834R, I682Q, V924R) were engineered into the ErbB-1 ICD-Flag construct by site-directed mutagenesis.

The sites for JM deletions were chosen based on the predicted structure of the JM region bound to micelles [63]. Specifically, the first deletion removes the first amphipathic helix, which contains the PKC phosphorylation site, and the larger deletion removes the first and second amphiphatic helices. Using ErbB-1 ICD-Flag as the template, forward primers were designed that incorporate a HindIII restriction site, a Kozak sequence, and a start codon immediately preceding the desired first residue (E663 or Q677). PCR-amplified cDNAs were digested with HindIII and ClaI and ligated into a similarly digested ErbB-1 ICD-Flag.

To create a Myc-tagged ErbB-1 ICD, the ErbB-1 ICD cDNA was shuttled from the ErbB-1 ICD-pFlag CMV 5.1+ vector into the pcDNA4-Myc/His A vector (Invitrogen). To prevent coding of the 6XHis tag at the C-terminus, a premature

stop codon was inserted between Myc and 6XHis by site-directed mutagenesis. Next, ErbB-1 ICD cDNA was shuttled from ErbB-1-Flag into the pcDNA4-Myc following digestion of both plasmids with HindIII and XbaI.

Table II-1: Primer sequences used to generate ErbB-1 ICD and mutations.

| | Primer sequences (5' to 3') | |
	Forward Primer	Reverse Primer
ErbB-1 ICD from EGFR-EGFP	GCCTGAAGCTTCACCATGCGA AGGCGCCACATCGTTCGG	CATCTAGATCATGCTCCAATAAA TTCACTGCTTTGTGGC
Mutation of stop codon in ErbB-1 ICD in pFlag	GAATTTATTGGAGCAGCATCTA GAGGATCCCGGGC	GCCCGGGATCCTCTAGATGCTG CTCCAATAAATTC
T654A ErbB-1 ICD-Flag	CGGAAGCGCGCGCTGCGGAG GCTGC	GCAGCCTCCGCAGCGCGCGCTT CCG
T654D ErbB-1 ICD-Flag	CGGAAGCGCGACCTGCGGAG GCTGC	GCAGCCTCCGCAGGTCGCGCTT CCG
K721R ErbB-1 ICD-Flag	CCCGTCGCTATCAGGGAATTA AGAGAAGCAAC	GTTGCTTCTCTTAATTCCCTGAT AGCGACGGG
I682Q ErbB-1 ICD-Flag	CAACCAAGCTCTCTTGAGGCA GTTGAAGGAAACTG	CAGTTTCCTTCAACTGCCTCAAG AGAGCTTGGTTG
V924R ErbB-1 ICD-Flag	CATGATCATGCGCAAGTGCTG GATGATAGACG	CGTCTATCATCCAGCACTTGCG CATGATCATG
Δ645-662 ErbB-1 ICD-Flag	GCCTGAAGCTTCACCATGGAG CTTGTGGAGCCTCTTACACCC AGTGGAGAAGC	CGATGATCAACTCACGGAACTTT GGG
Δ645-676 ErbB-1 ICD-Flag	GCCCGAAGCTTCACCATGCAA GCTCTCTTGAGGATCTTGAAG GAAACTG	CGATGATCAACTCACGGAACTTT GGG
Insertion of stop codon after myc in pcDNA4-myc/His	CAGAAGAGGATCTGTAGATGC ATACCGGTCATC	GATGACCGGTATGCATCTACAG ATCCTCTTCTGAG

Mutations and JM Deletions in Full-Length ErbB-1

Point mutations (T654A, T654D, I682Q, K721R, and V924R) were introduced into Flag-ErbB-1 (generously provided by Dr. Tony Burgess) by site-directed mutagenesis, and primers used for these mutations in ErbB-1 ICD (Table II-1) were used here. The strategy for introducing internal deletions into full-length ErbB-1 with an N-terminal Flag epitope is as follows. First, an EcoRV cut site was introduced by site-directed mutagenesis at nucleotides that

correspond to H648. Second EcoRV cut sites were added to this parental construct at nucleotides corresponding to either R662 or N676. Digestion with EcoRV and ligation generated either Δ648-662 or Δ648-676 Flag-ErbB-1. This cloning approach resulted in addition of two residues at deletion (Glu, Iso). All primers used for making the internal deletions are listed in Table II-2, and constructs were sequenced at the site of mutagenesis.

Table II-2: Primer sequences used to delete residues 648-662 and 648-676 in Flag-ErbB-1.

	Primer sequences (5' to 3')	
	Forward Primer	Reverse Primer
EcoRV648 Flag-ErbB-1	CATGCGAAGGCGCGATATCGTTCGG AAGC	GCTTCCGAACGATATCGCGCCTTCGCA TG
EcoRV662 Flag-ErbB-1	GAGGCTGCTGCAGGATATCGAGCTT GTGGAGC	GCTCCACAAGCTCGATATCCTGCAGCA GCCTC
EcoRV676 Flag-ErbB-1	CCCAGTGGAGAAGCTGATATCCAAG CTCTCTTG	CAAGAGAGCTTGGATATCAGCTTCTCC ACTGGG

Cell Culture and Transient Expression of ErbB-1 Constructs

COS-7 and NIH 3T3 cells were routinely maintained in 10% FBS-supplemented DMEM at 37°C with 5% CO_2. For ICD experiments in COS-7 cells: 2 ug of DNA was transiently transfected, using Lipofectamine 2000 (Invitrogen) per the manufacturer's instructions, into a 60-mm dish of COS-7 cells growing in 10% FBS/DMEM at approximately 80% confluency. When cells were co-transfected with ICD constructs, 1 ug of each construct was transfected into each 60-mm dish of COS-7 cells such that the total DNA in each dish was 2 μg. The ratio of DNA:Lipofectamine 2000 was 1 μg DNA: 3.5 μl Lipofectamine 2000 reagent in a final volume of 400 μl serum-free DMEM.

Full-length ErbB-1 constructs were transiently transfected into NIH 3T3 cells as described [3]. The ratio of DNA:FuGENE6 was 1.5 μg DNA: 4.5 μl FuGENE6 per well of 50% confluent 6-well plates of NIH 3T3 cells.

Immunoprecipitation and Blotting

For ICD experiments, transfected cells were harvested either 24 hrs. post-transfection, lysed with TGH buffer [1% Triton X-100, 10% glycerol, 50 mM Hepes (pH 7.2), 100 mM NaCl, 5 mM NaF, 1 mM Na_3VO_4, and Roche Complete-Mini protease inhibitor cocktail tablet] as described [117]. Lysates were precipitated with anti-FlagM2 (Sigma), anti-EGFR (1005, Santa Cruz Biotechnology), or anti-ErbB-4 prepared as described elsewhere [19]. Immunoprecipitates were subjected to immunoblotting with PY99 (Santa Cruz Biotechnology). To confirm equal expression, blots were stripped with 2% SDS, 100 mM β-mercaptoethanol, and 62.5 mM Tris-HCl (pH 6.8) for 20 min. at 60°C, then reprobed with anti-FlagM2, anti-EGFR (Upstate Biotech) or anti-ErbB-4. Densitometric analysis was performed using NIH ImageJ software. All results were normalized for expression levels and quantitated relative to wild-type.

For expression of full-length ErbB-1, NIH 3T3 cells were transfected for 40 hrs., starved for 60 min. with serum-free DMEM, and then treated for 5 min. with 50 ng/ml EGF (R&D) at 37°C. Lysis was performed with TGH as described above, and 100 μg of each lysate was directly subjected to immunoblotting with either EGFR PY1173 (Santa Cruz Biotechnology) or EGFR antibodies after separation by SDS-PAGE.

For co-immunoprecipitation assays, COS-7 cells were lysed 24 hrs. post-transfection with TGH and pre-incubated with Protein G-Sepharose beads (Invitrogen) to eliminate non-specific binding. Next, pre-cleared lysates were precipitated with anti-FlagM2 and blotted with anti-Myc (9E10, Santa Cruz Biotechnology) or precipitated with anti-Myc and blotted with anti-Flag. Blots were then stripped and re-probed with anti-EGFR. Whole-cell lysates were also blotted with anti-EGFR to confirm expression. Densitometric analysis was performed as for phosphotyrosine blots. Background binding of the Myc epitope to the FlagM2 antibody was subtracted; no non-specific binding to Protein G-Sepharose beads was detected (data not shown). Results are expressed relative to wild-type ErbB-1 ICD-Flag co-transfected with ErbB-1 ICD-Myc.

In Vitro Kinase Assays

In vitro kinase assays were performed essentially as described elsewhere [118]. Briefly, cells transiently transfected with 2 ug of each ICD were lysed and ICDs precipitated with anti-FlagM2. Immunoprecipitates were washed twice with TGH buffer and once with kinase assay buffer (25 mM Hepes, pH 7.4, 10 mM MgCl$_2$, 2.5 mM MnCl$_2$, 50 μM Na$_3$VO$_4$, and 0.5 mM DTT), then resuspended with 100 μl kinase assay buffer. Next, 10 μl of immunoprecipitated protein was incubated for 15 min. at room temperature with 25 μM ATP containing 62 μCi/ml [γ-^{32}P]-ATP in a total reaction volume of 40 μl. The reaction was quenched by addition of Laemmli buffer, boiled for 10 min. and separated by SDS-PAGE.

Immunostaining and Imaging of ErbB-1-Transfected Cells

NIH 3T3 cells were plated in MatTek dishes (MatTek Corporation) and transfected with ErbB-1 mutants as described above. After 24 hrs., the cells were fixed in 4% paraformaldehyde for 15 min., followed by blocking with 3% bovine serum albumin (BSA) in phosphate-buffered saline (PBS) for 15 min. at room temperature. Fixed cells were next stained with anti-Flag (rabbit polyclonal antibody, 5 µg/ml, Sigma-Aldrich) for 15 min. at 4°C in the blocking buffer. After 15-min. incubation with goat anti-rabbit Alexa-488-conjugated secondary antibody at 4°C, cells were imaged with a LSM510 confocal microscope and a Plan-Neofluar 40X oil immersion lens. The fluorophore was excited at 488 nm with an argon laser.

Results

Tyrosine Phosphorylation of the ErbB-1 ICD

To understand the contribution of the JM region to ErbB-1 receptor activation, a construct containing the entire ErbB-1 ICD (residues 645-1186) was engineered (Figure II-6A). When expressed in COS-7 cells, the ICD migrated at approximately 60-kDa and was tyrosine phosphorylated (Figure II-6B) in a manner dependent on its intrinsic kinase activity as revealed by mutagenesis of Lys721, a residue required for ATP binding in the kinase domain (Figure II-6C). The ErbB-4 ICD, which is generated by regulated intramembrane proteolysis of the full-length ErbB-4 receptor [119], is included for comparison and is similarly

tyrosine phosphorylated (Figure II-6B), as previously reported [118]. The data of

Zhang, *et al.,* show that high concentrations of purified ErbB-1 TKD promote

auto-activation [3]. However, tyrosine phosphorylation of the ICD occurs within a

milieu of intracellular proteins, thus avoiding the potential artifact of aggregation-

induced activation exhibited by the purified TKD. It also seems clear that the

expressed ICD is relatively stable because antibodies recognizing different

regions of the protein were used for analysis, and no major degradation products

were detected. Also, no aggregation of the ErbB-1 ICD was detected by

Figure II-6: Tyrosine phosphorylation of ErbB-1 ICD. **(A)** Lysates of COS-7 cells transfected with ErbB-4 or ErbB-1 ICDs were precipitated with the indicated antibodies followed by western blotting with a phosphotyrosine antibody (PY99, upper panel). Blots were stripped and reprobed with the indicated antibodies to detect either ErbB-4 ICD or ErbB-1 ICD. Similar results were obtained when lysates were directly blotted with anti-PY99 (data not shown). Asterisks (*) denote IgG. **(B)** Tyrosine phosphorylation of PKC-site mutants. The indicated ErbB-1 ICD constructs were expressed as in *(A)*, precipitated with anti-ErbB-1, and blotted with anti-PY99 (upper panel), stripped, and reprobed with anti-FlagM2 (lower panel). "Relative pY" refers to the tyrosine phosphorylation (pY) relative to wild-type after normalizing for expression levels.

immunostaining (data not shown).

Role of Thr654 Phosphorylation in Kinase Activation

To test whether modification of Thr654 influences activity of the ICD, T654A and T654D mutants were produced. Compared to the wild-type ICD, the T654A mutant ICD displays a 2.7-fold increase in tyrosine phosphorylation, while tyrosine phosphorylation of the phosphomimetic T654D mutant is decreased 2-fold (Figure II-6C). Phosphorylation of the T654A mutant is increased 8-fold relative to the T654D mutant. These results are consistent with data showing that phosphorylation of ErbB-1 at Thr654 results in a decrease in tyrosine kinase activity [120] and may imply that a population of wild-type ICD is phosphorylated on T654. Also, the data indicate that Thr654 modulates activity of the kinase domain within the context of the ICD fragment and that the mechanism does not require the presence of the ectodomain or transmembrane domain.

Based on *in vitro* interactions between a basic peptide comprising JM

Figure II-7: Effect of sphingosine treatment on tyrosine phosphorylation of ErbB-1 ICD. COS-7 cells were transiently transfected with ErbB-1 ICD or left untransfected, and then treated 24 hrs. post-transfection with vehicle (-) or 2 μM sphingosine (+) for 30 min at 37°C. Lysates were precipitated with anti-EGFR followed by blotting with anti-PY99 (upper panel) or anti-EGFR (lower panel). Sphingosine (2 μM) was maintained in lysis and immunoprecipitation buffers of sphingosine-treated samples.

residues 645-660 and phospholipid micelles, it has been proposed that an electrostatic interaction may regulate ErbB-1 kinase activation [88]. A similar interaction of the ErbB-1 ICD with the plasma membrane could potentially result in membrane-localized aggregation, which might promote constitutive kinase activation of the ICD. However, no decrease in wild-type ICD tyrosine phosphorylation occurred after treatment with 2 μM sphingosine (Figure II-7), which prevents the electrostatic interaction of JM peptides with phospholipids [65, 88].

JM Deletions Result in a Significant Loss of Kinase Activity

The preceding data suggested that phosphorylation of Thr654 alters kinase activity by either of two mechanisms: (1) phosphorylation at Thr654 promotes an autoinhibitory interaction of the JM region with the kinase domain, or (2) the JM region positively modulates the kinase domain and phosphoThr654 prevents the interaction. To test these possibilities, segments of the JM region were deleted in the ICD: Δ645-662 and Δ645-676 (Figure II-8A). The first shorter deletion removes the polybasic region and the larger deletion removes most of the JM region. When expressed in cells, the data revealed that tyrosine kinase activity is decreased by approximately 95% *in vivo* and 65% *in vitro* for the Δ645-662 mutant and about 95% for the Δ645-676 mutant *in vivo* and *in vitro* (Figure II-8B, C). This result demonstrates that the presence of the JM region is critical for maximal kinase activation.

The difference in the level of kinase activity detected for the two JM mutants also suggests that elements in both the N-terminal half of the JM, including the basic cluster and Thr654, and the C-terminal JM sequence participate in regulation of kinase activity. The studies of Zhang, *et al.*, identify
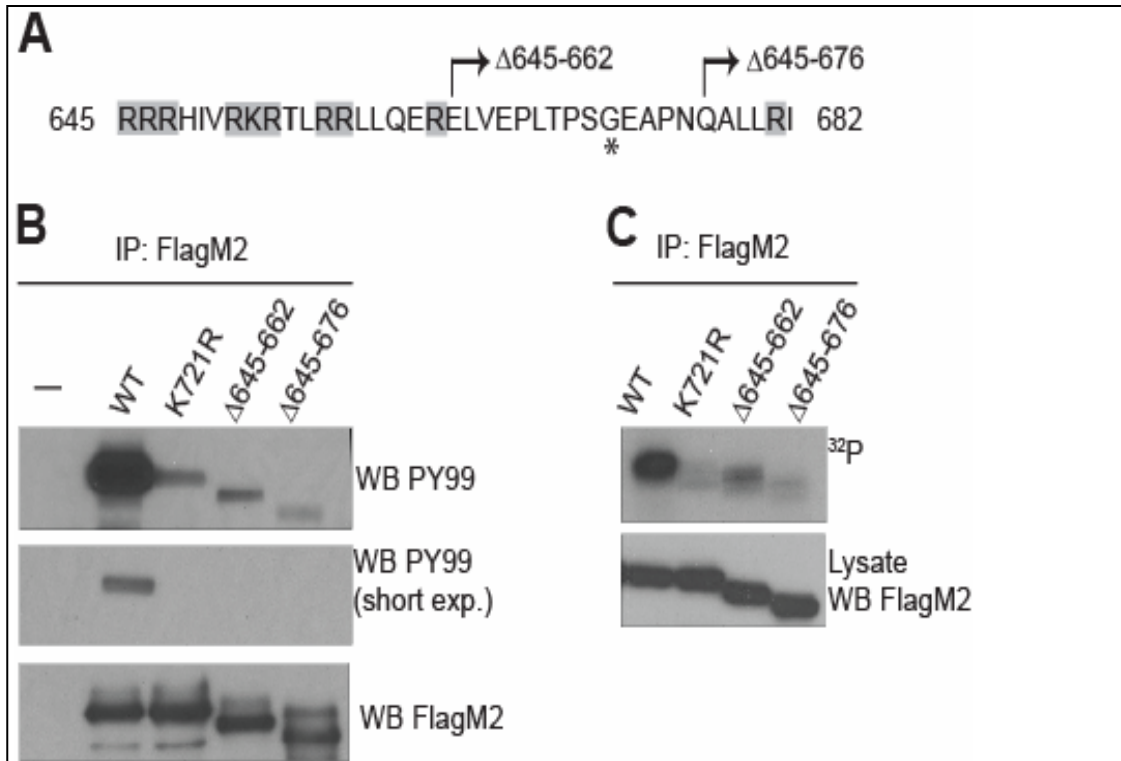
Figure II-8: Tyrosine phosphorylation of JM deletion mutants.
(A) JM residues in ErbB-1. Basic residues are shaded and Thr654 bolded as in Fig. II-6. Arrows denote the N-terminal residue of the two JM deletions in the ICD, Δ645-662 and Δ645-676. Asterisk (*) indicates the N-terminal residue of the TKD construct employed by Zhang, *et al.* [3], and Stamos, *et al.* [4], for crystallography. **(B)** Indicated ICD constructs were transiently transfected into COS-7 cells. Cell lysates were precipitated with anti-FlagM2 and blotted with anti-phosphotyrosine (PY99) or anti-FlagM2. **(C)** *In vitro* kinase assay comparing phosphorylation of ΔJM mutants to wild-type and K721R ICDs. After expression in COS-7 cells, lysis, and precipitation with anti-FlagM2, the immunoprecipitates were incubated with [γ-^{32}P]-ATP (upper panel), as described in *Materials and Methods*. Lysates were probed with anti-FlagM2 to confirm equal expression (lower panel).

Gly672-Ala677 as a likely element in the C-terminal JM region that participates in kinase activation, particularly Pro675 [3].

Contribution of the JM Region to Allosteric Kinase Activation

To address whether the JM region contributes to allosteric kinase activation, point mutations were engineered in the ICD at residues required for contacts at the asymmetric kinase dimer interface, I682Q in the N-lobe or V924R in the C-lobe of separate monomers [3]. The C-lobe V924R mutant can act only as an acceptor monomer, and the N-lobe I682Q mutant can function only as a donor to allosterically activate the acceptor monomer [3]. An experimental advantage of utilizing these mutations is that neither the N- nor the C-lobe point mutants homodimerize, thus any observed kinase activation is a result of asymmetrical dimerization of these mutants when expressed as individual monomers.

Compared to the wild-type ICD, the I682Q and the V924R ICD mutants were inactive when expressed alone (Figure II-9, lanes 3, 4). When co-expressed with a kinase-deficient K721R donor ICD, the V924R C-lobe acceptor mutant ICD was active (Figure II-9, lane 6). Co-expression of a C-lobe V924R acceptor ICD with an N-lobe I682Q donor ICD also resulted in kinase activation (Figure II-9, lane 5). This level of activation is approximately 20% of that obtained with wild-type ICD monomers (lane 1), which is comparable to that reported with the isolated TKD monomers having the same mutations [3]. One explanation for the decreased phosphorylation detected when I682Q and V924R

ICDs were co-expressed is that these mutants can only act as donors or acceptors, respectively, whereas both the N- and C-lobes of wild-type ICDs are able to participate in a dimer. These results confirm that the critical contacts between the N- and C-lobes of monomers previously shown to be required for allosteric kinase activation in the isolated TKD and the intact receptor [3] are preserved in the context of the ICD.

The results in Figure II-8 suggest, as one possibility, that the JM region may contribute to contacts at the asymmetric dimer interface and thereby influence kinase activation. Using these mutants, the capacity of the ΔJM mutants to act as donors or acceptors in allosteric kinase activation was assessed. To test ability of ΔJM mutants to act as acceptors, cells were co-transfected with either a ΔJM mutant also containing a C-lobe V924R mutation,
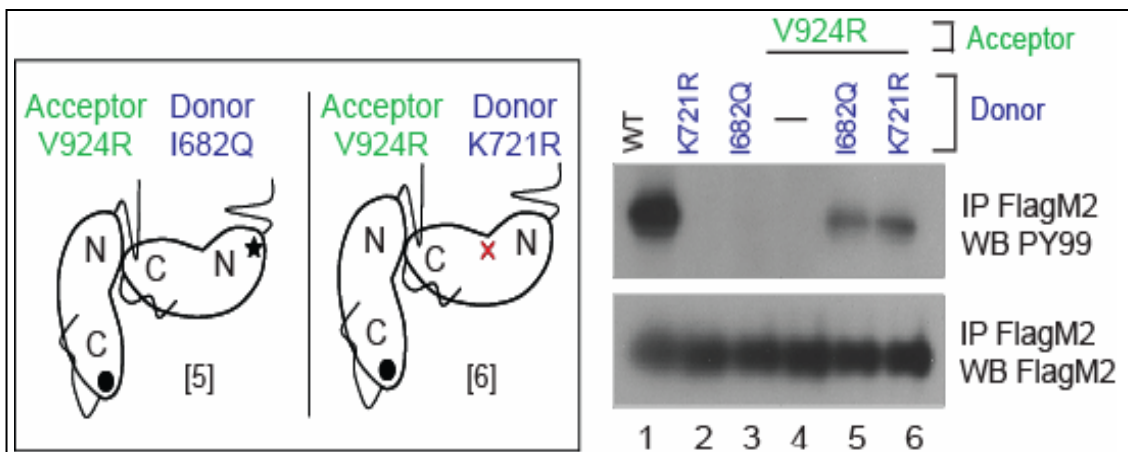
Figure II-9: Allosteric activation of ErbB-1 ICDs. *Left panel*: Cartoon of ICD mutants and predicted associations in co-expression experiments. Corresponding data lanes (right panel) are listed in brackets. Circles, V924R C-lobe mutation; stars, I682Q N-lobe mutation; X, K721R mutation; green text, acceptor monomer; blue text, donor monomer. *Right panel*: Acceptor (V924R) and donor (I682Q) monomers were expressed alone (lanes 3, 4) or co-expressed (lanes 5, 6). Lysates were precipitated with anti-FlagM2 and blotted with either anti-PY99 or anti-FlagM2.

to act as an acceptor monomer, and an N-lobe I682Q single mutant donor monomer (Figure II-9B, lanes 3 and 8). As a positive control, a V924R acceptor monomer (with an intact JM region) was co-expressed with an I682Q donor (Figure II-9B, lane 1). The data in Figure II-9B show that, compared to the positive control (lane 1), deletion of residues 645-662 decreases acceptor function by approximately 80% (lane 3), while deletion of residues 645-676 completely abrogates the capacity of that ICD to act as an acceptor monomer (lane 8).

Subsequently, the capacity of the ΔJM mutants to function as donor monomers was examined using a C-lobe V924R mutant as an acceptor monomer. To make certain the ΔJM mutants possess donor functions only, an N-lobe I682Q mutation was engineered into each ΔJM construct. Co-expression of a V924R acceptor mutant with either ΔJM donor mutant resulted in tyrosine phosphorylation of the acceptor V924R monomer (Figure II-10, lanes 5, 10), though at levels lower than the positive control, i.e., an I682Q donor with an intact JM region (lane 1). The Δ645-662 mutant demonstrated 40% of the positive control donor activity (lane 5), while the Δ645-676 mutant had 20% of the positive control activity (lane 10). This result indicates that the ΔJM mutants can still act as donors, but at a lower efficiency.

It is possible that the JM region facilitates but is not necessary for allosteric kinase activation. However, the kinase activity of the Δ645-676 mutant ICD was not rescued when a kinase-deficient K721R donor was over-expressed 10-fold relative to the Δ645-676 mutant ICD (data not shown), indicating that an

Figure II-10: Ability of JM mutants to act as acceptor or donor monomers. *Upper panel*: Cartoon of potential interactions of donor (I682Q) and acceptor (V924R) monomers with ΔJM mutants containing additional N-lobe (I682Q) or C- lobe (V924R) mutations. *Lower panel*: ΔJM mutants having N- or C-lobe mutations were co-expressed with acceptor (V924R) or donor (I682Q) monomers with intact JM regions. Tyrosine phosphorylation was assessed as in Figure II-9.

intact JM region must be present in an acceptor monomer and cannot be overcome by a concentration-dependent increase in the interaction of acceptor and donor monomers.   These data lead to the conclusion that the juxtamembrane region is essential for formation of an activated kinase acceptor.

Capacity of JM Mutants to Associate with a Wild-Type ICD

Since the ΔJM mutants are inactive, particularly as acceptors, in tyrosine kinase activation, the following experiments were performed to assess their capacity to interact with wild-type ICDs. This interaction of ΔJM and wild-type ICDs follows the strategy employed in Figures II-9 and II-10. Cells were co-transfected with Myc tagged wild-type and Flag tagged wild-type or Flag tagged ΔJM ICD constructs. All tags were placed at the carboxyterminus of each construct. Subsequently, lysates were precipitated with anti-Myc and blotted with anti-Flag. As a control for non-specific tag recognition, cells were singly transfected with the Myc or Flag tagged constructs (Figure II-11A, lanes 1-4). A low level of cross-reaction of the Flag epitope with the Myc antibody was

Figure II-11. Failure of ΔJM and T654D ICD mutants to interact with wild-type. **(A)** Flag-tagged wild-type and ΔJM mutant ICDs were transfected individually or co-transfected with wild-type-Myc ICD as described in *Materials and Methods*. Lysates were precleared on Protein G-Sepharose beads, then precipitated with anti-Myc and blotted with anti-FlagM2. The blot was stripped and re-probed with anti-EGFR. Lysates were also blotted with anti-EGFR. **(B)** T654D ICD-Flag was transfected with or without wild-type ICD-Myc as in *(A)*, and precleared lysates were precipitated with anti-Myc followed by blotting with anti-FlagM2. Expression was assessed as in *(A)*.

detected (lanes 2-4), and this background was subtracted from subsequent co-precipitation assays (lanes 5-7). The results in Figure II-11A show that interaction of Δ645-662-Flag ICD with wild-type-Myc ICD was reduced by 50% compared to wild-type-Flag ICD (lanes 5, 6), while the data in lane 7 show that the Δ645-676-Flag ICD interaction with wild-type-Myc ICD was decreased by 90%. The same results were achieved when transfected lysates were precipitated with anti-Flag and blotted with anti-Myc (data not shown). These data demonstrate that deletion of the JM region attenuates the association of the N-lobe of an acceptor with the C-lobe of a donor.
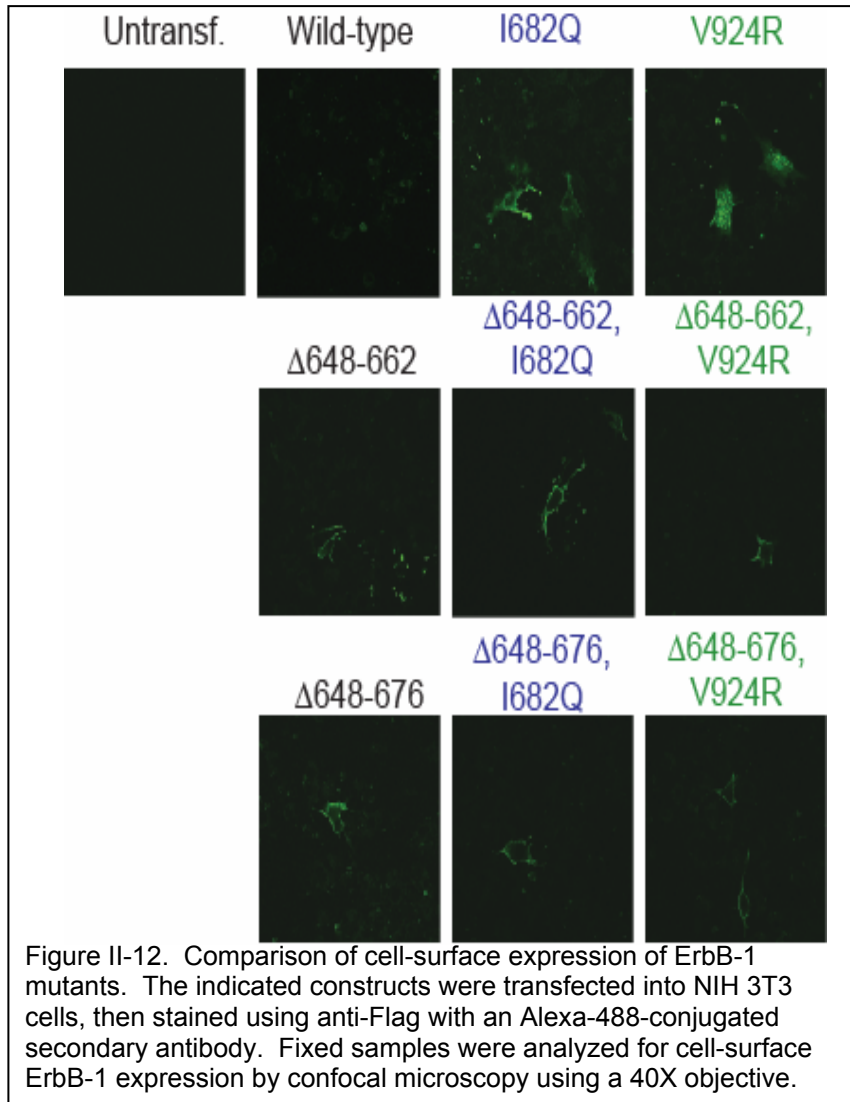
The data in Figure II-6C show that the T654D mutation in the JM region abrogates kinase activation of the ICD. In a co-precipitation experiment with Myc-tagged wild-type ICD, this Flag-tagged phosphomimetic mutant displayed a significantly decreased interaction with the wild-type ICD (Figure II-11B, lanes 4, 5), indicating that phosphorylation at Thr654 inhibits monomer:monomer associations.

Role of JM Region in Allosteric Activation of Full-Length ErbB-1

The above data collectively demonstrate that the JM region is vital for allosteric kinase activation in the ICD. This experimental model system allowed for large deletions within the JM region without concern for cell-surface expression. However, findings with fragments of a protein do not always reflect a general mechanism that is utilized by the intact receptor in a ligand-mediated fashion. Therefore, the experiments in Figures II-9 and II-10 were repeated

using full-length ErbB-1 with an N-terminal Flag epitope [5]. As a control, donor (I682Q) and acceptor (V924R) mutants in the context of intact ErbB-1 were expressed in NIH 3T3 cells as described [3], and EGF treatment resulted in tyrosine phosphorylation of these mutants only when co-expressed (Figure II-13A). These data indicate that co-expression of donor and acceptor mutants does not alter EGF-dependent activation. Previous experiments with the ICD resulted in a lower level of phosphorylation of the co-expressed donor (I682Q) and acceptor (V924R) ICD mutants compared to wild-type ICD (Figure II-9), similar to the published report using the isolated TKD [3]. Zhang, *et al.,* did not co-express the donor (I682Q) and acceptor (V924R) full-length receptor mutants, so the decrease in phosphorylation in the ICD (Figure II-9) and TKD [3] mutants compared to wild-type may be compensated for in full-length ErbB-1 by other regions of the molecule.

To aid in membrane insertion and stability, the first three charged residues (R645-R647) of the JM region that are part of the stop transfer sequence were included, so the two deletion mutants are Δ648-662 and Δ648-676 ErbB-1. All ΔJM deletion constructs were assessed for cell-surface expression by fluorescence microscopy using anti-Flag (Figure II-12) and Texas Red-conjugated EGF and cell sorting with anti-Flag (data not shown). Detection of the Flag epitope confirms cell-surface expression whereas Texas Red-EGF binding verifies that the ΔJM deletions are capable of binding EGF.

Figure II-12. Comparison of cell-surface expression of ErbB-1 mutants. The indicated constructs were transfected into NIH 3T3 cells, then stained using anti-Flag with an Alexa-488-conjugated secondary antibody. Fixed samples were analyzed for cell-surface ErbB-1 expression by confocal microscopy using a 40X objective.

The ability of the ΔJM ErbB-1 mutants to act as donors was assessed by co-expression of ΔJM,I682Q double mutants either alone (Figure II-13B, lanes 5-6 and 9-10) or with acceptors containing an intact JM region (lanes 7-8, 11-12). Consistent with the data obtained using ICD fragments, the Δ648-662,I682Q ErbB-1 donor mutant retains activity when co-expressed with a V924R ErbB-1 acceptor mutant, and the level of EGF-stimulated tyrosine phosphorylation was similar to phosphorylation of the positive control (Figure II-13B, lanes 4 and 8).
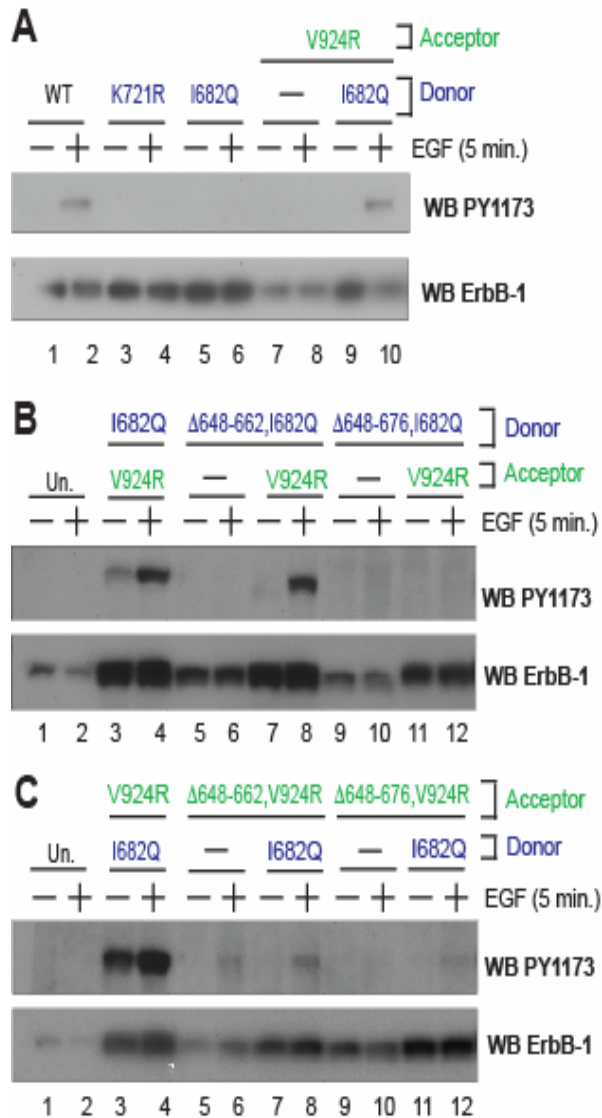
Figure II-13: Role of JM region in allosteric activation of EGF-treated ErbB-1. **(A)** NIH 3T3 cells were transiently transfected with the indicated constructs. Forty hrs. later, cells were starved for 60 min. in serum-free media, then treated with EGF (50 ng/ml) for 5 min. Lysates were immediately blotted with either ErbB-1 (upper panels) or phosphosite-specific ErbB-1 PY1173 (lower panels). Panels **(B)** and **(C)** represent experiments assessing the ability of JM deletions to act either as donors **(B)** or acceptors **(C)**. It should be noted that the larger deletion, Δ648-676, had dramatically reduced expression compared to mutants with an intact JM region.

This result is especially important because it verifies cell-surface expression, ligand binding, and activation of the Δ648-662,I682Q ErbB-1 mutant equivalent to the control. In contrast, the larger deletion displayed marked reduction in phosphorylation (lanes 9, 10). Although Δ648-676 ErbB-1 acceptor and donor mutants were detected on the cell surface by anti-Flag staining (Figure II-12), analysis by flow cytometry revealed that cell surface expression of Δ648-676 ErbB-1 is significantly less than that of wild-type ErbB-1 (data not shown). This decrease in cell-surface expression is by no means unexpected due to the large region deleted. Because the JM linker between the TM domain and the TKD has been removed, the TKD is now directly adjacent to the plasma membrane. This may present a steric hindrance to efficient membrane insertion or sequences in the deleted region may be required for processing to the cell surface. Since the shorter deletion does reach the cell surface, this would imply that the region defined by residues 663-676 may be required for trafficking the intact receptor to the cell surface. Already identified in this region are basolateral sorting signals [67].

In agreement with the hypothesis that the JM region facilitates interactions required for allosteric kinase activation, deletion of the JM region in the intact receptor abrogated acceptor functions for both ΔJM constructs (Figure II-13C, lanes 8, 12). The loss in tyrosine phosphorylation for the ΔJM ErbB-1 mutants is greater than 80% that of the positive control. This result confirms the conclusions drawn from experiments using the ICD by showing that deletion of
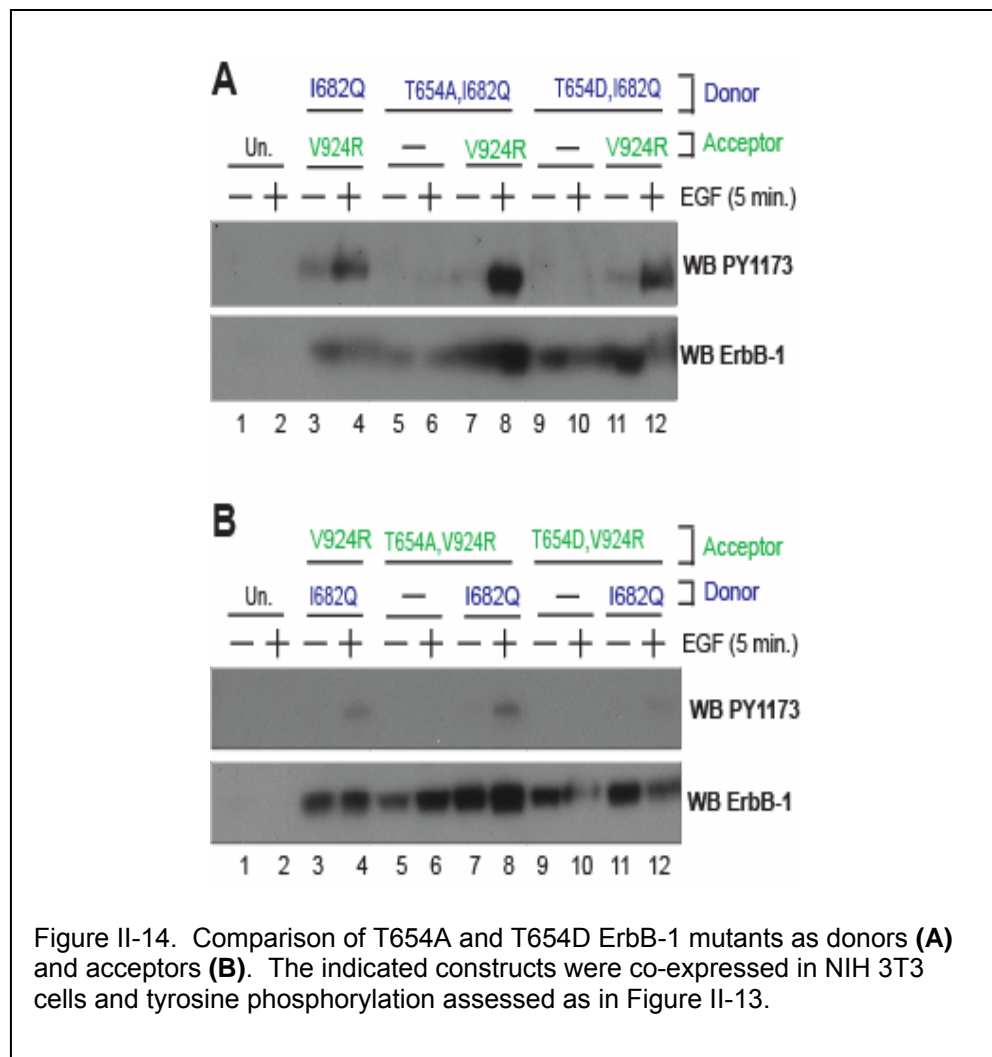
the JM region prevents ligand-stimulated activation in the transmembrane receptor.

It was hypothesized that PKC phosphorylation inhibits the interactions required for allosteric kinase activation based on three pieces of information: 1) PKC phosphorylation of T654 results in decreased kinase activation [69]; 2) the phosphomimetic T654D mutant ICD exhibited a 50% reduction in tyrosine phosphorylation compared to wild-type (Figure II-6B); and 3) the phosphomimetic mutant displayed a 50% decrease in interaction with a wild-type ICD (Figure II-11B). Thus, the ability of T654A and T654D ErbB-1 mutants to act as donors and acceptors was assessed in the intact receptor.

The data in Figure II-14 demonstrate that the T654A ErbB-1 mutant is a better donor than the positive control as measured by tyrosine phosphorylation in response to EGF stimulation (Figure II-14A, lanes 4, 8). This finding is consistent with the T654A ICD mutant that displays a significant increase (about 2.7-fold) in tyrosine phosphorylation compared to the wild-type phosphorylation (Figure II-6). However, mechanistically it is not clear how preventing PKC phosphorylation of the donor N-lobe affects activity of the acceptor monomer in the Kuriyan model of allosteric kinase activation. No difference in tyrosine phosphorylation of the I682Q donor mutant and the T654D,I682Q donor mutant was detected (Figure II-14A, lanes 4, 12), indicating that, in contrast to the T654A mutant, the phosphomimetic mutation did not affect donor activity.

Next tested were the capabilities of T654 mutants to act as acceptors. The results obtained in this experiment were not as striking as deletion of the JM

region. As shown in Figure II-14B, the T654A/V924R ErbB-1 acceptor mutant was a slightly better acceptor than the positive control (lanes 4, 8), and the acceptor function decreased slightly with the T654D/V924R acceptor mutant (lane 12). These data are not sufficient to conclude that phosphorylation of T654 disrupts the asymmetric dimer in the intact receptor stimulated with EGF.

Figure II-14. Comparison of T654A and T654D ErbB-1 mutants as donors **(A)** and acceptors **(B)**. The indicated constructs were co-expressed in NIH 3T3 cells and tyrosine phosphorylation assessed as in Figure II-13.

Effect of ErbB-1 Tyrosine Kinase Inhibitor on T654A ICD Activity

Several reports in the literature describe how mutations in the ErbB-1 TKD affect binding of ATP and the ATP analog TKIs such as gefitinib (Iressa) and erlotinib (Tarceva, reviewed in ref. [23]). In an effort to understand why the T654A ErbB-1 ICD had a nearly 3-fold increase in tyrosine phosphorylation as

Figure II-15: T654A ICD displays increased sensitivity to erlotinib (Tarceva). COS-7 cells were transiently transfected with either wild-type or T654A ICD and treated 24 h later with the indicated concentrations of erlotinib for 60 min. Lysates were precipitated with anti-ErbB-1 and blotted with either anti-PY99 (upper panel) or anti-ErbB-1 (lower panel). Right panel: quantitation of results. Numbers in bars indicated percent decrease in tyrosine phosphorylation compared to untreated controls (0).

compared to wild-type ICD, COS-7 cells expressing T654A ICD were treated with increasing concentrations of erlotinib for 60 min. and tyrosine phosphorylation assessed. The data in Figure II-15 reveal a dose-dependent decrease in tyrosine phosphorylation for T654A ICD, with a significant decrease in tyrosine phosphorylation at lower concentrations of inhibitor than wild-type. This experiment supports the idea that the JM region has an influence on the ATP

binding site and thereby kinase activity. Further experiments are necessary to test if the T654A mutant has a higher affinity for ATP like the TKD mutations, but it is intriguing that mutation at a site distal to the ATP binding site affects sensitivity to an ATP analog.

CHAPTER III

CONCLUSIONS

Several RTKs, excluding the ErbB receptors, contain one or more tyrosine residues in the JM region that must be phosphorylated in *trans* for complete kinase activation [121]. Gain-of-function, oncogenic mutations in the JM region of the RTK Kit are frequently found in patients with gastrointestinal stromal tumors (GIST) [122], hinting at a consistent autoinhibitory role for the JM region. In fact, 67% of GIST patients harbor mutations in the Kit JM region [123], compared to ErbB-1 in which ICD mutations have only been detected in the TKD [23]. The crystal structure of the intracellular domain of Kit revealed that the JM region interacts in *cis* with the A-loop of the TKD to lock the protein in an inactive conformation [124]. Autophosphorylation of a critical tyrosine residue in the Kit JM region destabilizes the closed conformation, allowing for activation of kinase activity [124], and mutations in the JM region disrupt the autoinhibitory interaction of the JM region with its TKD [125, 126]. Thus, in Kit JM mutants, the kinase domain is in a constitutively open and active conformation. A similar mechanism for kinase inactivation exists for the related receptors FLT3 [127], c-fms [128] and most likely PDGF receptor-β [121], as well as the ephrin receptors EphB2 [129] and EphA4 [130].

In contrast, PKC phosphorylation of the ErbB-1 and ErbB-2 JM region promotes kinase inactivation [69, 89, 90]. The insulin receptor contains three JM

tyrosine residues, but none of these contribute to regulation of kinase activity [121]. Hence, the role of the JM region in kinase activity is not conserved amongst all RTKs, and the data presented in the previous chapter indicate the JM region of ErbB-1 has a distinct function from that of Kit, i.e., that the ErbB-1 JM region promotes rather than inhibits kinase activity and phosphorylation of T654 destabilizes this relationship. Unclear, however, is how phosphorylation of T654 within the JM region attenuates activation. It was initially proposed that the JM region serves as autoinhibitory region similar to that of Kit, and T654 phosphorylation stabilizes the auto-inhibited state. By that logic, deletion of the JM region should result in an increase in tyrosine phosphorylation similar to the results with the T654A mutant ICD. In direct contrast to that theory, the data in the previous chapter clearly demonstrate that the JM region is not responsible for autoinhibition.

In the experiments evaluating the capacity of T654D ErbB-1 to act as an acceptor, only a slight decrease in tyrosine phosphorylation of the phosphomimetic mutant was detected compared to the positive control (Figure II-14). This modest decrease in activity does not correspond to the 50% reduction in tyrosine phosphorylation of the T654D ICD mutant (Figure II-6). In the full-length system, EGF-stimulated tyrosine phosphorylation of the T654D mutant with no acceptor or donor mutations was not tested. In a parallel experiment, I attempted to validate T654 phosphorylation of wild-type ICD after TPA treatment by immunoblotting with a PKC phosphosite-specific antibody and by mass spectrometery, but both were unsuccessful. The antibody recognized TPA-

treated T654A ICD in addition to wild-type ICD, so the specificity of this reagent is questionable. Due to the large stretch of lysines and arginines flanking T654, traditional trypsin digest was not an option. Digestion with Glu-C (cleaves peptide bond C-terminal to Glu) did not yield a fragment containing T654. In data not presented, a T654D ICD acceptor (V924R) mutant was co-expressed with a ΔJM donor (I682Q) mutant to test whether T654 phosphorylation affected allosteric kinase activation. The ΔJM mutant was used as a donor because its lower molecular weight allows for comparing phosphorylation of each ICD expressed. Again, only a slight decrease in tyrosine phosphorylation of was detected when T654D was expressed as an acceptor compared to the positive control. Collectively, these data suggest that T654 phosphorylation may not completely disrupt acceptor N-lobe interactions with the donor C-lobe.

The critical finding that initiated this study was the loss of kinase activity with the ΔJM mutants (Figure II-8). These data strongly suggested that the JM region in some way facilitates intracellular kinase activity. By first expressing the entire ICD of ErbB-1 in cells, the contribution of the JM region in the formation of an active kinase was assessed. The data presented in the preceding chapter indicate that the JM region is essential for maximal allosteric activation of ICD kinase activity (Figure II-10). Extending these experiments to incorporate the intact receptor revealed that the requirement for the JM region is preserved in the context of the full-length receptor in a ligand-dependent manner (Figure II-13).

While other studies have demonstrated that deletion of portions the JM region (residues 645-657) abrogates kinase activity in the intact receptor [108,

131], this is the first report to elucidate the mechanism by which the JM region regulates kinase activation. The study of Zhang *et al.,* which includes residues 672-682 of the JM region, showed that Pro675 within the JM region of an acceptor TKD interacts with Val956 in the C-lobe of a donor TKD, and a P675G TKD mutant has diminished activity *in vitro* [3]. However, this proline residue is contained in our Δ645-662 ICD construct. Therefore, this study defines residues distal to Pro675 in allosteric kinase activation, implicating new residues within the JM region.

No crystallographic studies include the complete juxtamembrane or carboxyterminal regions [3, 4], so the contribution of these regions to the allosteric mechanism of activation remains poorly defined. While the study by Kuriyan's group made a significant advance in understanding how kinase activation of ErbB receptors is initiated, several questions remain. First, what other structural changes must occur for complete activation? Trimers were ruled out as a mode of oligomerization [3], so how does the donor monomer become an active kinase? Is the donor monomer able to also act as an acceptor? What is the structure of an active dimer? How is the kinase inactivated? The data presented here indicate that the JM region facilitates formation of an active kinase, but does the carboxyterminal region also contribute to the mechanism of activation? Lemmon has used X-ray scattering in solution to measure structural changes of ErbB-1 ectodomain (personal communication), and this technique can differentiate between intra- and inter-molecular interactions. This approach would be valuable to ask where the JM region of the acceptor monomer connects

the donor monomer, as well as the location of the carboxyterminal region in context of the asymmetrical dimer.

Previous studies using peptides representing the polybasic JM region of ErbB-1 identified an acidic region in the C-lobe of the TKD that interacts with the polybasic JM peptide [106]. Deletion of the polybasic region results in an inactive receptor [131], consistent with our findings. Therefore, this may be the region in the donor monomer makes contacts with the JM region from an acceptor monomer to facilitate allosteric kinase activation.

A related issue is to determine how the mutations in the ErbB-1 TKD in lung cancer alter the structure of the ErbB-1 TKD to increase affinity for TKIs. Yun, *et al.,* recently reported crystal structures of wild-type and L858R ErbB-1 TKD bound to gefitinib (ErbB-1 TKI) and AEE788 (dual ErbB-1/vascular endothelial growth factor receptor TKI) [36]. Not surprisingly, this group found that the L858R mutant, which lies in the A-loop, bound gefitinib with a 20-fold higher affinity and displayed a 50-fold increase in activity *in vitro* compared to wild-type [36]. As expected, the L858R mutant TKD was crystallized in an active conformation [36].

My data indicate that a T654D/L834R (alternative numbering) double mutant in the context of the ErbB-1 ICD has elevated tyrosine phosphorylation similar to that of L834R alone (data not shown). If the L858R mutant is in a constitutively active conformation, this conformation may circumvent the need for intracellular dimerization for kinase activation, although one study detected cross-linked dimers of full-length L858R ErbB-1 in a lung cancer cell line in the

absence of EGF stimulation [132]. A relevant experiment would be to investigate whether oncogenic mutations in the TKD, such as L858R and Δ746-750, influence allosteric kinase activation using the experimental strategy in this and Kuriyan's study [3]. In other words, does introduction of an N-lobe (donor) or a C-lobe (acceptor) mutation in the context of the L858R mutation abrogate basal or EGF-stimulated activity? If ICD dimerization is not required for transition to the active conformation, then the dimer interface mutants will not affect activity of the oncogenic mutants.

The study comparing phosphorylation of wild-type and the T654A mutant ICDs after treatment with the tyrosine kinase inhibitor (TKI) erlotinib yielded insight into the possibility that the JM region interacts with the TKD of the ICD because mutation at a site distal to the kinase active site affected not only basal kinase activity, but also sensitivity to the TKI. In an attempt to understand why TKD mutations L858R and Δ746-750 are more sensitive to TKIs, kinetic analysis revealed that mutant ICDs have higher affinity for ATP and kinase activity towards an exogenous substrate [116]. While no human mutations in the JM region of ErbB-1 have been reported, analysis of this activating T654A mutant will potentially advance the knowledge of the fold of the ICD and how one region interacts with another either in *cis* or in *trans* on an adjacent monomer to facilitate activation. It is still unclear mechanistically why this mutation is more active than the wild-type.

By far the most important finding of this project is that the JM region is able to modulate activity of the kinase. The unusual mechanism of allosterically

regulating kinase activity presents an interesting alternative for traditional TKIs. The current TKIs are most effective in patients harboring activating mutations in ErbB-1 TKD, but that population of patients only represents a small subset of all tumors that overexpress ErbB-1, so other approaches for inhibiting activity of wild-type receptors are necessary. Inhibitory molecules that target to the JM region of ErbB-1 and not the active site may be therapeutically advantageous since the JM region of other RTKs, such as Kit, have a divergent function in kinase activation and do not contain the polybasic region. One downside to targeting the JM region is that so many other pieces of information are contained within this relatively small region, and the importance of these other signaling entities are not fully undersood.

With over 30 years of research on ErbB-1, it is fascinating that the basic mechanisms of activation are still being uncovered. The structural study by Kuriyan's group last year made great strides in understanding how kinase activation is initiated intracellularly in addition to disproving the generally-accepted dogma of symmetrical TKD dimerization. This study fills in another gap of knowledge by elucidating how the JM region participates in activation, and serves to open "old" doors towards understanding how each of the regions in the intracellular domain cooperate to form an active kinase.

REFERENCES

1.   Linggi, B. and G. Carpenter. (2006). ErbB receptors: new insights on mechanisms and biology. *Trends in Cell Biology* **16**: 649.

2.   Yarden, Y. and M.X. Sliwkowski. (2001). Untangling the ErbB signalling network. *Nat Rev Mol Cell Biol* **2**: 127-37.

3.   Zhang, X., J. Gureasko, K. Shen, P.A. Cole, and J. Kuriyan. (2006). An allosteric mechanism for activation of the kinase domain of epidermal growth factor receptor. *Cell* **125**: 1137-49.

4.   Stamos, J., M.X. Sliwkowski, and C. Eigenbrot. (2002). Structure of the epidermal growth factor receptor kinase domain alone and in complex with a 4-anilinoquinazoline inhibitor. *J Biol Chem* **277**: 46265-72.

5.   Garrett, T.P., N.M. McKern, M. Lou, T.C. Elleman, T.E. Adams, G.O. Lovrecz, et al. (2002). Crystal structure of a truncated epidermal growth factor receptor extracellular domain bound to transforming growth factor alpha. *Cell* **110**: 763-73.

6.   Ogiso, H., R. Ishitani, O. Nureki, S. Fukai, M. Yamanaka, J.H. Kim, et al. (2002). Crystal structure of the complex of human epidermal growth factor and receptor extracellular domains. *Cell* **110**: 775-87.

7.   Wahl, M.I., T.O. Daniel, and G. Carpenter. (1988). Antiphosphotyrosine recovery of phospholipase C activity after EGF treatment of A-431 cells. *Science* **241**: 968-70.

8.   Nishibe, S., M.I. Wahl, S.M. Hernandez-Sotomayor, N.K. Tonks, S.G. Rhee, and G. Carpenter. (1990). Increase of the catalytic activity of phospholipase C-gamma 1 by tyrosine phosphorylation. *Science* **250**: 1253-6.

9.   Lowenstein, E.J., R.J. Daly, A.G. Batzer, W. Li, B. Margolis, R. Lammers, et al. (1992). The SH2 and SH3 domain-containing protein GRB2 links receptor tyrosine kinases to ras signaling. *Cell* **70**: 431.

10. Gale, N.W., S. Kaplan, E.J. Lowenstein, J. Schlessinger, and D. Bar-Sagi. (1993). Grb2 mediates the EGF-dependent activation of guanine nucleotide exchange on Ras. *Nature* **363**: 88.

11. Lin, S.-Y., K. Makino, W. Xia, A. Matin, Y. Wen, K.Y. Kwong, et al. (2001). Nuclear localization of EGF receptor and its potential new role as a transcription factor. *Nat Cell Biol* **3**: 802.

12. Liao, H.-J. and G. Carpenter. (2007). Role of the Sec61 Translocon in EGF Receptor Trafficking to the Nucleus and Gene Expression. *Mol. Biol. Cell* **18**: 1064-1072.

13. Wickner, W. and R. Schekman. (2005). Protein Translocation Across Biological Membranes. *Science* **310**: 1452-1456.

14. Sandvig, K. and B. van Deurs. (2002). Transport of protein toxins into cells: pathways used by ricin, cholera toxin and Shiga toxin. *FEBS Lett* **529**: 49-53.

15. Ostman, A., C. Hellberg, and F.D. Bohmer. (2006). Protein-tyrosine phosphatases and cancer. *Nat Rev Cancer* **6**: 307.

16. Carpenter, G. and S. Cohen. (1976). 125I-labeled human epidermal growth factor. Binding, internalization, and degradation in human fibroblasts. *J. Cell Biol.* **71**: 159-171.

17. Beguinot, L., R.M. Lyall, M.C. Willingham, and I. Pastan. (1984). Down-Regulation of the Epidermal Growth Factor Receptor in KB Cells is due to Receptor Internalization and Subsequent Degradation in Lysosomes. *Proc Natl Acad Sci U S A* **81**: 2384-2388.

18. Hanover, J.A., M.C. Willingham, and I. Pastan. (1984). Kinetics of transit of transferrin and epidermal growth factor through clathrin-coated membranes. *Cell* **39**: 283-93.

19. Baulida, J., M.H. Kraus, M. Alimandi, P.P. Di Fiore, and G. Carpenter. (1996). All ErbB receptors other than the epidermal growth factor receptor are endocytosis impaired. *J Biol Chem* **271**: 5251-7.

20. Di Guglielmo, G.M., P.C. Baass, W.J. Ou, B.I. Posner, and J.J. Bergeron. (1994). Compartmentalization of SHC, GRB2 and mSOS, and hyperphosphorylation of Raf-1 by EGF but not insulin in liver parenchyma. *Embo J* **13**: 4269-77.

21. Vieira, A.V., C. Lamaze, and S.L. Schmid. (1996). Control of EGF Receptor Signaling by Clathrin-Mediated Endocytosis. *Science* **274**: 2086-2089.

22. Downward, J., Y. Yarden, E. Mayes, G. Scrace, N. Totty, P. Stockwell, et al. (1984). Close similarity of epidermal growth factor receptor and v-erb-B oncogene protein sequences. *Nature* **307**: 521-7.

23. Sharma, S.V., D.W. Bell, J. Settleman, and D.A. Haber. (2007). Epidermal growth factor receptor mutations in lung cancer. *Nat Rev Cancer* **7**: 169-81.

24. Cruz, J.J., A. Ocana, E. Del Barco, and A. Pandiella. (2007). Targeting receptor tyrosine kinases and their signal transduction routes in head and neck cancer. *Ann Oncol* **18**: 421-430.

25. Zhang, W., M. Gordon, and H.J. Lenz. (2006). Novel approaches to treatment of advanced colorectal cancer with anti-EGFR monoclonal antibodies. *Ann Med* **38**: 545-51.

26. Hochster, H.S., D.G. Haller, A. de Gramont, J.D. Berlin, P.A. Philip, M.J. Moore, et al. (2006). Consensus report of the international society of gastrointestinal oncology on therapeutic progress in advanced pancreatic cancer. *Cancer* **107**: 676-85.

27. Yao, M., T. Shuin, H. Misaki, and Y. Kubota. (1988). Enhanced Expression of c-myc and Epidermal Growth Factor Receptor (C-erbB-1) Genes in Primary Human Renal Cancer. *Cancer Res* **48**: 6753-6757.

28. Posadas, E.M., M.S. Liel, V. Kwitkowski, L. Minasian, A.K. Godwin, M.M. Hussain, et al. (2007). A phase II and pharmacodynamic study of gefitinib in patients with refractory or recurrent epithelial ovarian cancer. *Cancer* **109**: 1323-30.

29. Aklilu and Ilson. (2007). Targeted Agents and Esophageal Cancer-The Next Step? *Seminars in Radiation Oncology* **17**: 62.

30. Yamazaki, H., Y. Fukui, Y. Ueyama, N. Tamaoki, T. Kawamoto, S. Taniguchi, et al. (1988). Amplification of the structurally and functionally altered epidermal growth factor receptor gene (c-erbB) in human brain tumors. *Mol Cell Biol* **8**: 1816-20.

31. Paez, J.G., P.A. Janne, J.C. Lee, S. Tracy, H. Greulich, S. Gabriel, et al. (2004). EGFR mutations in lung cancer: correlation with clinical response to gefitinib therapy. *Science* **304**: 1497-500.

32. Lynch, T.J., D.W. Bell, R. Sordella, S. Gurubhagavatula, R.A. Okimoto, B.W. Brannigan, et al. (2004). Activating mutations in the epidermal growth factor receptor underlying responsiveness of non-small-cell lung cancer to gefitinib. *N Engl J Med* **350**: 2129-39.

33. Pao, W., V. Miller, M. Zakowski, J. Doherty, K. Politi, I. Sarkaria, et al. (2004). EGF receptor gene mutations are common in lung cancers from "never smokers" and are associated with sensitivity of tumors to gefitinib and erlotinib. *Proc Natl Acad Sci U S A* **101**: 13306-13311.

34. Ji, H., X. Zhao, Y. Yuza, T. Shimamura, D. Li, A. Protopopov, et al. (2006). Epidermal growth factor receptor variant III mutations in lung tumorigenesis and sensitivity to tyrosine kinase inhibitors. *Proc Natl Acad Sci U S A* **103**: 7817-22.

35. Ji, H., D. Li, L. Chen, T. Shimamura, S. Kobayashi, K. McNamara, et al. (2006). The impact of human EGFR kinase domain mutations on lung tumorigenesis and in vivo sensitivity to EGFR-targeted therapies. *Cancer Cell* **9**: 485.

36. Yun, C.-H., T.J. Boggon, Y. Li, M.S. Woo, H. Greulich, M. Meyerson, et al. (2007). Structures of Lung Cancer-Derived EGFR Mutants and Inhibitor Complexes: Mechanism of Activation and Insights into Differential Inhibitor Sensitivity. *Cancer Cell* **11**: 217.

37. Wood, E.R., A.T. Truesdale, O.B. McDonald, D. Yuan, A. Hassell, S.H. Dickerson, et al. (2004). A unique structure for epidermal growth factor receptor bound to GW572016 (Lapatinib): relationships among protein

conformation, inhibitor off-rate, and receptor activity in tumor cells. *Cancer Res* **64**: 6652-9.

38.   Jackman, D.M., B.Y. Yeap, L.V. Sequist, N. Lindeman, A.J. Holmes, V.A. Joshi, et al. (2006). Exon 19 deletion mutations of epidermal growth factor receptor are associated with prolonged survival in non-small cell lung cancer patients treated with gefitinib or erlotinib. *Clin Cancer Res* **12**: 3908-14.

39.   Bonner, J.A., P.M. Harari, J. Giralt, N. Azarnia, D.M. Shin, R.B. Cohen, et al. (2006). Radiotherapy plus Cetuximab for Squamous-Cell Carcinoma of the Head and Neck. *N Engl J Med* **354**: 567-578.

40.   Burtness, B., M.A. Goldwasser, W. Flood, B. Mattar, and A.A. Forastiere. (2005). Phase III Randomized Trial of Cisplatin Plus Placebo Compared With Cisplatin Plus Cetuximab in Metastatic/Recurrent Head and Neck Cancer: An Eastern Cooperative Oncology Group Study. *J Clin Oncol* **23**: 8646-8654.

41.   Yarden, Y. and J. Schlessinger. (1987). Epidermal growth factor induces rapid, reversible aggregation of the purified epidermal growth factor receptor. *Biochemistry* **26**: 1443-51.

42.   Cho, H.S. and D.J. Leahy. (2002). Structure of the extracellular region of HER3 reveals an interdomain tether. *Science* **297**: 1330-3.

43.   Cho, H.S., K. Mason, K.X. Ramyar, A.M. Stanley, S.B. Gabelli, D.W. Denney, Jr., et al. (2003). Structure of the extracellular region of HER2 alone and in complex with the Herceptin Fab. *Nature* **421**: 756-60.

44.   Bouyain, S., P.A. Longo, S. Li, K.M. Ferguson, and D.J. Leahy. (2005). The extracellular region of ErbB4 adopts a tethered conformation in the absence of ligand. *Proc Natl Acad Sci U S A* **102**: 15024-15029.

45.   Mendrola, J.M., M.B. Berger, M.C. King, and M.A. Lemmon. (2002). The single transmembrane domains of ErbB receptors self-associate in cell membranes. *J Biol Chem* **277**: 4704-12.

46. Ferguson, K.M., M.B. Berger, J.M. Mendrola, H.-S. Cho, D.J. Leahy, and M.A. Lemmon. (2003). EGF Activates Its Receptor by Removing Interactions that Autoinhibit Ectodomain Dimerization. *Mol Cell* **11**: 507.

47. Mattoon, D., P. Klein, M.A. Lemmon, I. Lax, and J. Schlessinger. (2004). The tethered configuration of the EGF receptor extracellular domain exerts only a limited control of receptor function. *Proc Natl Acad Sci U S A* **101**: 923-928.

48. Lemmon, M.A., Z. Bu, J.E. Ladbury, M. Zhou, D. Pinchasi, I. Lax, et al. (1997). Two EGF molecules contribute additively to stabilization of the EGFR dimer. *Embo J* **16**: 281-94.

49. Cho, H.-S., K. Mason, K.X. Ramyar, A.M. Stanley, S.B. Gabelli, D.W. Denney, et al. (2003). Structure of the extracellular region of HER2 alone and in complex with the Herceptin Fab. *Nature* **421**: 756.

50. Chu, C.T., K.D. Everiss, C.J. Wikstrand, S.K. Batra, H.J. Kung, and D.D. Bigner. (1997). Receptor dimerization is not a factor in the signalling activity of a transforming variant epidermal growth factor receptor (EGFRvIII). *Biochem J* **324 (Pt 3)**: 855-61.

51. Senes, A., D.E. Engel, and W.F. DeGrado. (2004). Folding of helical membrane proteins: the role of polar, GxxxG-like and proline motifs. *Current Opinion in Structural Biology* **14**: 465.

52. Gerber, D., N. Sal-Man, and Y. Shai. (2004). Two Motifs within a Transmembrane Domain, One for Homodimerization and the Other for Heterodimerization. *J. Biol. Chem.* **279**: 21177-21182.

53. Bargmann, C.I., M.-C. Hung, and R.A. Weinberg. (1986). Multiple independent activations of the neu oncogene by a point mutation altering the transmembrane domain of p185. *Cell* **45**: 649.

54. Weiner, D.B., J. Liu, and M.I. Greene. (1989). A point mutation in the neu oncogene mimics ligand induction of receptor aggregation. *Nature* **339**: 230.

55.   Vidal, G.A., D.E. Clark, L. Marrero, and F.E. Jones. (2006). A constitutively active ERBB4/HER4 allele with enhanced transcriptional coactivation and cell-killing activities. *Oncogene*.

56.   Hubbard, S.R. and W.T. Miller. (2007). Receptor tyrosine kinases: mechanisms of activation and signaling. *Current Opinion in Cell Biology* **19**: 117.

57.   Hubbard, S.R. (1997). Crystal structure of the activated insulin receptor tyrosine kinase in complex with peptide substrate and ATP analog. *Embo J* **16**: 5572-81.

58.   Hubbard, S.R., L. Wei, and W.A. Hendrickson. (1994). Crystal structure of the tyrosine kinase domain of the human insulin receptor. *Nature* **372**: 746.

59.   Biscardi, J.S., M.-C. Maa, D.A. Tice, M.E. Cox, T.-H. Leu, and S.J. Parsons. (1999). c-Src-mediated Phosphorylation of the Epidermal Growth Factor Receptor on Tyr845 and Tyr1101 Is Associated with Modulation of Receptor Function. *J. Biol. Chem.* **274**: 8335-8343.

60.   Gotoh, N., A. Tojo, M. Hino, Y. Yazaki, and M. Shibuya. (1992). A highly conserved tyrosine residue at codon 845 within the kinase domain is not required for the transforming activity of human epidermal growth factor receptor. *Biochemical and Biophysical Research Communications* **186**: 768.

61.   Tice, D.A., J.S. Biscardi, A.L. Nickles, and S.J. Parsons. (1999). Mechanism of biological synergy between cellular Src and epidermal growth factor receptor. *Proc Natl Acad Sci U S A* **96**: 1415-1420.

62.   Jeffrey, P.D., A.A. Russo, K. Polyak, E. Gibbs, J. Hurwitz, J. Massague, et al. (1995). Mechanism of CDK activation revealed by the structure of a cyclinA-CDK2 complex. *Nature* **376**: 313.

63.   Choowongkomon, K., C.R. Carlin, and F.D. Sonnichsen. (2005). A structural model for the membrane-bound form of the juxtamembrane domain of the epidermal growth factor receptor. *J Biol Chem* **280**: 24043-52.

64.   Choowongkomon, K., M.E. Hobert, C. He, C.R. Carlin, and F.D. Sonnichsen. (2004). Aqueous and micelle-bound structural characterization of the epidermal growth factor receptor juxtamembrane domain containing basolateral sorting motifs. *J Biomol Struct Dyn* **21**: 813-26.

65.   Sato, T., P. Pallavi, U. Golebiewska, S. McLaughlin, and S.O. Smith. (2006). Structure of the membrane reconstituted transmembrane-juxtamembrane peptide EGFR(622-660) and its interaction with Ca2+/calmodulin. *Biochemistry* **45**: 12704-14.

66.   Kil, S.J., M. Hobert, and C. Carlin. (1999). A leucine-based determinant in the epidermal growth factor receptor juxtamembrane domain is required for the efficient transport of ligand-receptor complexes to lysosomes. *J Biol Chem* **274**: 3141-50.

67.   He, C., M. Hobert, L. Friend, and C. Carlin. (2002). The epidermal growth factor receptor juxtamembrane domain has multiple basolateral plasma membrane localization determinants, including a dominant signal with a polyproline core. *J. Biol. Chem.* **277**: 38284-38293.

68.   Hsu, S.-C. and M.-C. Hung. (2007). Characterization of a Novel Tripartite Nuclear Localization Sequence in the EGFR Family. *J. Biol. Chem.* **282**: 10432-10440.

69.   Hunter, T., N. Ling, and J.A. Cooper. (1984). Protein kinase C phosphorylation of the EGF receptor at a threonine residue close to the cytoplasmic face of the plasma membrane. *Nature* **311**: 480.

70.   Davis, R.J. and M.P. Czech. (1985). Tumor-promoting phorbol diesters cause the phosphorylation of epidermal growth factor receptors in normal human fibroblasts at threonine-654. *Proc Natl Acad Sci U S A* **82**: 1974-8.

71.   Takishima, K., I. Griswold-Prenner, T. Ingebritsen, and M.R. Rosner. (1991). Epidermal growth factor (EGF) receptor T669 peptide kinase from 3T3-L1 cells is an EGF-stimulated "MAP" kinase. *Proc Natl Acad Sci U S A* **88**: 2520-2524.

72.   Northwood, I.C., F.A. Gonzalez, M. Wartmann, D.L. Raden, and R.J. Davis. (1991). Isolation and characterization of two growth factor-

stimulated protein kinases that phosphorylate the epidermal growth factor receptor at threonine 669. *J Biol Chem* **266**: 15266-76.

73.   Martin-Nieto, J. and A. Villalobo. (1998). The human epidermal growth factor receptor contains a juxtamembrane calmodulin-binding site. *Biochemistry* **37**: 227-36.

74.   Sun, H., Z. Chen, H. Poppleton, K. Scholich, J. Mullenix, G.J. Weipz, et al. (1997). The Juxtamembrane, Cytosolic Region of the Epidermal Growth Factor Receptor Is Involved in Association with alpha -Subunit of Gs. *J. Biol. Chem.* **272**: 5413-5420.

75.   Friedman, B., A.R. Frackelton, Jr., A.H. Ross, J.M. Connors, H. Fujiki, T. Sugimura, et al. (1984). Tumor promoters block tyrosine-specific phosphorylation of the epidermal growth factor receptor. *Proc Natl Acad Sci U S A* **81**: 3034-8.

76.   Cochet, C., G.N. Gill, J. Meisenhelder, J.A. Cooper, and T. Hunter. (1984). C-kinase phosphorylates the epidermal growth factor receptor and reduces its epidermal growth factor-stimulated tyrosine protein kinase activity. *J Biol Chem* **259**: 2553-8.

77.   Downward, J., M.D. Waterfield, and P.J. Parker. (1985). Autophosphorylation and protein kinase C phosphorylation of the epidermal growth factor receptor. Effect on tyrosine kinase activity and ligand binding affinity. *J. Biol. Chem.* **260**: 14538-14546.

78.   Davis, R.J. (1988). Independent mechanisms account for the regulation by protein kinase C of the epidermal growth factor receptor affinity and tyrosine-protein kinase activity. *J Biol Chem* **263**: 9462-9.

79.   Morrison, P., K. Takishima, and M.R. Rosner. (1993). Role of threonine residues in regulation of the epidermal growth factor receptor by protein kinase C and mitogen-activated protein kinase. *J. Biol. Chem.* **268**: 15536-15543.

80.   Davis, R.J. and M.P. Czech. (1985). Platelet-derived growth factor mimics phorbol diester action on epidermal growth factor receptor phosphorylation at threonine-654. *Proc Natl Acad Sci U S A* **82**: 4080-4.

81.   King, C.S. and J.A. Cooper. (1986). Effects of protein kinase C activation after epidermal growth factor binding on epidermal growth factor receptor phosphorylation. *J. Biol. Chem.* **261**: 10073-10078.

82.   Whiteley, B. and L. Glaser. (1986). Epidermal growth factor (EGF) promotes phosphorylation at threonine-654 of the EGF receptor: possible role of protein kinase C in homologous regulation of the EGF receptor. *J. Cell Biol.* **103**: 1355-1362.

83.   Crotty, T., J. Cai, F. Sakane, A. Taketomi, S.M. Prescott, and M.K. Topham. (2006). Diacylglycerol kinase {delta} regulates protein kinase C and epidermal growth factor receptor signaling. *Proc Natl Acad Sci U S A* **103**: 15485-15490.

84.   Beguinot, L., J.A. Hanover, S. Ito, N.D. Richert, M.C. Willingham, and I. Pastan. (1985). Phorbol Esters Induce Transient Internalization without Degradation of Unoccupied Epidermal Growth Factor Receptors. *Proc Natl Acad Sci U S A* **82**: 2774-2778.

85.   Lin, C.R., W.S. Chen, C.S. Lazar, C.D. Carpenter, G.N. Gill, R.M. Evans, et al. (1986). Protein kinase C phosphorylation at Thr 654 of the unoccupied EGF receptor and EGF binding regulate functional receptor loss by independent mechanisms. *Cell* **44**: 839-48.

86.   Lund, K.A., C.S. Lazar, W.S. Chen, B.J. Walsh, J.B. Welsh, J.J. Herbst, et al. (1990). Phosphorylation of the epidermal growth factor receptor at threonine 654 inhibits ligand-induced internalization and down-regulation. *J. Biol. Chem.* **265**: 20517-20523.

87.   Bao, J., I. Alroy, H. Waterman, E.D. Schejter, C. Brodie, J. Gruenberg, et al. (2000). Threonine phosphorylation diverts internalized epidermal growth factor receptors from a degradative pathway to the recycling endosome. *J Biol Chem* **275**: 26178-86.

88.   McLaughlin, S., S.O. Smith, M.J. Hayman, and D. Murray. (2005). An electrostatic engine model for autoinhibition and activation of the epidermal growth factor receptor (EGFR/ErbB) family. *J Gen Physiol* **126**: 41-53.

89.   Cao, H., S. Decker, and D.F. Stern. (1991). TPA inhibits the tyrosine kinase activity of the neu protein in vivo and in vitro. *Oncogene* **6**: 705-11.

90. Ouyang, X., T. Gulliford, H. Zhang, G.C. Huang, and R. Epstein. (1996). Human Cancer Cells Exhibit Protein Kinase C-dependent c-erbB-2 Transmodulation That Correlates with Phosphatase Sensitivity and Kinase Activity. *J. Biol. Chem.* **271**: 21786-21792.

91. Fujii, K., G. Zhu, Y. Liu, J. Hallam, L. Chen, J. Herrero, et al. (2004). Kinase peptide specificity: Improved determination and relevance to protein phosphorylation. *Proc Natl Acad Sci U S A* **101**: 13744-13749.

92. Gandino, L., P. Longati, E. Medico, M. Prat, and P.M. Comoglio. (1994). Phosphorylation of serine 985 negatively regulates the hepatocyte growth factor receptor kinase. *J. Biol. Chem.* **269**: 1815-1820.

93. Gandino, L., M.F. Di Renzo, S. Giordano, F. Bussolino, and P.M. Comoglio. (1990). Protein kinase-c activation inhibits tyrosine phosphorylation of the c-met protein. *Oncogene* **5**: 721-5.

94. Takayama, S., M.F. White, and C.R. Kahn. (1988). Phorbol ester-induced serine phosphorylation of the insulin receptor decreases its tyrosine kinase activity. *J. Biol. Chem.* **263**: 3440-3447.

95. Downward, J., P. Parker, and M.D. Waterfield. (1984). Autophosphorylation sites on the epidermal growth factor receptor. *Nature* **311**: 483-5.

96. Walton, G.M., W.S. Chen, M.G. Rosenfeld, and G.N. Gill. (1990). Analysis of deletions of the carboxyl terminus of the epidermal growth factor receptor reveals self-phosphorylation at tyrosine 992 and enhanced in vivo tyrosine phosphorylation of cell substrates. *J. Biol. Chem.* **265**: 1750-1754.

97. Hsuan, J.J., J. Downward, S. Clark, and M.D. Waterfield. (1989). Proteolytic generation of constitutive tyrosine kinase activity of the human insulin receptor. *Biochem J* **259**: 519-27.

98. Levkowitz, G., H. Waterman, S.A. Ettenberg, M. Katz, A.Y. Tsygankov, I. Alroy, et al. (1999). Ubiquitin Ligase Activity and Tyrosine Phosphorylation Underlie Suppression of Growth Factor Signaling by c-Cbl/Sli-1. *Mol Cell* **4**: 1029.

99. Honegger, A.M., A. Schmidt, A. Ullrich, and J. Schlessinger. (1990). Evidence for epidermal growth factor (EGF)-induced intermolecular autophosphorylation of the EGF receptors in living cells. *Mol. Cell. Biol.* **10**: 4035-4044.

100. Honegger, A.M., R.M. Kris, A. Ullrich, and J. Schlessinger. (1989). Evidence that Autophosphorylation of Solubilized Receptors for Epidermal Growth Factor is Mediated by Intermolecular Cross-Phosphorylation. *Proc Natl Acad Sci U S A* **86**: 925-929.

101. Honegger, A., T.J. Dull, F. Bellot, E. Van Obberghen, D. Szapary, A. Schmidt, et al. (1988). Biological activities of EGF-receptor mutants with individually altered autophosphorylation sites. *Embo J* **7**: 3045-52.

102. Honegger, A., T.J. Dull, D. Szapary, A. Komoriya, R. Kris, A. Ullrich, et al. (1988). Kinetic parameters of the protein tyrosine kinase activity of EGF-receptor mutants with individually altered autophosphorylation sites. *Embo J* **7**: 3053-60.

103. Heldin, C.-H., A. Ostman, and L. Ronnstrand. (1998). Signal transduction via platelet-derived growth factor receptors. *Biochimica et Biophysica Acta (BBA) - Reviews on Cancer* **1378**: F79.

104. Sasaoka, T., W.J. Langlois, F. Bai, D.W. Rose, J.W. Leitner, S.J. Decker, et al. (1996). Involvement of ErbB2 in the Signaling Pathway Leading to Cell Cycle Progression from a Truncated Epidermal Growth Factor Receptor Lacking the C-terminal Autophosphorylation Sites. *J. Biol. Chem.* **271**: 8338-8344.

105. Lee, N.Y. and J.G. Koland. (2005). Conformational changes accompany phosphorylation of the epidermal growth factor receptor C-terminal domain. *Protein Sci* **14**: 2793-2803.

106. Aifa, S., N. Miled, F. Frikha, M.R. Aniba, S.P. Svensson, and A. Rebai. (2006). Electrostatic interactions of peptides flanking the tyrosine kinase domain in the epidermal growth factor receptor provides a model for intracellular dimerization and autophosphorylation. *Proteins* **62**: 1036-43.

107. Sorokin, A. (1995). Activation of the EGF receptor by insertional mutations in its juxtamembrane regions. *Oncogene* **11**: 1531-40.

108. Yamane, K., C. Toyoshima, and S. Nishimura. (1992). Ligand-induced functions of the epidermal growth factor receptor require the positively charged region asymmetrically distributed across plasma membrane. *Biochemical and Biophysical Research Communications* **184**: 1301.

109. Segatto, O., F. Lonardo, D. Wexler, F. Fazioli, J.H. Pierce, D.P. Bottaro, et al. (1991). The juxtamembrane regions of the epidermal growth factor receptor and gp185erbB-2 determine the specificity of signal transduction. *Mol Cell Biol* **11**: 3191-202.

110. Castagnino, P., Z. Biesova, W.T. Wong, F. Fazioli, G.N. Gill, and P.P. Di Fiore. (1995). Direct binding of eps8 to the juxtamembrane domain of EGFR is phosphotyrosine- and SH2-independent. *Oncogene* **10**: 723-9.

111. Morrison, P., K.C. Chung, and M.R. Rosner. (1996). Mutation of Di-leucine residues in the juxtamembrane region alters EGF receptor expression. *Biochemistry* **35**: 14618-24.

112. Koland, J.G., K.M. O'Brien, and R.A. Cerione. (1990). Expression of epidermal growth factor receptor sequences as E. coli fusion proteins: Applications in the study of tyrosine kinase function. *Biochemical and Biophysical Research Communications* **166**: 90.

113. Cadena, D.L., C.L. Chan, and G.N. Gill. (1994). The intracellular tyrosine kinase domain of the epidermal growth factor receptor undergoes a conformational change upon autophosphorylation. *J. Biol. Chem.* **269**: 260-265.

114. Hsu, C.Y., M. Mohammadi, M. Nathan, A. Honegger, A. Ullrich, J. Schlessinger, et al. (1990). Generation of recombinant cytoplasmic domain of epidermal growth factor receptor with intrinsic protein tyrosine kinase activity. *Cell Growth Differ* **1**: 191-200.

115. Timms, J.F., M.E. Noble, and M. Gregoriou. (1995). An investigation of the role of Glu-842, Glu-844 and His-846 in the function of the cytoplasmic domain of the epidermal growth factor receptor. *Biochem J* **308 (Pt 1)**: 219-29.

116. Mulloy, R., A. Ferrand, Y. Kim, R. Sordella, D.W. Bell, D.A. Haber, et al. (2007). Epidermal Growth Factor Receptor Mutants from Human Lung

Cancers Exhibit Enhanced Catalytic Activity and Increased Sensitivity to Gefitinib. *Cancer Res* **67**: 2325-2330.

117.   Zhou, W. and G. Carpenter. (2000). Heregulin-dependent trafficking and cleavage of ErbB-4. *J Biol Chem* **275**: 34737-43.

118.   Linggi, B., Q.C. Cheng, A.R. Rao, and G. Carpenter. (2006). The ErbB-4 s80 intracellular domain is a constitutively active tyrosine kinase. *Oncogene* **25**: 160-3.

119.   Ni, C.Y., M.P. Murphy, T.E. Golde, and G. Carpenter. (2001). gamma - Secretase cleavage and nuclear localization of ErbB-4 receptor tyrosine kinase. *Science* **294**: 2179-81.

120.   Cochet, C., G.N. Gill, J. Meisenhelder, J.A. Cooper, and T. Hunter. (1984). C-kinase phosphorylates the epidermal growth factor receptor and reduces its epidermal growth factor-stimulated tyrosine protein kinase activity. *J. Biol. Chem.* **259**: 2553-2558.

121.   Hubbard, S.R. (2004). Juxtamembrane autoinhibition in receptor tyrosine kinases. *Nat Rev Mol Cell Biol* **5**: 464-71.

122.   Hirota, S., K. Isozaki, Y. Moriyama, K. Hashimoto, T. Nishida, S. Ishiguro, et al. (1998). Gain-of-function mutations of c-kit in human gastrointestinal stromal tumors. *Science* **279**: 577-580.

123.   Corless, C.L., J.A. Fletcher, and M.C. Heinrich. (2004). Biology of gastrointestinal stromal tumors. *Journal of Clinical Oncology* **22**: 3813.

124.   Mol, C.D., D.R. Dougan, T.R. Schneider, R.J. Skene, M.L. Kraus, D.N. Scheibe, et al. (2004). Structural basis for the autoinhibition and STI-571 inhibition of c-Kit tyrosine kinase. *J. Biol. Chem.* **279**: 31655-31663.

125.   Kitayama, H., Y. Kanakura, T. Furitsu, T. Tsujimura, K. Oritani, H. Ikeda, et al. (1995). Constitutively activating mutations of c-kit receptor tyrosine kinase confer factor-independent growth and tumorigenicity of factor-dependent hematopoietic cell lines. *Blood* **85**: 790-798.

126.	Casteran, N., P. De Sepulveda, N. Beslu, M. Aoubala, S. Letard, E. Lecocq, et al. (2003). Signal transduction by several KIT juxtamembrane domain mutations. *Oncogene* **22**: 4710-22.

127.	Griffith, J., J. Black, C. Faerman, L. Swenson, M. Wynn, F. Lu, et al. (2004). The Structural Basis for Autoinhibition of FLT3 by the Juxtamembrane Domain. *Molecular Cell* **13**: 169.

128.	Walter, M., I.S. Lucet, O. Patel, S.E. Broughton, R. Bamert, N.K. Williams, et al. (2007). The 2.7 A Crystal Structure of the Autoinhibited Human c-Fms Kinase Domain. *J Mol Biol* **367**: 839.

129.	Wybenga-Groot, L.E., B. Baskin, S.H. Ong, J. Tong, T. Pawson, and F. Sicheri. (2001). Structural Basis for Autoinhibition of the EphB2 Receptor Tyrosine Kinase by the Unphosphorylated Juxtamembrane Region. *Cell* **106**: 745.

130.	Binns, K.L., P.P. Taylor, F. Sicheri, T. Pawson, and S.J. Holland. (2000). Phosphorylation of Tyrosine Residues in the Kinase Domain and Juxtamembrane Region Regulates the Biological and Catalytic Activities of Eph Receptors. *Mol. Cell. Biol.* **20**: 4791-4805.

131.	Aifa, S., J. Aydin, G. Nordvall, I. Lundstrom, S.P.S. Svensson, and O. Hermanson. (2005). A basic peptide within the juxtamembrane region is required for EGF receptor dimerization. *Experimental Cell Research* **302**: 108.

132.	Okabe, T., I. Okamoto, K. Tamura, M. Terashima, T. Yoshida, T. Satoh, et al. (2007). Differential Constitutive Activation of the Epidermal Growth Factor Receptor in Non-Small Cell Lung Cancer Cells Bearing EGFR Gene Mutation and Amplification. *Cancer Res* **67**: 2046-2053.